Influence of the chemokine CXCL12 on the progression and the signalling in colorectal cancer

Dissertation

Zur Erlangung des Grades Doktor der Naturwissenschaften

Am Fachbereich Biologie

Der Johannes Gutenberg-Universität Mainz

vorgelegt von

M.Sc. Biotechnology

Risala Hussein Allami

aus

Baghdad, Iraq

Mainz 2013

بِسۡمِ ٱللَّهِ ٱلرَّحۡمَٰنِ ٱلرَّحِيمِ

وَقُل رَّبِّ زِدۡنِي عِلۡمٗا

سُورَةُ طٰه

Translation in English

In the name of Allah, the Beneficent, the Merciful

"O my Lord! Increase me in knowledge."

Surah Ta-Ha

TABLE OF CONTENTS

TABLE OF CONTENTS

Abbreviations

AIDS	Acquired immune deficiency syndrome
APC	Adenomatosis polyposis coli
AKT	v-akt murine thymoma viral oncogene homolog 1 / PKB – protein kinase B
ATF	activating transcription factor
B-ATF	B-cell-activating transcription factor
BM	Bone marrow
BSA	Bovine serum albumin
Bp	Base pare
CCL	CC family chemokine ligand
CCR	CC family chemokine receptor
cDNA	Complementary DNA
CXCL	CXC family chemokine ligand
CXCR	CXC family chemokine receptor
CRC	Colorectal cancer
DNA	Deoxyribonucleic acid
DNase	Deoxyribonuclease
dNTP	Deoxynuclaotide triphosphate
EGFR	Epidermal growth factor receptor

ABBREVIATIONS

ERK	extra-cellular signal-regulated kinase / MAPK1
FACS	Fluorescence activated cell sorting
FAP	Familial Adenomatous Polyposis
FBS	Fetal bovine Serum
GFP	Green fluorescence protein
G418	Geneticin
HNPCC	Hereditary non-polyposis colorectal cancer
JNK	jun terminal kinase
MAPK	Mitogen Activated Protein Kinase
MEK	MAPK kinase/ERK kinase
ml	Millilitre
mg	Milligram
MMP	Matrix-Metalloproteinase
mRNA	Messenger RNA
p38	Protein 38
PAGE	polyacrylamide gel electrophoresis
PB	Peripheral blood
PBS	Phosphate Buffered Saline
PCR	Polymerase chain reaction

PI3K	phosphoinositide 3-kinases
PKC	protein kinase C
PPAR	peroxisome proliferative receptor
RNA	Ribonucleic acid
RT	Reverse transcription
Rpm	Rotation per minute
SDF-1	Stromal cell-derived factor 1
SNP	Single nucleotide polymorphism
Temp	Temperature
TCF-4	transcription factor 4
TNFα	tumor necrosis factor α
TNM	Tumour-Node-Metastasis
UICC	Union international contra le cancer
UV	Ultraviolet light
VEGF	Vascular endothelial growth factor
WB	Western blot
WT	Wild type
µg	Microgram
µl	Microliter

1. Introduction

1.1 Epidemiology

1.1.1 The mortality statistics in Germany

Diseases of the circulatory system have been for many years the most frequent cause of death in both men and women. Whereas malignant neoplasms are the second leading cause of death in men nearly with 28.9 % and in women with 22.4 % (Fig 1). At present, approximately every third death is due to circulatory disease and every fourth death is due to cancer [1]. The burden of cancer is increasing in economically developing and developed countries as a result of aging population and an adoption of cancer-associated lifestyle choices including tobacco smoking, obesity, physical inactivity and diet with high calories [2]. About 12.7 million cancer cases and 7.6 million cancer deaths are estimated to have occurred in 2008 worldwide and with 1.24 million new cases diagnosed in 2008, colorectal cancer is the third most common cancer worldwide. [2]. In addition, colorectal cancer sums up to the second most frequent type of cancer concerning men and women in developed countries [1].

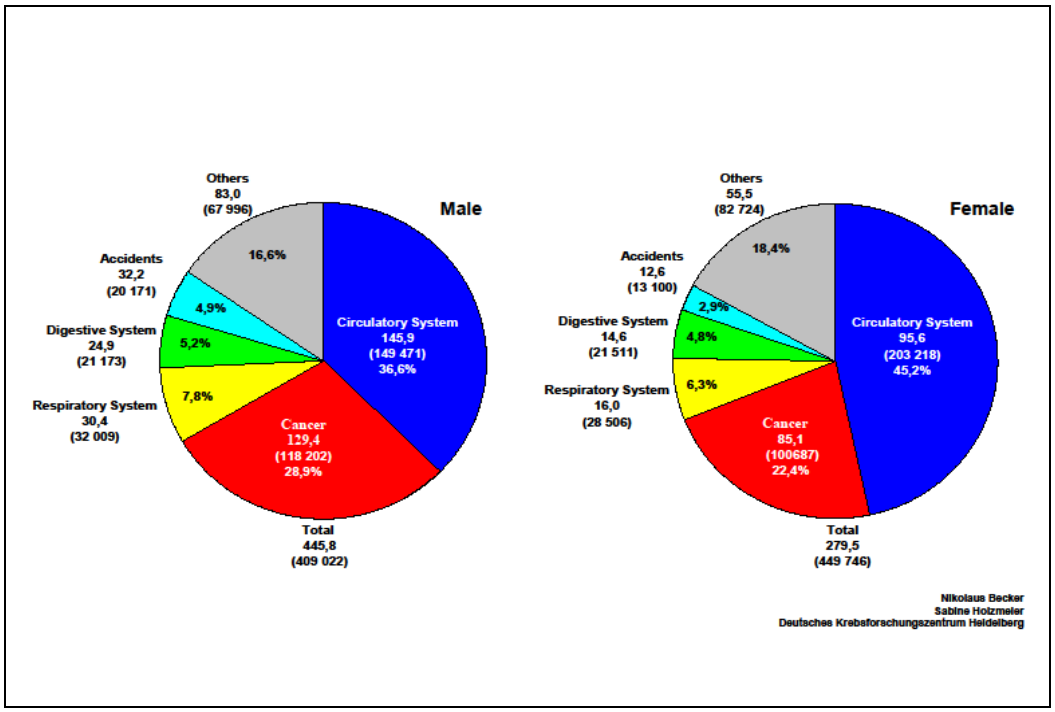

Fig 1- The Most Frequent Causes of Death in Germany in 2010 [1]

In Germany, in 2008, there were nearly 65,000 cases of colorectal cancer and almost 26,000 deaths and in 2012, according to projections of the Robert-Koch-Institute, up to 73,000 new cases [3].

The trend graphs for the five leading groups of causes of death in Germany (Fig 2) indicate that cancer mortality continues to show a slight, gradual downtrend compared to the more pronounced decline for cardiovascular diseases. Cancer will become the leading cause of death in Germany in the next 15-20 years, whereas the age-adjusted mortality rates from diseases of the circulatory system have declined significantly among females for decades and among males since about 1970, and that these rates are continuing to fall.

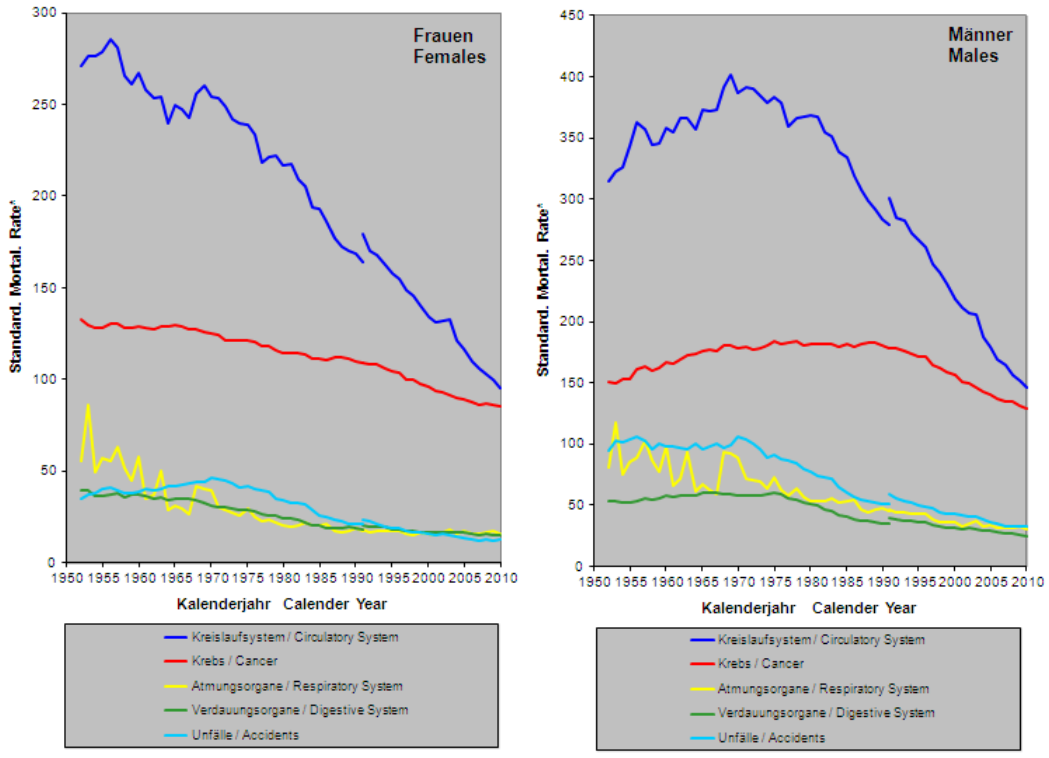

A B

Fig 2- Trend graph for the five leading groups of causes of death in Germany for male (A) and female (B) [4]

1.1.2 Incidence and Mortality Data

According to the World Health Organization, cancer is the leading cause of death in economically developed countries and the second leading cause of death in developing countries [5]. Today, millions of people all over the world are living with cancer or have had cancer [6].

The five most common types of cancer are largely identical for each sex in both parts of Germany.

Lung cancer is the leading cause of cancer death in males (25.5 %) followed by colorectal cancer (11.0 %), and prostate cancer (9.09 %) (Fig 3).

Breast cancer is the leading cause of cancer death in females (19.2 %) followed by lung cancer (16.0 %) and colorectal cancer (10.3 %) [3].

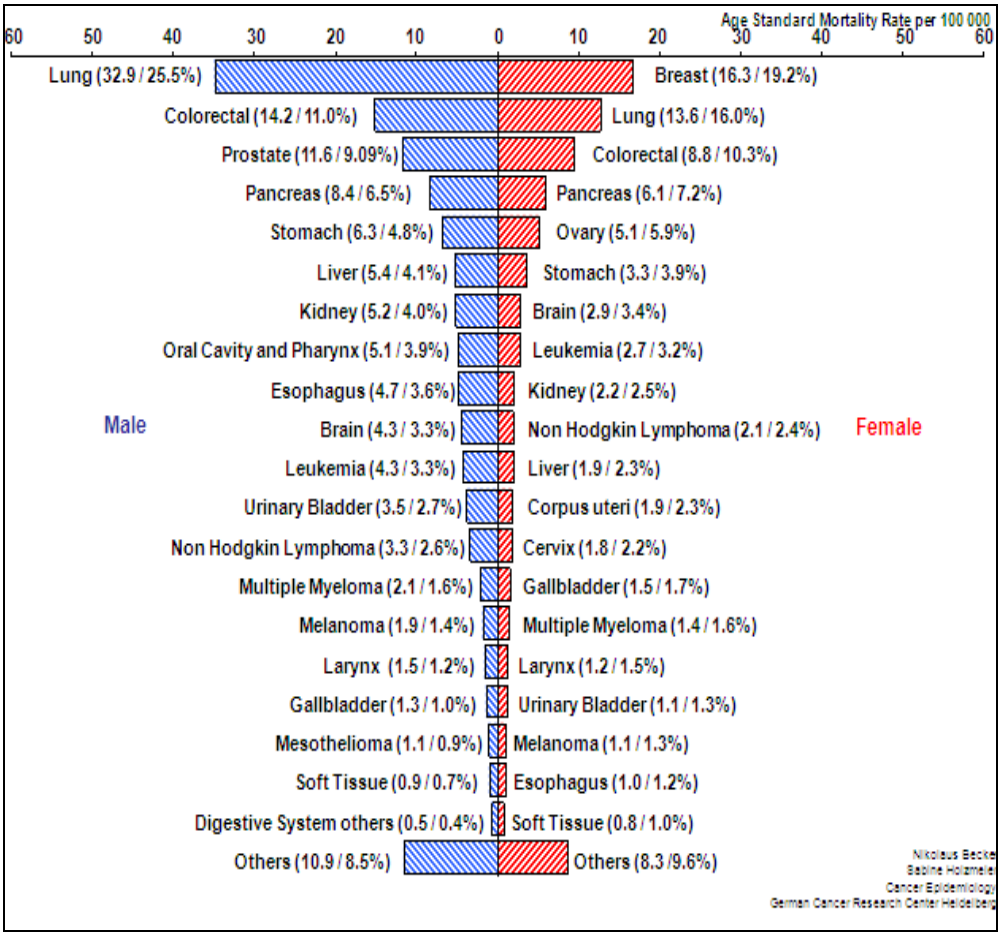

Fig 3- The 20 Most Frequent Causes of Cancer Deaths in Germany 2010 [7]

1.2 Definition of cancer

Cancer is not just one disease but many diseases. There are more than 200 different types of cancer and each is classified by the type of cell that is initially affected. There are over 60 different organs in the body where a cancer can develop [8].

When cells become abnormal and divide without control or order, cancer occurs like all other organs of the body. Normally, cells divide to produce more cells only when the body needs them. This orderly process helps keep us healthy. If cells keep dividing when new cells are not needed, a mass of tissue forms. This mass of extra tissue, called a tumor, can be benign or malignant [9]. Depending on whether or not they can spread by invasion and metastasis, tumors are classified as:

- **Benign tumors** aren't cancerous. They can often be removed, and, in most cases, they do not come back. Cells in benign tumors do not spread to other parts of the body. Benign tumors are rarely threats to life
- **Malignant tumors** are cancerous. Cells in these tumors can invade nearby tissues and spread from the original (primary) tumor to form new tumors in other parts of the body. The spread of cancer from one part of the body to another is called metastasis [10].

Anywhere in the body cancer can originate [11].

- **Carcinomas:** are cancers arising from the cells that cover external and internal body surfaces. Lung, breast and colon cancers are the most common types of cancer.
- **Sarcomas**: are cancers arising from cells found in the supporting tissues of the body such as bone, cartilage, fat, connective tissue and muscle.
- **Lymphomas:** are cancers that arise in the lymph nodes and tissues of the body's immune system.
- **Leukemias:** are cancers of the immature blood cells that grow in the bone marrow and tend to accumulate in large numbers in the bloodstream.

1.2.1 Carcinogenesis – The development of cancer

Every cancer and its carcinogenesis are unique; cancers usually develop over years and sometimes decades until they become clinically overt. During this time they gradually develop from normal cells into neoplastic lesions. Nevertheless most cancers share common features and progress by similar steps [12].

A genomic alteration is often preceded by hyperplasia of the tissue, caused by deregulation and increased cell proliferation. However, there are no DNA mutations. Hyperplasia is mostly induced by inflammation. It can develop into a neoplasia but it can also regress in order to become normal tissue again. Once a cell acquires a persistent genomic alteration the carcinogenesis can become irreversible (Fig 4) [12].

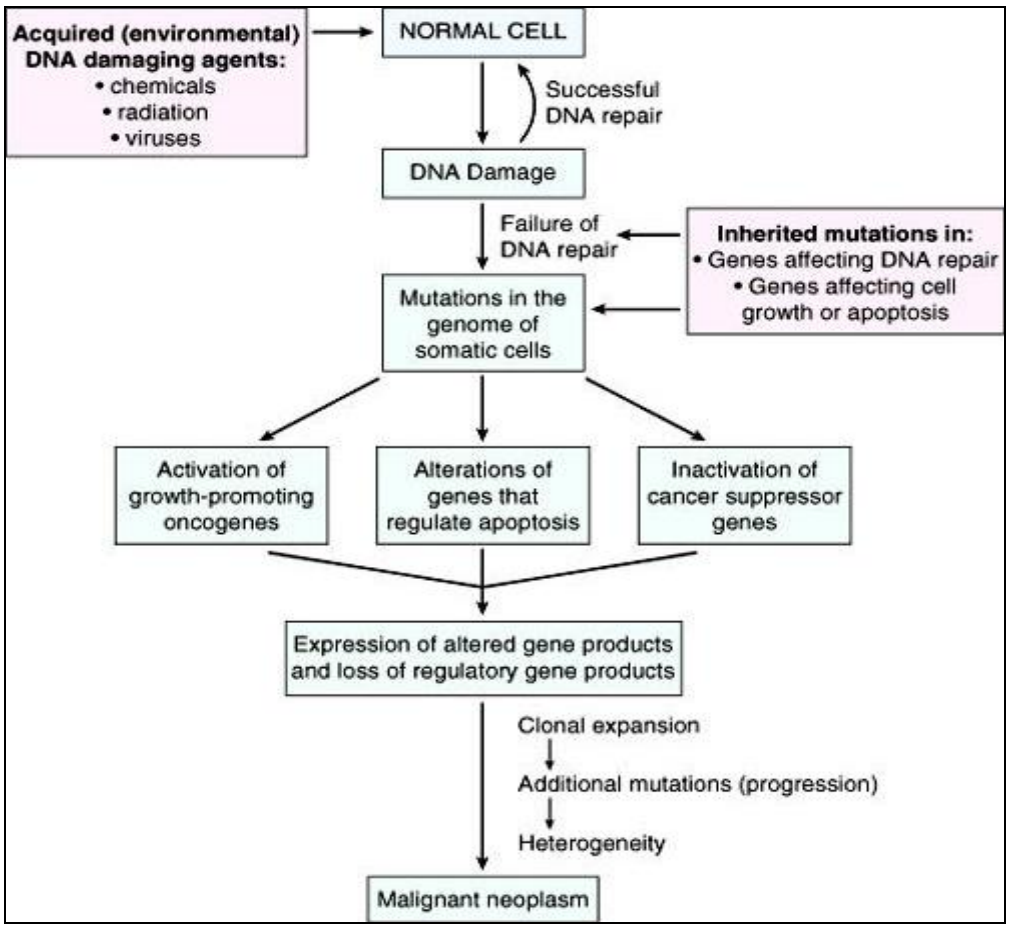

Fig 4 - Molecular basis of cancer [12]

According to present knowledge the process of a normal cell turning into a cancer cell appears arbitrary.

Cancer is caused by both internal factors (including inherited mutations, hormones, immune conditions, and mutations that occur from metabolism) and external factors (including tobacco, infectious organisms, chemicals, and radiation). These causal factors may act together or in sequence to initiate carcinogenesis [13].

Mutations occur rarely and randomly. An accumulation of mutations within oncogenes, tumor suppressor genes, apoptosis related genes or DNA repair genes is very improbable. Most cells will die off or remain at an early stage of carcinogenesis. Several factors can promote the carcinogenesis. Hereditary predisposition, such as mutations in DNA repair genes, exposition to carcinogenic substances, ionizing radiation or certain retroviruses can lead to an increased mutation frequency. Once a cell has acquired enough mutations to become a tumor cell, it will be driven by selective pressure into increased malignancy [12].

1.3 Colorectal cancer

Colorectal cancer (CRC) develops in the colon or the rectum. The colon is the part of the digestive system where the waste material is stored and fluids as well as electrolytes are being resoled. The rectum is the end of the colon adjacent to the anus. Together, they form a long, muscular tube called the large intestine (also known as the large bowel) [14].

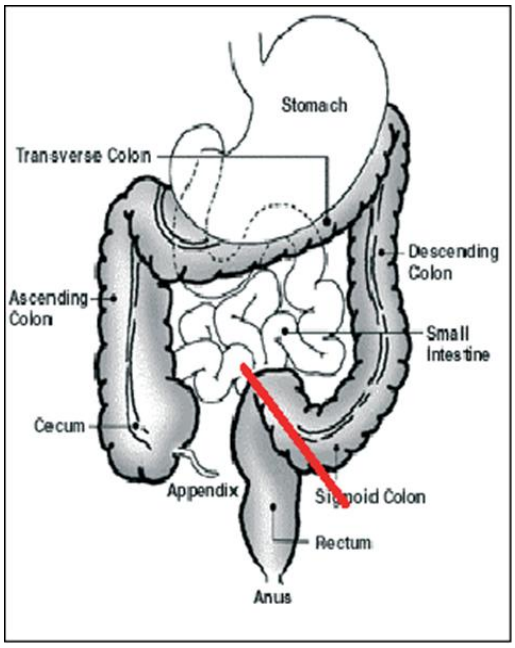

Fig 5- The anatomy of the gastrointestinal tract [14]

The colon is divided into five sections: caecum and ascending, transverse, descending, and sigmoid. The rectum forms the most distal portion of the large intestine [14]

Colorectal cancer may occur at any age, more than 90% of the patients are over age 40, at which point the risk doubles every ten years. In addition to age, other high risk factors include a family history of colorectal cancer and polyps and a personal history of ulcerative colitis, colon polyps or cancer of other organs, especially of the breast or uterus [15].The etiology of CRC is complex involving an inter-play of environmental and genetic factors. Some other risk factors enhancing the likelihood of CRC are obesity, sedentary lifestyle and smoking [16].

There are three variants of CRC, two of which are hereditary [17].

- **FAP** (familial adenomatous polyposis) is a hereditary colon cancer syndrome where the affected family members will develop countless numbers (hundreds, sometimes thousands) of colon polyps, starting during early adulthood. FAP is accounting for an estimated 1% - 2% of incident cases of colorectal cancer.
- **HNPCC** (hereditary nonpolyposis colon cancer) is a hereditary colon cancer syndrome. Affected family members can develop colon polyps and cancers. It accounts for 3% of incident cases of colorectal cancer.
- **Sporadic cancer** is the third variant and counts for the majority of cases (about 80%).

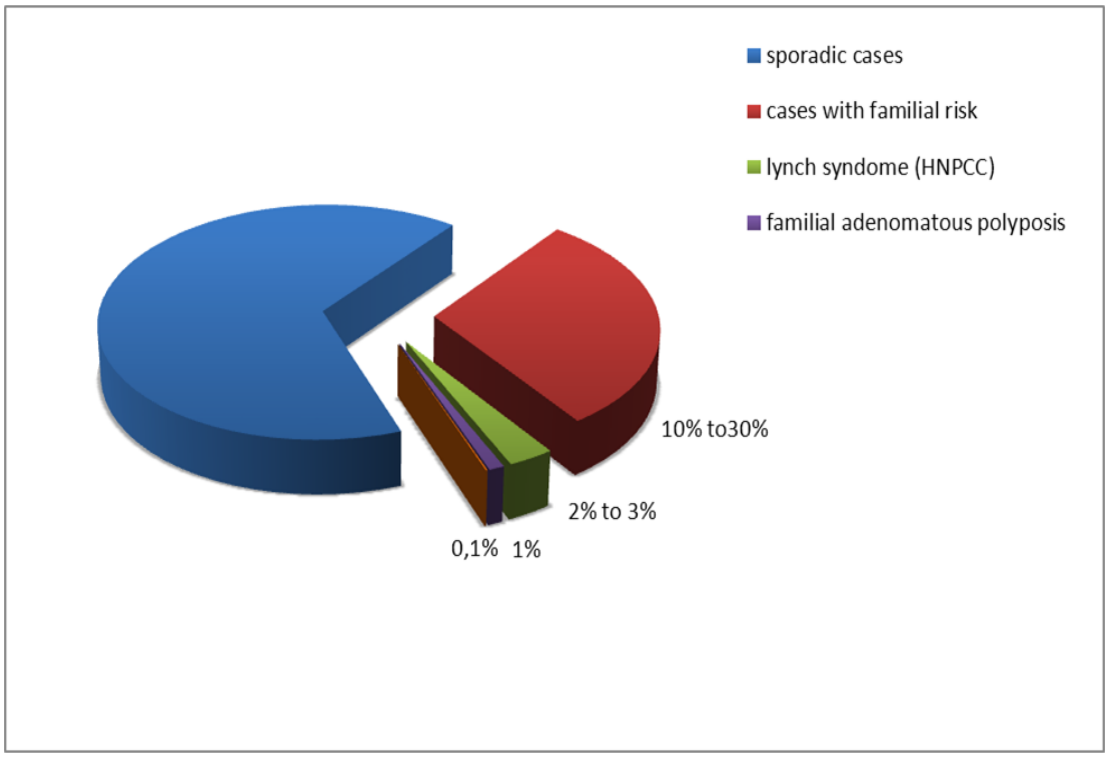

Fig 6- Family risk settings in colon cancer

1.3.1 Carcinogenesis of colorectal cancer

The carcinogenesis of colorectal cancer is intensely studied. In 1990, Fearon and Vogelstein proposed a model for describing the genetic tumor progression in CRC [18]. Vogelstein et al postulated that alterations of oncogenes (K-ras) and proto-oncogenes (APC, DCC, p53) are required for the development of colorectal cancers [19, 20]. Mutation of the tumor suppressor APC, a key protein in the Wnt signaling pathway, is suggested as the start of CRC. Likewise this mutation was presumed to be the cause of the hereditary variant FAP (familial adenomatous polyposis) of CRC.

Transition from adenoma to dysplastic tissue may be caused by several genetic changes as well as changes in the adenoma microenvironment. KRAS activation due to mutation is found in 40-50% of adenomas and carcinomas and leads to a constant signal to the nucleus for division [21]. A mutation that occurs in the majority of CRC cases appears in the tumor suppressor p53 gene which is responsible for regulation of cell cycle in Wild type [22]. Another well-known mutation is in the DCC gene (deleted in colorectal carcinoma). The DCC protein has a possible roll in cell-environment interactions [23]. The different phases of colon cancer progression are described by Markowitz SD and Bertagnolli MM (Fig.7) [24].

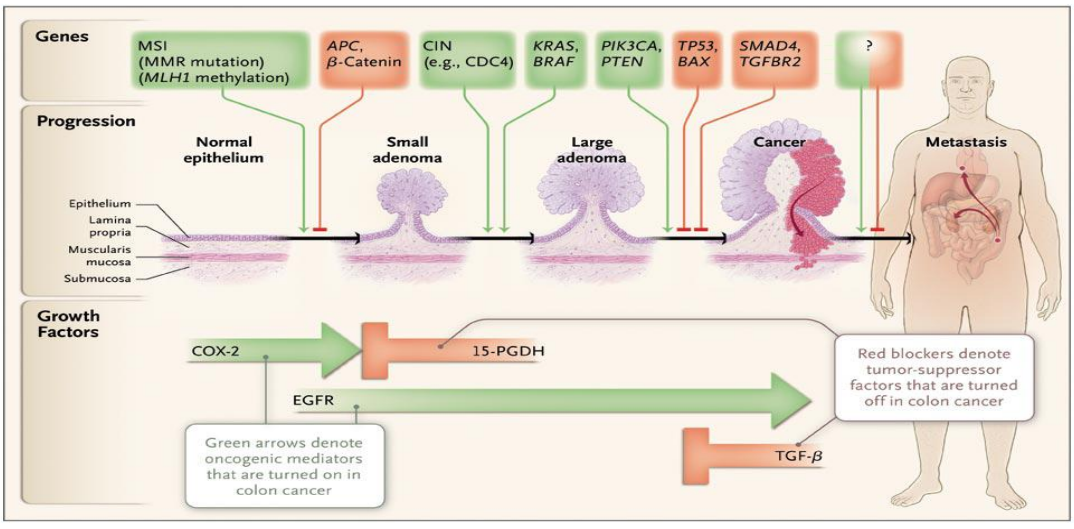

Fig 7- Biological and genetic events during colon cancer [24].

1.3.2 Classification and staging of colon cancers

Classification according to Dukes was first proposed by Dr. C.E. Dukes in 1932 and describes the stages of colorectal cancer as: A – tumor confined to intestinal wall, B – tumor invading through the intestinal wall, C – with lymph node (s) involvement and D – with distant metastasis [25]. The most common current staging system is the TNM (Tumors/Nodes/Metastases) system [26]. Dukes staging was used in the present work and can be converted to approximate TNM staging (Table 1).

Dukes	**TNM**
A	T1/T2; N0; M0
B	T3/T4; N0; M0
C	Tx; N1/N2; M0
D	Tx; Nx; M1

Table 1- Relationships between Dukes staging and TNM classification.

The central aim of the TNM system for classification is the unambiguous description of tumors and cancers in respect to their histopathology and anatomical extent [27].

The TNM system is based on three components:

- The extent of the primary tumor (T)
- The absence or presence and extent of regional lymph node metastasis (N)
- The absence or presence of distant metastasis (M)

T – Primary tumor	
Tx	Primary tumour cannot be assessed
T0	No evidence of primary tumour
Tis	Carcinoma in situ: intraepithelial or invasion of lamina propria
T1	Tumour invades submucosa
T2	Tumour invades muscularis propria
T3	Tumour invades subserosa or into non-peritonealised pericolic or perirectal tissue
T4	Tumour directly invades other organs or structures and/or perforates visceral peritoneum • T4a Tumour perforates visceral peritoneum • T4b Tumour directly invades other organs or structures
N – Regional lymp node	
Nx	Regional lymph nodes cannot be assessed
N0	No regional lymph node metastasis
N1	Metastasis in 1 – 3 regional lymph nodes • N1a Metastasis in 1 regional lymph node • N1b Metastasis in 2 – 3 regional lymph nodes • N1c Tumour deposit(s), i.e., satellites, in the subserosa, or in non pericolic or perirectal soft tissue without regional lymph node metastasis
N2	Metastasis in 4 or more regional lymph nodes • N2a Metastasis in 4 – 6 regional lymph nodes • N2b Metastasis in 7 or more regional lymph nodes
M – Distant metastasis	
M0	No distant metastasis
M1	Distant metastasis • M1a Metastasis confined to one organ (liver, lung, ovary, non-regional lymph node(s) • M1b Metastasis in more than one organ or the peritoneum

Table 2- TNM classification for colon and rectum tumours [27].

According to UICC (International Union against Cancer) patients can be grouped into clinical stages, which have similar clinical characteristics and shared prognosis (Table 3)

Stage grouping (according to UICC)			
Stage 0	Tis	N0	M0
Stage 1	T1, T2	N0	M0
Stage 2	T3, T4	N0	M0
Stage 2a	T3	N0	M0
Stage 2b	T4a	N0	M0
Stage 2c	T4b	N0	M0
Stage 3	Any T	N1,N2	M0
Stage 3a	T1, T2 T1,	N1 N2a	M0
Stage 3b	T3, T4a T2,T3 T1,T2	N1 N2a N2b	M0
Stage 3c	T4a T3,T4a T4b	N2a N2b N1,N2	M0
Stage 4a	Any T	Any N	M1a
Stage 4b	Any T	Any N	M1b

Table 3- Stage grouping for colon and rectum tumours according to UICC [27].

The primary tumors are also regularly characterised by their histopathological grading (G) which characterises cell differentiation of the cancer cells (Table 4).

G – Histopathological grading	
G1	Well differentiated
G2	Moderately differentiated
G3	Poorly differentiated
G4	Undifferentiated

Table 4- Histopathological grading for colon and rectum tumors [27].

1.4 Chemokines and their structure

1.4.1 What are chemokines?

More than 200 **Cytokines** are a category of signaling molecules which are important in inter-cellular communication and regulate cell proliferation, differentiation, maturation and death [28, 29, 30].

The general cytokine network includes several cytokine families (**lymphokines, interleukins, chemokines**) that can be classified in terms of ligand and receptor structure, although most cytokines have little homology in their DNA or amino acid sequence. One exception to this is the family of chemoattractant cytokines or chemokines. With approximately 50 closely related members and at least 19 receptors, chemokines are now the largest known cytokine family [28, 29, 30].

1.4.2 Chemokine structure and nomenclature

Chemokines are a superfamily of chemoattracting cytokine like protein (8-14 kDa), which bind to their cognate G-protein coupled receptors (GPCRs). It consists of approximately 70-130 amino acids and they are classified into four subfamilies **CXC, CC, CX3C** and **C.**

Chemokines are based on the positioning of the served two N-terminal cysteine residues of the chemokines. (Fig 8) [31]

- The CXC is known as α chemokine that has one amino acid present in between the first two cysteine residues near the amino or N-terminus.
- The CX3C is known as δ chemokine that has three amino acid residues between the first and second cysteines near the N-terminus
- The CC is known as β chemokines. The first two cysteines are adjacent to each other, near the Nterminus, which are the largest families of chemokines.
- The C is known as γ chemokines. The fourth chemokine subtype lacks two (the first and third) of the four conserved cysteine residues [32, 33, 34].

Group of chemokine	Structure
C:	**……...C……..……..C…….**
CC:	**……C------C……C…….C…….**
CXC:	**……CX----C……C…… C…….**
CX3C:	**……CXXXC……C…….C…….**
C – cysteine; X - an amino acid other than cysteine	

Fig 8- Structural classification of the chemokine family [31]

Chemokines are important in many biological processes, such as migration of leukocytes, embryogenesis, wound healing, angiogenesis, hematopoiesis, atherosclerosis, inflammatory diseases, tumor growth and metastasis and HIV-infection [35, 36].

As a result, a new nomenclature system was developed several years ago, in which the chemokine structural code (**CXC, CC, CX3C, or C**) is followed by the letter 'L' (ligand) for each chemokine (as in CXCL1) or by the letter 'R' (receptor) for each receptor (as in CXCR1) [37].

Table (5) list of the chemokines identified to date together with their synonyms and official names.

Systematic names	Common names	Chemokine receptor
CXCL1	GROα, MGSAα	CXCR2
CXCL2	GROβ, MIP-2α	CXCR2
CXCL3	GROγ, MIP-2β	CXCR2
CXCL4	Platelet factor-4	Unknown
CXCL5	ENA-78	CXCR2
CXCL6	GCP-2	CXCR1
CXCL7	PBP, βTG	CXCR2
CXCL8	IL-8	CXCR1
CXCL9	Mig	CXCR3
CXCL10	γYP-10, CRG-2	CXCR3
CXCL11	I-TAC, IP9, H174	CXCR3
CXCL12	**SDF-1α, -1β, -1γ, - 1δ ,-1ε , -1ϕ**	**CXCR4, CXCR7**
CXCL13	BCA-1, BLC	CXCR5
CXCL14	BRAK, Bolekine	Unknown
CXCL16	STRC33, BUNZO	CXCR6
CCL1	I-309, TCA-3	CCR8
CCL2	MCP-1, MCAF	CCR11
CCL3	MIP-1α	CCR1, CCR5
CCL4	MIP-1β	CCR5
CCL5	RANTES	CCR1, CCR3, CCR5
CCL6	GCP-2	Unknown
CCL7	MCP-3	CCR1, CCR2, CCR3, CCR11
CCL8	MCP-2	CCR1, CCR2, CCR3, CCR5
CCL11	Eotaxin	CCR3
CCL13	MCP-4	CCR1, CCR2, CCR3, CCR11
CCL14	CC-1, HCC-1, MCIF	CCR1
CCL15	HCC-2, MIP-5	CCR1, CCR3
CCL16	HCC-4, LEC	CCR1
CCL17	TARC	CCR4
CCL18	MIP-4, PARC, AMAC-1	Unknown
CCL19	MIP-3β, ELC, exodus-3	CCR7
CCL20	MIP-3α, LARC, exodus1	CCR6
CCL21	SLC, exodus-2, TCA4	CCR7
CCL22	MDC, de/ β-ck	CCR4
CCL23	MPIF-1, MIP	CCR1
CCL24	MPIF-2, eotaxin-2	CCR3
CCL25	TECK	CCR9
CCL26	eotaxin-3, MIP-4α	CCR3
CCL27	CTACK, ALP, ILC	CCR10
CCL28	MEC	CCR3, CCR10
XCL1	Lymphotactin α, SCM-1α	XCR1
XCL2	Lymphotactin β, SCM-1β	XCR1
CX3CL1	Fractalkine	CX3R1

Table 5- chemokines and chemokine receptors

1.4.3 Chemokine receptors

The chemokine receptors are seven-transmemberane receptors coupled to G protein, which include receptors for hormones, neurotransmitters, paracrine substances and inflammatory mediators**.** There are four classes of chemokine receptors **CXCR1, CCR1, XCR1** and **CX3CR1** [38, 39].

The human chemokine system currently contains more than 50 human chemokines and 20 chemokine receptors [33] (Table 6) (Fig 9).

Chemokine receptor	Chemokine ligand
CXCR1	CXCL6, CXCL8
CXCR2	CXCL1, CXCL2, CXCL3, CXCL5, CXCL6, CXCL7, CXCL8
CXCR3	CXCL4, CXCL9, CXCL10, CXCL11
CXCR4	CXCL12
CXCR5	CXCL13
CXCR6	CXCL16
CXCR7	CXCL11, CXCL12,
CCR1	CCL3, CCL4, CCL5, CCL7, CCL8, CCL9/CCL10, CCL14, CCL15, CCL16, CCR2
CCL2,	CCL6, CCL7, CCL8, CCL12, CCL13, CCL16
CCR3	CCL7, CCL8, CCL11, CCL13, CCL15, CCL24, CCL26, CCL28
CCR4	CCL3, CCL5, CCL17, CCL22
CCR5	CCL3, CCL4, CCL5, CCL8, CCL13, CCL16
CCR6	CCL20
CCR7	CCL19, CCL21
CCR8	CCL1, CCL16
CCR9	CCL25
CCR10	CCL27, CCL28
XCR1	XCL1, XCL2
CX3CR1	CX3CL1

The Duffyreceptor is not included in this table– this is a non-signalling receptor

Table 6- The four classes of chemokine receptors and their ligands* (some chemokines may bind other receptors) [39]

Among the 7 receptors that selectively bind certain CXC chemokines are the chemokine receptors CXCR1 to CXCR7, whereas the CC receptor family consists of 10 receptors, CCR1 to CCR10.

The receptor for CX3CL1 (fractalkine) is CX3CR1, and XCR1 is the receptor for XCL1 and 2 (lymphotactin). Another chemokine receptor, known as the Duffy antigen receptor for chemokines (DARC) which has been shown to bind to both CXC and CC chemokines. Yet, this is a non-signalling receptor, as no function has been observed on chemokine ligand binding. Each receptor is able to bind to more than one chemokine and each chemokine was shown to be able to use more than one receptor [38, 39, 40].

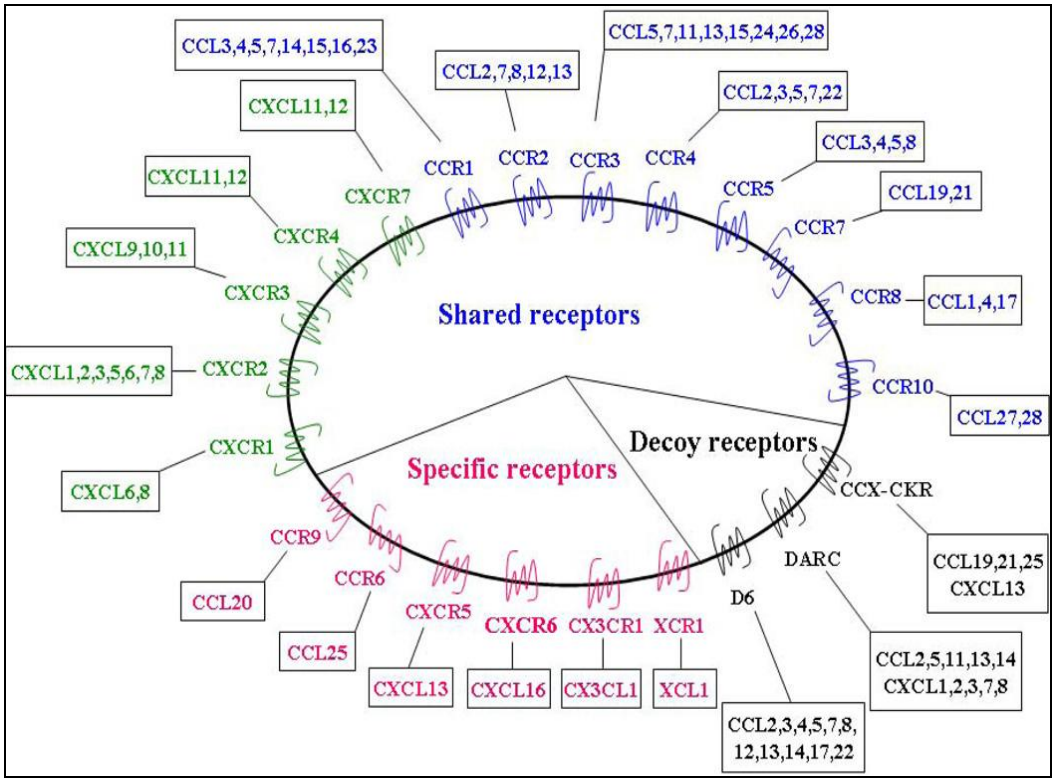

Fig 9- Chemokine family and their cognate receptors (some chemokines may bind other receptors) [40]

1.4.4 Chemokine receptor signalling

Both chemokine and chemokine receptor signalling have been described as modulators of metastasis and anoikis in several cancers, respectiely [41].

The specific effects of chemokines on their target cells are mediated by members of a family of 7-transmembrane-domain, G-protein-coupled receptors that elicit intracellular signalling primarily through Gαi heterotrimeric protein complexes.

Chemokine receptors are activated by heterotrimeric protein complex functioning through exchange of guanosine diphosphate (GDP) for guanosine triphosphate (GTP) leading to the dissociation of the Gα and Gβγ subunits to establish two unique signalling circuits. The Gα subunit thus can inhibit adenylcyclase activity and formation of the second messenger cAMP. The process on intracellular calicum adoption is steered by the Gβγ dimeric complex that causes phospholipase C (PLC) activation and formation of both inositol triphospate (IP3) and diacylglyceral (DAG), resulting in mobilization of intracellular calcium (Fig10). The G protein subunit propel likewise other pathways such as mitogen activated protein kinase (MAPK) and PI3K pathways [42,43].

Chemotaxis is partly coordinated through activation of focal adhesion proteins and Rho family members such as Rho and Rac. CXC1L2 mediated activation of Rho take a leading role for polarizing acting filaments which is essential for intestinal epithelial cell migration [44].

Activation and desensitization of chemokine receptor signalling typically occurs through intracellular phosphorylation of serine residues at the C-terminus by G-protein receptor kinases (GRKs) after ligand binding [45]. This process is typically mediated through β arrestin and clatherin dependent endocytosis [46].

A new family of chemokine receptors is called scavenger or a typical receptors. These receptors include members D6 [47] and DARC [48]. They tend to be promiscuous and bind several chemokine ligands.

Yet, chemokine binding to these receptors does not entice cellular chemotaxis or activate calcium flux [49].

(Fig10). Represents some of the key signalling pathways throught to be involved in CXCR4 signal transduction. The binding of chemokine CXCL12 to chemokine receptor CXCR4 initiates divergent signalling pathway downstream of ligand binding, which can result in a variety of responses including chemotaxis, cell proliferation, and survival, increase intracellular calcium and gene transcription [50].

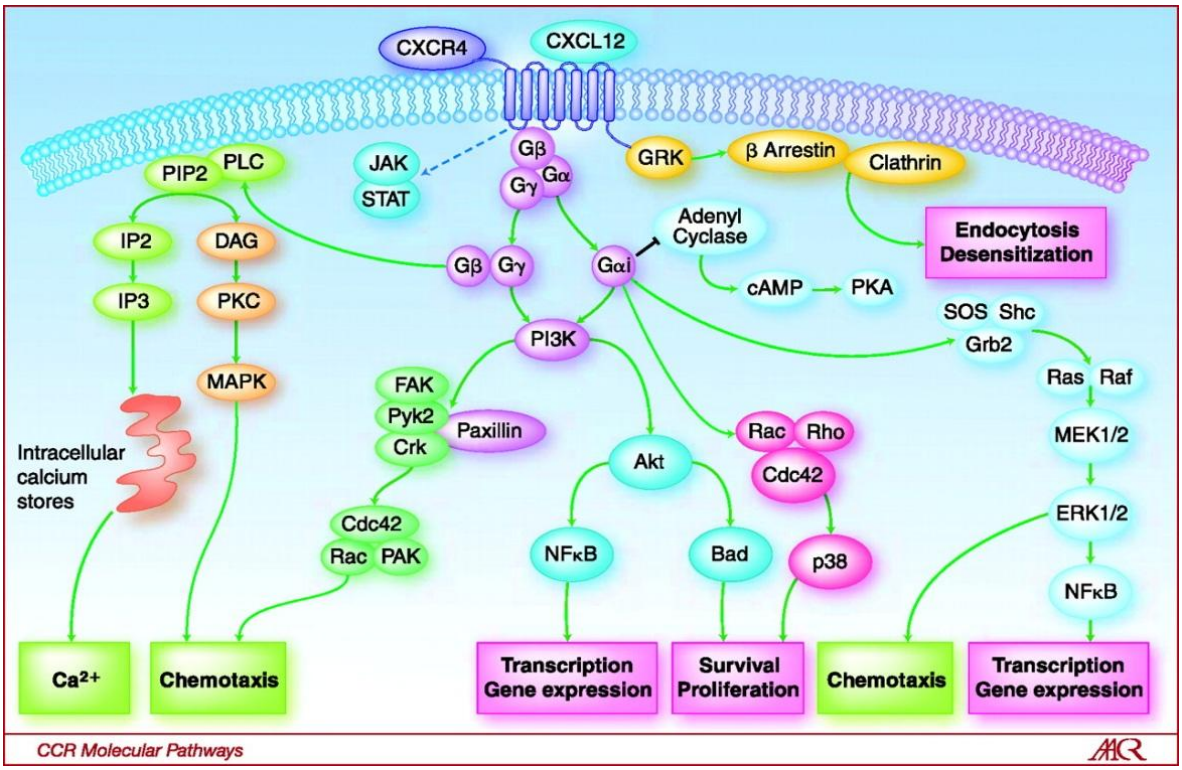

Fig10- A schematic of the CXCL12/CXCR4 intracellular signal transduction pathways [50].

1.5 CXCL12 and its receptors

Stromal cell-derived factor 1 (SDF-1) or CXCL12, also known as Pre-B-cell growth stimulating factor (PBSF), is a small cytokine belonging to the CXC subfamily [51]. The receptors for chemokine CXCL12 are CXCR4 and CXCR7.

1.5.1 CXCR4

CXCR4 is seven-span transmembrane G-protein-coupled receptor (GPCRs) that binds the ligand CXCL12. CXCR4 was initially discovered as an orphan receptor called fusin or LESTR. It serves as a co-receptor for entry of T-tropic HIV viruses that target $CD4^+$ T cells [40].

CXCR4 is widely expressed on many cell types, including the immune and the central nervous systems, and can mediate migration of resting leukocytes and hematopoietic progenitors in response to CXCL12 functioning in a number of physiological processes [40]. CXCR4 is over-expressed in many human cancers, including breast cancer, ovarian cancer, melanoma, and prostate cancer (PCa) [52].

It is known from several studies that the interaction between SDF-I and its receptor CXCR4 promotes angiogenesis and the migration of cancer cells into the metastatic sites in many cancers like breast [53], lung [54], ovarian [55], renal [56], prostate [57], neuroblasoma [58], These CXCR4 expressing tumors preferentially spread to tissues that express CXCL12/SDF-1 highly, including lung, liver, lymph nodes and bone marrow [59].

1.5.2 CXCR7/RDC-1

CXCL12 binds to another seven transmembrane span receptor named CXCR7 (or RDC-1) [60]. CXCR7 is expressed in a number of cells including endothelial cells, T lymophocytes, dendritic cells, B cells, chondrocytes, and endometrial stromal cells [61]. CXCR7 is also expressed in tumor cells that can produce a proliferative effect. Thus, SDF-1 can modulate the migrational capacity of tumor cells and CXCR7 can enhance tumor growth [62].

1.6 Biology of SDF-1

1.6 .1 SDF-1 (CXCL12) and human tumor microenviroment

The chemokine CXCL12 (SDF-1) is a small protein (8-14 KDa) that regulates leukocyte trafficking and is variably expressed in a number of normal and cancer tissues such as BM, heart, liver, kidney, thymus, spleen, skeletal muscle and brain [51,63].
Many essential biological processes are regulated by the chemokine stromal cell derived factor-1(CXCL12/SDF-I), including cardiac and neuronal development, stem cell motility, neovascularization and tumorgenesis [64-68].

It is known from several studies that multiple modes of action are implicated in CXCL12-mediated tumor pathogenesis; CXCL12 promotes tumor growth and malignancy, enhances tumor angiogenesis, participates in tumor metastasis, fosters an immunosuppressive network within the tumor microenvironment and mediates tumor cell adhesion, migration and invasion, myeloid dendritic cells (mDC) and plasmacytoid dendritic cells (pDC) (Fig11).

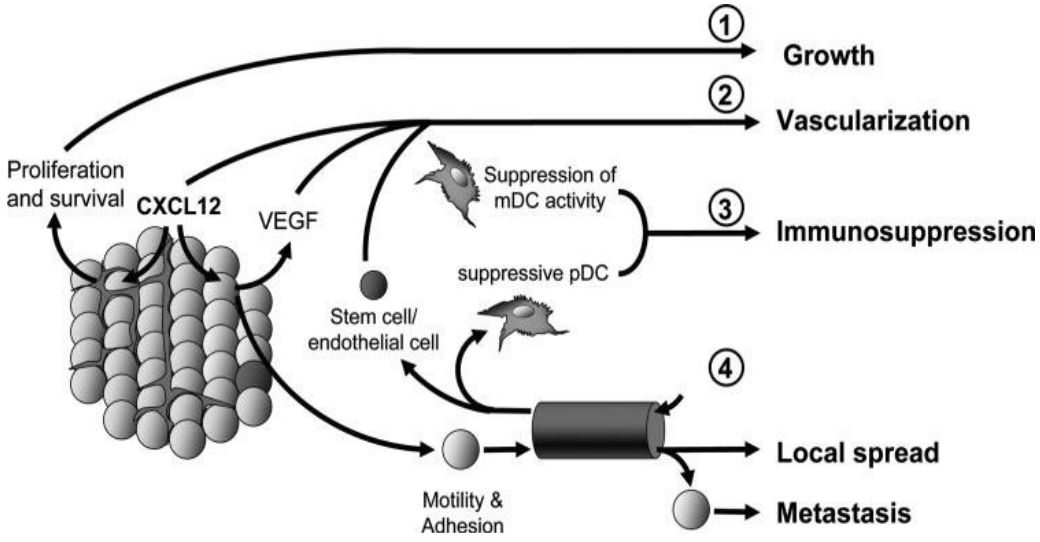

Fig 11- CXCL12 plays multiple roles in tumor biology [69]

1.6.2 Molecular Structure of SDF-1 Splice variants

SDF-1 proteins are found in living organisma as monomers, being expressed in six isoforms (SDF-1 alpha, beta, gamma, delta, epsilon und theta) all sharing the same first three exons except exon 4 in each case stems from different regions of the human SDF-1 gene [70]. The CXCL12 gene is mapped on chromosome 10 whereas most of the other genes encoding CXC chemokines are situated on chromosome 4. Fig12 shows the exon/intron structures of those different SDF-1 isoforms [71, 72, 73].

The analysis of the genomic structure of SDF-1 in human and mouse revealed two isoforms, SDF-1α and SDF-1β. These two isoforms arise from a single gene through alternative splicing [72, 73, 74].
The functional diversity and differential proteolytic processing abilities of these two isoforms are well investigated and characterized: SDF-1α is 270 base-pairs long and encodes a 89 amino acid protein; likewise SDF-1β is 282 base-pairs long and encodes a 93 amino acid protein, of which the first 89 amino acids are identical to that of SDF-1α except for the last four amino acids of SDF-1β, which are absent in SDF-1α [70,71,72,73].

It was later revealed that a third splice variant SDF-1γ, 361 base-pairs long, encodes a 119 amino acid proteins. The first three exons of SDF-1γ are identical with SDF-1α and SDF-1β but use a different fourth exon [73]. The fourth exon is located 3200 bp downstream from the third exon on the SDF-1 gene locus and is situated between the third exon and the fourth exon of SDF-1β. It has a polyadenylation signal sequence and a poly-A stretch. Thus, human SDF-1γ may represent the human ortholog of rat SDF-1γ. Yet, human SDF-1γ mRNA has a much shorter 3′ untranslated region (UTR). SDF-1γ is expressed in adult rat brain, heart and lung with the strongest expression observed in heart [70, 75].

SDF-1δ is a fourth alternative splicing isoform, 423 base-pairs long and encodes an 140 amino acid proteins. It is alternatively spliced in the last codon of the SDF-1α open reading frame (ORF), leading to a 731 base-pair intron, with the terminal exon of SDF-1α being split into two. Human SDF-1δ shares the same 3′ UTR and polyadenylation signal sequence as human SDF-1α. The deduced AA sequence of human SDF-1δ predicts a peptide of 140 AA. The first 89 AA are identical with SDF-1α, the C-terminal additional 51 AA are unique [73].

Human SDF-1ε cDNA is a fifth splice isoform, 273 base-pairs long, and human SDF-1ϕ cDNA is a sixth splice isoform 303 base-pairs long, encoding a 90 amino acid protein and a SDF-1ϕ 100 amino acid protein respectively [73].

The first three exons of SDF-1ε and SDF-1ϕ are identical with SDF-1β and SDF-1γ isoforms. The SDF-1ε and SDF-1ϕ mRNAs have very similar genomic organization, with the fourth exon located approximately 81 kilobase-pairs downstream form the third exon. SDF-1ε and SDF-1ϕ differ by 7 bp in the ORF of the fourth exon via the use of an alternative splicesome acceptor site. [73] .

```
                  *        20         *        40         *        60
SDF-1α  : MNAKVVVVLVLVLTALCLSDGKPVSLSYRCPCRFFESHVARANVKHLKILNTPNCALQIV :  60
SDF-1β  : MNAKVVVVLVLVLTALCLSDGKPVSLSYRCPCRFFESHVARANVKHLKILNTPNCALQIV :  60
SDF-1γ  : MNAKVVVVLVLVLTALCLSDGKPVSLSYRCPCRFFESHVARANVKHLKILNTPNCALQIV :  60
SDF-1δ  : MNAKVVVVLVLVLTALCLSDGKPVSLSYRCPCRFFESHVARANVKHLKILNTPNCALQIV :  60
SDF-1ε  : MNAKVVVVLVLVLTALCLSDGKPVSLSYRCPCRFFESHVARANVKHLKILNTPNCALQIV :  60
SDF-1ϕ  : MNAKVVVVLVLVLTALCLSDGKPVSLSYRCPCRFFESHVARANVKHLKILNTPNCALQIV :  60

                  *        80         *       100         *       120
SDF-1α  : ARLKNNNRQVCIDPKLKWIQEYLEKALNK*------------------------------ :  89
SDF-1β  : ARLKNNNRQVCIDPKLKWIQEYLEKALNKRFKM*-------------------------- :  93
SDF-1γ  : ARLKNNNRQVCIDPKLKWIQEYLEKALNKGRREEKVGKKEKIGKKKRQKKRKAAQKRKN* : 119
SDF-1δ  : ARLKNNNRQVCIDPKLKWIQEYLEKALNNLISAAPAGKRVIAGARALHPSPPRACPTARA : 120
SDF-1ε  : ARLKNNNRQVCIDPKLKWIQEYLEKALNNC*----------------------------- :  90
SDF-1ε  : ARLKNNNRQVCIDPKLKWIQEYLEKALNKIWLYGNAETSR*------------------- : 100

                  *       140
SDF-1α  : ---------------------- :   -
SDF-1β  : ---------------------- :   -
SDF-1γ  : ---------------------- :   -
SDF-1δ  : LCEIRLWPPPEWSWPSPGDV* : 140
SDF-1ε  : ---------------------- :   -
SDF-1ϕ  : ---------------------- :   -
```

Fig 12- Genomic structures of human SDF-1 splice variants [71]

Fig (13) Predicted amino acid sequences of CXCL12 splice variants. Capital letters indicate amino acids conserved between the splice variants. Lowercase letters indicate divergent amino acids at the carboxyl termini of the splice variants. The underlined sequences are BBXB domains. The numbers to the right indicate the number of amino acids in each variant.

All splice sites conform to the predicted consensus motif for splice in some recognition sites (GU for donor sites and AG for acceptor sites). The predicted amino acid sequences of all human SDF-1 isoforms are aligned and compared in Fig.13 [73, 76].

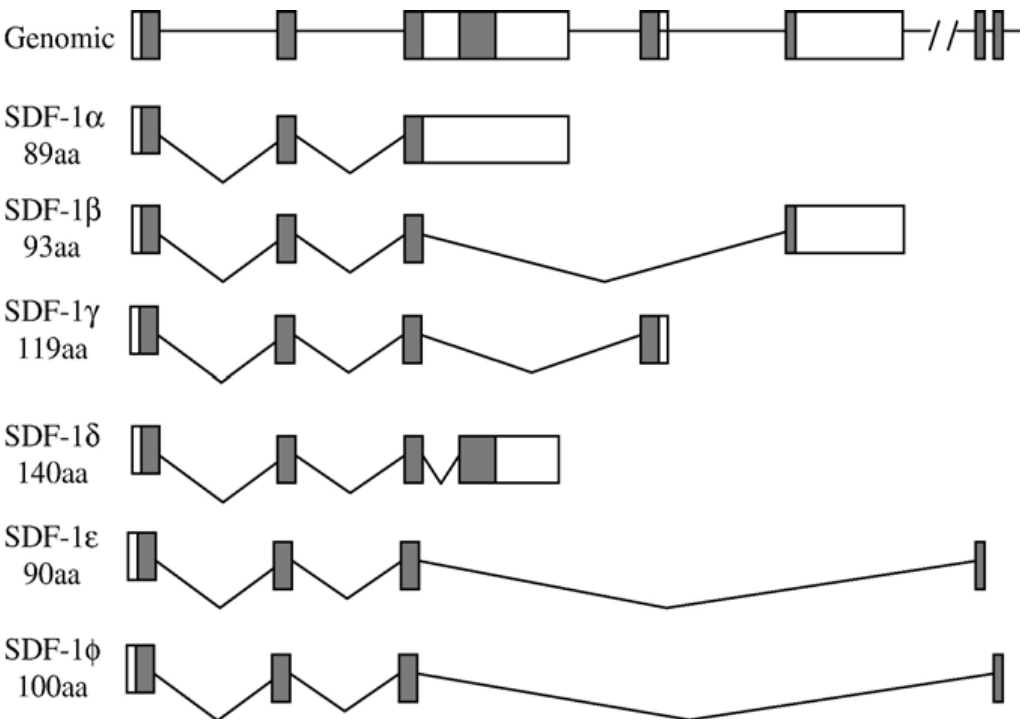

Fig 13- The predicted amino acid sequences of human SDF-1 splice variants [73].

1.7 Objective of the study

The chemokine CXCL12 and its receptor CXCR4 have been implicated in cancer metastasis of many different neoplasms. The major function of this chemokine is to regulate hematopoietic cell trafficking and secondary lymphoid tissue architecture. The potential role of the novel CXCL12 splice variants (SDF-1α, SDF-1β, SDF-1γ, SDF-1δ**,** SDF-1ε and SDF-1θ) axis in cancer development and function is not well understood. Besides that, the pathophysiological role of CXCL12 variants in colorectal cancer progression is needed to be elucidated. The present study aimed to determine the role of the novel CXCL12 variants (SDF-1α, SDF-1β, SDF-1γ, SDF-1δ**,** SDF-1ε and SDF-1θ) in the developmental processes of tumor formation, immune invasion and pathophysiological mechanisms of carcinogenesis. This prompted us to investigate expression, signal transduction and specific functions of the chemokine CXCL12 splice variants in CRC cells by using different experimental systems, animal's models, human in vitro systems and biopsy material derived from colorectal carcinoma patients.

2 Materials and Methods

2.1 Chemical materials

Product	Manufacturer
Albumin Fraction	Carl Roth GmbH+Co.KG, Germany
AMD3100	Sigma , Germany
Anti-biotic-Anti mycotic	Invitrogen , U.S.A.
CellTiter-Glo	Promega, U.S.A.
Dimethylsulfoxid	Carl Roth GmbH+Co.KG, Germany
D PBS Puffer	Invitrogen, U.S.A.
Fetal Bovine Serum	Invitrogen, U.S.A.
Fibronectin,Human	Invitrogen, U.S.A.
FUJI Medical X-Ray Film, Super RX, 18x24	FUJI Film, Japan
Geneticin (G418)	Invitrogen, U.S.A.
Lipofectamine2000	Invitrogen, U.S.A.
Loading Dye solution	Fermentas, U.S.A.
NuPAGE® 10% Bis-Tris-Gel 1,0 mm,12well	Invitrogen, U.S.A.
NuPAGE® MES SDS Running Buffer	Invitrogen, U.S.A.
NuPAGE® Tris-Acetat SDS Running Buffer	Invitrogen, U.S.A.
Propidium iodide solution	Sigma-Aldrich,Germany
RNeasy Mini-Kit	Qiagen, Germany
Roti-Block Lösung	Carl Roth GmbH+Co.KG, Germany
Roti-Blot A Anodenbuffer 10x	Carl Roth GmbH+Co.KG, Germany
Roti-Blot K Kathodenbuffer 10x	Carl Roth GmbH+Co.KG, Germany
Roti-Lumin	Carl Roth GmbH+Co.KG, Germany

Product	Manufacturer
Roti-PVDF	Carl Roth GmbH+Co.KG, Germany
RPMI 1640	Invitrogen, U.S.A.
Taq PCR Core Kit	Qiagen, Germany
Triton X-100	Carl Roth GmbH+Co.KG, Germany
Trypsin-EDTA	PAA Laboratories GmbH, Austria
Trypan Blue Solution 0.4%	Sigma , Germany
Haemotoxylin	Merck , Germany
100bpDNA Ladder	Invitrogen, U.S.A.
50bpDNA Ladder	Invitrogen, U.S.A.

Table 7- List of Chemical materials which have used in completion of this study

2.1.2 Devices

Device	Manufacturer
AE21 microscope	Motic, Germany
Bio photometer	Eppendorf, Germany
Bio fuge fresco	Heraeus, Germany
Biological Safety Cabinets	Nuaire, Germany
Curix 60	AGFA, Belgium
Duomax 1030	Heidolph, Germany
Electrophoresis Power Supply (EV231)	Consort, Germany
Fastblot B32	Biometra, Germany
FACS Vantage SE	BD, Germany
FluroScan	Thermo Fisher Scientifc, Germany
Gel Doc EZ Imager	BioRAD, Germany
Rotanta/RP	Hettich Zentrifugen, Germany
Thermo cycler	PTC-200, Germany
Universal 320R	Hettich Zentrifugen, Germany
Water bath	Köttermann, Germany
X-Cell Surelock Gelkammer	Invitrogen, U.S.A.
X-Omatic cassette	Kodak, Germany

Table 8- List of Devices which have used in completion of this study

2.1.3 Antibodies

2.1.3.1 Primary Antibody

Antibody	Immunogenic origin	Dilution	Reference
AKT	rabbit, Monoclonal	1:1000	Cell Signaling, MA,USA
P-AKT	rabbit, polyclonal (Thr 450)	1:1000	Cell Signaling, MA,USA
MEK1/2	rabbit, polyclonal	1:1000	Cell Signaling, MA,USA
P- MEK1/2	rabbit, polyclonal (Ser 217/221)	1:1000	Cell Signaling, MA,USA
P38 MAP Kinase	rabbit, polyclonal	1:500	Cell Signaling, MA,USA
P- P38 MAP Kinase	rabbit, polyclonal (Thr180/Tyr182)	1:500	Cell Signaling, MA,USA
SAPK/JNK	rabbit, polyclonal	1:500	Cell Signaling, MA,USA
P- SAPK/JNK	rabbit, polyclnal (Thr183/Tyr185)	1:500	Cell Signaling, MA,USA
TUBULIN	rabbit, polyclonal	1:1000	Cell Signaling, MA,USA

Table 9- List of Primary antibodies which have used in completion of this study

2.1.3.2 Secondary Antibody

Antibody	dilution	reference
Goat anti-mouse	1:10.000	SantaCruz Biotechnology ,USA
Goat anti-rabbit	1:10.000	SantaCruz Biotechnology,USA

Table 10- List of Secondary antibodies which have used in completion of this study

2.1.4 Cell lines

Cell line	origin	reference
SW-480 SW-620	Human colorectal adenocarcinoma Human colorectal adenocarcinoma	ATCC, USA ATCC, USA
D05 D14	Human melanoma cells Human melanoma cells	ATCC, USA ATCC, USA

Table11- List of Cell lines which have used in completion of this study

2.1.5 Plasmids & Vector

Plasmids & Vector	Manufacturer
Plasmid SDFI alpha	Intel chon, Germany
Plasmid SDFI beta	Intel chon, Germany
Plasmid SDFI gamma	Intel chon, Germany
Plasmid SDFI delta	Intel chon, Germany
Plasmid SDFI epsilon	Intel chon, Germany
Plasmid SDFI theta	Intel chon, Germany
NT-GFP FusionTopo TA Expression Kit.	Invitrogen, U.S.A.

Table12- List of Plasmids & Vector which have used in completion of this study

2.1.6 Primers

The primers for DNA sequencing of all SDF1 plasmids were synthesized by the company Eurofins MWG operon, Germany and delivered in a lyophilized state. The lyophilized oligonucleotides were diluted in water to 50 μM or 50 pmol/μl concentrations and stored at -20 °C for long term usage. The primers diluted to final working concentration of 5μM for PCR reactions.

2.2 Molecular Biological Methods

2.2.1 Tumor cell lines and culture conditions

The human colorectal adenocarcinoma cell line SW480 was initially isolated from the tissue of a 50-year-old Caucasian. The SW620 cell line was established from a lymph node metastasis taken from the same patient one year later.
The melanoma cell lines D05 and D14 were kindly provided by the laboratory of Prof. Wölfel (Department of Tumor Immunological, III Medical Clinic and Polyclinic).
Tumor cell lines were grown in RPMI-1640 medium supplemented with 10% fetal calf serum, 100 Units/ml penicillin, 100 mg/ml streptomycin at 5% CO2 in a 37 °C humidified atmosphere. All cell culture work was performed aseptic in a sterile hood (Heraeus, Laminair). The cells were passaged regularly and the media was changed every other day. In addition, the cultures were checked routinely for infection with mycoplasma. The cells were frozen in a media containing 90% FCS and 10% DMSO for long term storage in liquid nitrogen. A coulter counter (Beckton Dickinson) was used for counting the cells. All cell lines were purchased from the American Type Culture Collection (ATCC).

2.3 Polymerase Chain Reaction (PCR)

The polymerase chain reaction (PCR) technique was described in the mid 1980's by Kary Mullis and is used to amplify specific DNA sequences [77]. PCR is based on thermal cycling where a cycle involves three steps**:** (1) denaturation of DNA/amp icons (PCR copies), (2) annealing of template and primers, (3) extension of DNA. Two sequence specific oligonucleotide primers are needed; one forward (P1) and one reverse (P2) to get the specific amplification of the DNA sequence of interest. The primers bind to denatured DNA. Copies of the DNA sequence are produced during extension in the presence of a heat-stable DNA polymerase and deoxynucleoside triphosphates (dNTPs) [78] (Fig14).

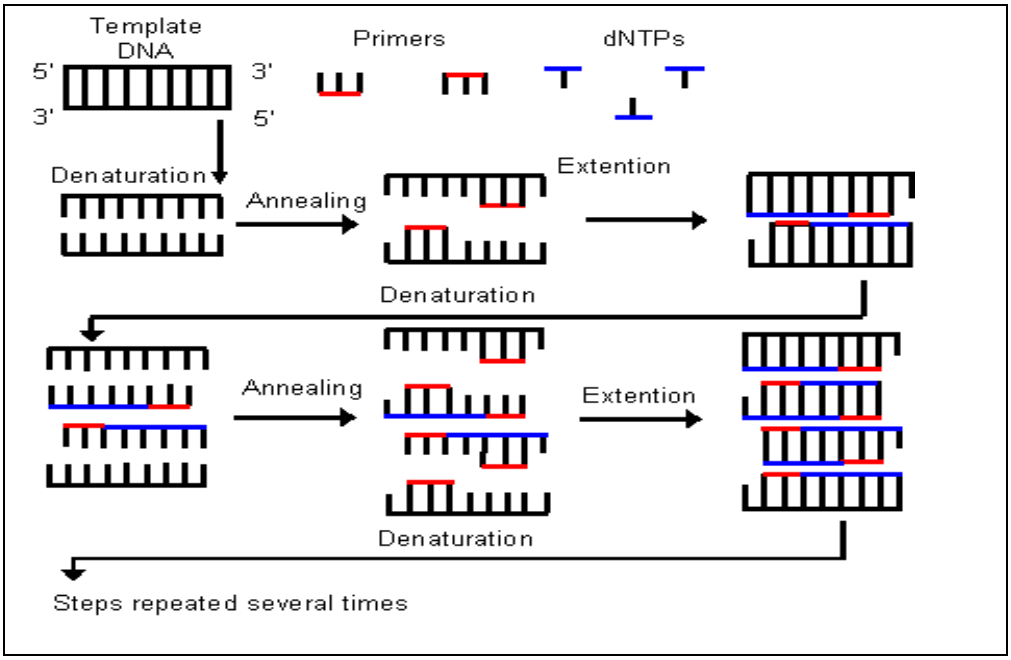

Fig 14- The polymerase chain reaction with denaturation of double stranded DNA followed by annealing with primers and extension [79]

2.3.1 Detection of CXCL12 gene polymorphism in CRC Patients by PCR-RFLP

The present study was conducted 73 CRC patients of all stages. The aim of this work was to study the CXCL12 polymorphisms at codon G801A by restriction fragment length polymorphism (PCR-RFLP) assay and to correlate them with the clinical presentation and tumor characteristics.

The PCR reaction for amplification of CXCL12 G801A gene was performed according to the method described by Dimberg et a l [80].

The master mix typically contained all of the components needed for PCR except the template DNA, according to (Table 13).

Master mix	**Volume**
10x PCR Buffer	2.5µl
H_20 Distilled water	21.375
$dNTP_S$	0.5µl
Primer forward	0.25 µl
Primer backward	0.25 µl
Taq polymerase	0.125 µl
Template DNA	0.5µl(100ng)
Total volume	**25.5 µl**

Table 13-Reaction components for PCR

The primers used for CXCL12 genotyping were as follows:

The CXCL12 forward primer, 5´- CAGTCA ACC TGG GCA AAG CC-´3. and

The CXCL12 reverse primer, 5´- AGCTTT GGT CCT GAG AGT CC-´3. Primers were synthesized commercially (Euro fins MWG operon, Germany). PCR reactions were carried out using an automated thermal cycler (Eppendorf, Germany).

The following standard protocol was adjusted to each specific application:

Temp	Time	Step
94°C	4 Min	Initial activation step
94°C	45 Sec	Denaturation
62.4°C	45 Sec	Annealing
72°C	1.30 Min	Extension
72°C	71.30 Min.	Final extension
4°C	15 Min	Indefinite
Number of cycles 35		

Table 14-Thermal Cycler Conditions for PCR

2.3.2 Separation of DNA on Agarose Gel Electrophoresis

Agarose gel electrophoresis was used to visualize the amplified products. 1-2% (w/v) agarose gels were used to separate the DNA molecules depending on their molecular size. The DNA samples were mixed with 0.1 volumes of 10x DNA loading buffer and loaded on agarose gel lanes and placed in the electrophoresis chamber. The gel electrophoresis chamber was filled with 1x TAE buffer and run at 90 V / 300 mA/ 150W for one hour. Gels were viewed on an UV Transilluminator. To visualize the DNA, the agarose gels contained 0.5 g / ml ethidium bromide and were irradiated under UV light transilluminator (wave length 312 nm). Size of DNA bands was estimated by comparison with a product size-marking DNA ladder (SM0373). Images were captured using the Gel Doc system (Quantity One software, Biorad, Germany). For the CXCL12 polymorphism, a 302- bp fragment was amplified.

2.3.3 Digestion of PCR product by specific restriction enzyme for detection of CXCL12 gene polymorphism

The restriction enzyme digestion was performed by incubating double-stranded DNA molecules with an appropriate amount of restriction enzyme in their respective buffer as recommended by the supplier at optimal reaction temperature.
After amplification, the PCR products (302 bp) were digested at 37°C for one hour with 1 µl MspI according toTable 15.

PCR Amplificate	15µl
PCR water	13µl
Tango buffer	2µl
MSPI Enzyme	1µl

Table 15- Reaction components for digestion

The digested products were visualized by electrophoresis on a 2% agarose gel (Oxoid Limited, Hampshire, UK) containing ethidium bromide (0.5 mg/ml).

2.3.4 Expression of CXCL12 Splice Variants in human colorectal carcinoma and human normal mucosa

The expression of CXCL12 splicing variants (alpha, beta, gamma, delta, epsilon, and theta) was analysed in 40 colorectal tumour and 20 human mucosa cDNA samples.
PCR reactions contained all of the components needed for PCR and the template cDNA from colorectal carcinoma and normal mucosa, as described in Table 16.

Master mix	**Volume**
10x PCR Buffer	2.5µl
H_20 Distilled water	21.375
$dNTP_S$	0.5µl
Primer forward	0.25 µl
Primer backward	0.25 µl
Taq polymerase	0.125 µl
Template DNA	0.5µl(100ng)
Total volume	**25.5 µl**

Table 16- Reaction components for PCR

In order to determine the expression patterns of the human SDF-1 isoforms in colorectal and mucosa tissues, we designed PCR primers (Table 17) that could detect each SDF-1 isoform specifically. We used beta-actin as control for our samples. PCR reactions were carried out using an automated thermal cycler (Eppendorf, Germany).

Gene	Primer Sequence	Temp.	Cycles
SDF1alpha	**for: 5'-ATGAACGCCAAGGTCGTGGTC-3'** **rev: 5'-AAGTGCTTACTTGTTTAAAGCTTTCTC -3'**	60.8°C	38
SDF1beta	**for: 5'-ATGAACGCCAAGGTCGTGGTC-3'** **rev: 5'-ACCCTCTCACATCTTGAACCTCTT -3'**	61.3°C	38
SDF1gamma	**for: 5'-ATGAACGCCAAGGTCGTGGTC-3'** **rev: 5'-AGATAACTAGTTTTTCCTTTTCTGGGC -3'**	61.2°C	38
SDF1delta	**for: 5'-ATGAACGCCAAGGTCGTGGTC-3'** **rev: 5'-ACACCATTACACATCCCCAGGAGA -3'**	61.8°C	38
SDF1epsilon	**for: 5'-CGCCATGAACGCCAAGGTCGTGGTCG -3'** **rev: 5'-CTAATTACTTCAGTGGCAGATCATAC -3'**	62°C	38
SDF1theta	**for: 5'-CGCCATGAACGCCAAGGTCGTGGTCG -3'** **rev: 5'-CACACTAATTACTTCAGTGGCAGATC -3'**	62°C	38
B-actin	**for: 5'-GAGAAGCTGTGCTACGTCGCCC -3'** **rev: 5'-TGCTCGCTCCAACCGACTGCTG -3'**	58°C	20

Table 17- Sequences of primers used in PCR assay

2.4 RNA Isolation and Semiquantitative Reverse Transcription-PCR

2.4.1 RNA extraction from Cell lines

RNA isolation was performed using the RNeasy Mini Kit according to the manufacturer's recommendations (Qiagen, Germany).

Cells were grown to 70-80% confluence in a cell culture flask and were harvested by trypsinisation and subsequently lysed with a mixture of B-mercaptoethanol and RLT buffer (guanidine isothiocynate GITC-containing lysis buffer). The latter is highly denaturing and immediately inactivates RNeases to ensure isolation of intact RNA. The cell lysate was homogenized using a QIA shredder spin Column. Homogenization was necessary to reduce the viscosity of the cell lysates produced by disruption. Incomplete homogenization results in inefficient binding of RNA to the RNeasy membrane and therefore significantly reduced

yields. An equal volume of 70% ethanol was then added to the homogenized lysate to ensure selective binding of RNA onto the silica based RNeasy spin column and the sample was loaded onto the RNeasy column. A wash with RW1 buffer followed by two washes with RPE buffer to removed sheared genomic DNA and protein contaminants. RNA was eluated from the RNeasy spin column with 30 µl DEPC-treated water and recovered by centrifugation. RNA was stored at -80°C.

RNA concentrations were measured by UV Biophotometer (Eppendorf). 1µl of eluted RNA was diluted in 1:100 (W/L) sterile water. Added to a microcuvette it was blanked with water.

2.4.2 Reverse transcription PCR (RT-PCR)

RT is a techinique used to generate complementary DNA (cDNA) from an RNA template [81, 82]. We mainly used RT- PCR which is a method to quantify the expression of specific genes. The principle is the same as for PCR. However, in a first separate step mRNA is transformed to cDNA. The RNA strand is converted to cDNA by the use of the enzyme reverse transcriptase and oligo-dT primers that are mRNA selective by binding to the poly A-tails. Primers are designed to generate products spanning over exon-exon boundaries as a second step to ensure that it is only cDNA and not genomic DNA in the PCR. The RT-PCR conditions were optimised and performed according to general rules.
The master mix typically contains all of the components needed for PCR except the template RNA, according to Table 18.

Master mix	Volume
10x RT-Buffer	2µl
dNTP Mix	2µl
Oligo-dt primer	0.3µl
Reverse Transcriptase	1 µl
RNaisn(RNase inhibitor)	0.25 µl
dH20(RNase-free water)	XµL
Template RNA	2µg in 20 µl
Total volume	**20 µl**

Table18- Reaction components for Reverse Transcription

The following Standard Protocol was adjusted to each specific application

Temp	Time
37°C	1h
94°C	3 min
4°C	1h

Table 19-Thermal Cycler Conditions for RT-PCR

2.5 Transfection

2.5.1 Transfection of Colon carcinoma cell line (SW480) and Melanoma cell line (D05) with plasmid SDFI isoforms using Lipofectamine 2000

Transfection: is the process of introducing nucleic acids into cells by non-viral methods [83]. The goal of transfection is to isolate individual stable clones containing transfected DNA that have integrated into the cellular genome [84].

2.5.2 Transfection protocol

5 x 10^5 cells were seeded in 2 ml of RPMI1640 medium containing 10% FCS in six well plates 24 h before transfection aiming to achieve 80-90% confluency. For each transfection reaction, 1µg of Plasmid SDFI (pcDNA3.1/NT-GFP-SDF-I) or of Vector (pcDNA3.1/NT-GFP) was diluted in a 50 µl of RPMI1640 medium (serum-free) and gently mixed. 10µl from Lipofectamine 2000 were diluted in 50 µl of RPMI1640 medium serum-free. Boths were incubated for 5 minutes at room temperature.

Plasmid&Vector	DNA amount	Lipofectamine2000 amount
pcDNA3.1/NT-GFP-SDF-1- alpha	1µg	10-15µl
pcDNA3.1/NT-GFP-SDF-1-beta	1µg	10-15µl
pcDNA3.1/NT-GFP-SDF-1-gamma	1µg	10-15µl
pcDNA3.1/NT-GFP-SDF-1-delta	1µg	10-15µl
pcDNA3.1/NT-GFP-SDF-1-epsilon	1µg	10-15µl
pcDNA3.1/NT-GFP-SDF-1-theta	1µg	10-15µl
pcDNA3.1/NT-GFP-TOPO	1µg	10-15µl

Table 20- The constructs used in transfection experiment

After incubation, the diluted plasmid was mixed with the diluted Lipofectamine 2000 (total volume 100 µl). It was mixed gently and incubated for 20-45 minutes at room temperature to allow the DNA-Lipofectamine 2000 complexes to form.
100 µl of DNA-Lipofectamine 2000 complexes were added to each well containing cells and medium. They were gently mixed by rocking the plate back and forth.
The cells were incubated at 37°C in a CO2 incubator for 24-48 hours until they were ready to assay for transgene expression. However, growth medium was replaced after 4-6 hours without loss of transfection activity. Stable plasmid integration was selected using G418.

Green Fluorescent Protein (GFP), an inherently fluorescent protein was used to determine transfection efficiency (percentage of transfected cells in the population) either visually by fluorescence microscopy or quantitatively by flowcytometry.

2.5.3 Stable Transfection

2.5.3.1 Selection of Stably Transfected Cells

After cells were transfected, selection of positive transfected cells occurred with the antibiotic G418 (Geneticin), used as a selective drug to kill untransfected cell. The effective concentration of G418 varies with the cell type, growth concentration, cells metabolic, rate and position in the cell cycle. We have used a concentration (700µg/ml) of antibiotic G418 with cell line SW480 and (500µg/ml) with cell line D05.

Antibiotic	Working Concentration	Stock Solution
G-418 or Geneticin	G-418 is used for initial selection at 500µg/ml with a range of 50–1,000µg/ml	50 mg/ml in either water or 100 mM HEPES (pH 7.3); the latter buffer helps maintain culture medium pH

Table 21- Antibiotic G418 used to select and maintain stable transfectants

Cells were harvested 24–72 hours post-transfection for studies designed to analyze transient expression of transfected gene SDF-1/CXCL12 and its splice variants e.g., isolation of RNA, Western blots assays and FACS analysis.

2.6 FACS Vantage (Fluorescence Activated cell sorting)

All samples contained about 10^{6-7} cells per ml from SW480 and DO5 transfected with SDFI isoforms and GFP. A negative control with no expression (native cells) was always used. Sorting medium contained 5% dissociation PBS buffer and not more than 0.2% serum (FCS). We filtered the cell suspension before sorting through a cell strainer cap in order to eliminate cell aggregates, which might lead to clogging of the nozzle. A collection tube with 3-5 ml medium containing up to 20% FCS serum was used to collect positive transfected cells.

2.7 Western blot

Western blotting (or immunoblotting), is an analytical method that involves the immobilization of proteins on the nitrocellulose membranes or PVDF [85]. Before detection by monoclonal or polyclonal antibodies, sample proteins are separated using SDS polyacrylamide gel electrophoresis (SDS-PAGE) providing information about molecular weight and the potential existence of different isoforms of the proteins under study [86].

RIPA cell lysis buffer 2x:

240 mM NaCl
100 mM Tris-HCL, pH 8,0
2% NP-40
0,2% SDS

Lysis buffer

2x RIPA-Puffer	1/2 of the approach
Protease-Inhibitor	50xconcentrated 1/50 of the approach
PMSF 100x concentrated	1/100 of the approach
NaF 25x concentrated	1/25 of the approach
Vanadat 1000x concentrated	1/1000 of the approach
DTT 1000xconcentrated	1/1000 of the approach
Benzoate 300U/ml	0,08 µl pro 100 µl Lysis puffer

Table 22- lysis buffer components used in western blot analysis

2.7.1 Samples preparation

10^6-10^7 cells (SW480 and DO5) were transfected with SDFI plasmids and pcDNA3.1/NT-GFP-TOPO vector as a negative control. For total protein extraction, cultured cells were trypsinized and resuspend in 105 µL lysis buffer. Cells were homogenized under ice to fragment the genomic DNA; cell debris was pelleted at 13,000 rpm for 30-minutes at 4ºC. The supernatant was transferred to a new tube. Protein is determined by Lowry program as follows**:** the samples were boiled in LSD buffer for 9 minutes at 95° C. For longer storage, the specimens were aliquots and frozen at -80°C. Protein samples were loaded for electrophoresis. Protein Ladder (Fermentas) was used to determine band size.

2.7.2 Western blot analysis

100 µg of protein were loaded on a 10% SDS-PAGE gel. The samples were run on the gel, until the blue marker reached the lower end of the gel.

After electrophoresis, the proteins were transferred to a sheet of special blotting paper called PVDF membrane. The membrane was washed with TPBS Puffer and blocked for 1 h at room temperature with Roti-block (blocking buffer).

Proteins (AKT/pAKT , MEK/pMEK , JNK/pJNK , P38/pP38 and Tubulin) were detected with specific primary antibodies, that were diluted in blocking buffer and incubated at 4 °C overnight with gentle agitation on a platform shaker. Secondary antibodies were diluted in TBS-T and incubated for 1 h at room temperature with gentle agitation. Table 23 summarizes the antibodies used.

Antibodies	Gel	Puffer
phospho AKT	10% Bis-TRIS-Gel	MES-Puffer
AKT	10% Bis-TRIS-Gel	MES-Puffer
phospho MEK	10% Bis-TRIS-Gel	MES-Puffer
MEK	10% Bis-TRIS-Gel	MES-Puffer
Phospho P38	10% Bis-TRIS-Gel	MES-Puffer
P38	10% Bis-TRIS-Gel	MES-Puffer
Phospho SAPK / JNK	10% Bis-TRIS-Gel	MES-Puffer
SAPK / JNK	10% Bis-TRIS-Gel	MES-Puffer
TUBULIN	10% Bis-TRIS-Gel	MES-Puffer

Table 23- List of Antibodies which have used in completion of this study

For visualisation, proteins bands were visualized by incubation of the membrane for one minute in chemi-luminescent with Roti-Lumin systems 1 and 2, a substrate that will luminesce, when exposed to the reporter on the secondary antibody. The light is then detected by a photographic film. The image is analyzed by densitometry, which evaluates the relative amount of protein staining and quantifies the results in terms of optical density. The membrane was exposed to the film for different time periods (for 1 sec to 30 min). When the membrane should be re-probed with another antibody, the bound antibodies were removed by stripping for one hour at 50°C. Each condition was performed in duplicates.

2.8 AMD3100

2.8.1 Structure of AMD3100

Plerixafor (AMD3100) is an immunostimulant used to mobilize hematopoietic stem cells (HSCs) in cancer patients and acts as an antagonist of the chemokine receptor CXCR4 and as allosteric agonist of the chemokine receptor CXCR7**.**The bicyclam AMD3100 was originally described as selective inhibitor of HIV-1and HIV-2 replication and it is known as a small synthetic inhibitor of the CXCR4 receptor for the chemokine SDF-1. Plerixafor is highly specific in its interaction with CXCR4 [87, 88].

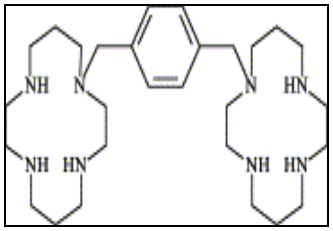

Fig15- Structure of AMD3100 originally termed [1,1′-[1,4-phenylene- bis(methylene)]-bis -1,4,8,11-tetra-azacyclotetradecane [88].

2.8.2 Western blot analysis after treatment with different concentration of AMD3100.

To study the effect of AMD3100 on SDFI isoforms in SW480 and D05, $5x10^5$ cells were seeded in a six-well culture plate. Cells were treated with different concentration of AMD3100 (0 µg/mL) (5 µg/mL) and (10µg/mL) and afterwards incubated overnight at 37°C. Cells were collected and analyses were performed as described.

2.9 Cell Proliferation

Cell proliferation, also known as cell growth, cell division, or cell replication is the basic process through which cells create new cells [89].

Degenerative diseases, such as arthritis, diabetes mellitus and cancer, occur from errors in cell replication and as a result of errors in DNA transcription during the cell cycle. Cancer in particular, is often the final result of a progressive accumulation of DNA transcription errors occurring in transformed cells, ultimately leading to uncontrolled cell proliferation and malignancy [89].

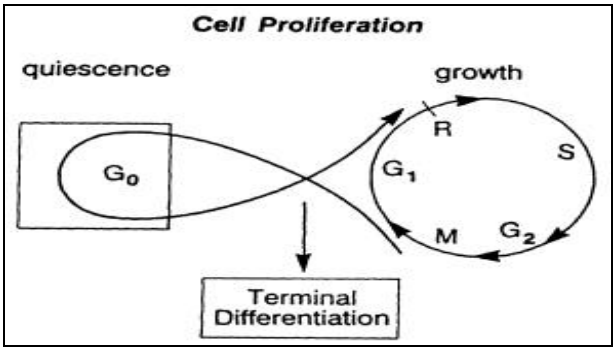

Fig 16- The cell cycle can be divided into two functional phases, S and M phases, and two preparatory phases, G1 and G2 [89].

2.9.1 Cell Proliferation assay

To study the effect of SDFI isoforms on tumor cell proliferation, 5000 cells (SW480, D05) were seeded in 100 µl RPMI medium supplemented with 10% FBS per well in a 96-well plate. On the first day, the first row was measured for all isoforms and control. Measurements were repeated every 24 h for 5 days. All measurements were performed in quadruplicate. Cell proliferation was determined by luminescence assay.

The CellTiter-Glo® Luminescent Cell Viability Assay is a homogeneous method to determine the number of viable cells in culture, based on quantitation of ATP, which signals the presence of metabolically active cells. 30µL CellTiter-GLO was added to each well containing 105 µL medium in a 96-well plate. Contents were carefully mixed and incubated for 2 minutes. They were measured after 12 minutes according to the recommendation of the manufacturer.

2.9.2 Cell Proliferation assay after treatment with different concentration from AMD3100

Cells (SW480, D05) were seeded in 96-well culture plates at a density of 5000 cells per well followed by the addition of AMD3100 in various concentration (0µg/ml) (5µg/ml) (10µg/ml). Then cells were incubated for 24 h. Cellular proliferation assay was performed as previously described.

2.10 Cell adhesion

Adhesion occurs between cells of a single type or heterophilic adhesion between cells of different types using cell adhesion molecules (CAMs) such as selectins, integrins, and cadherins.

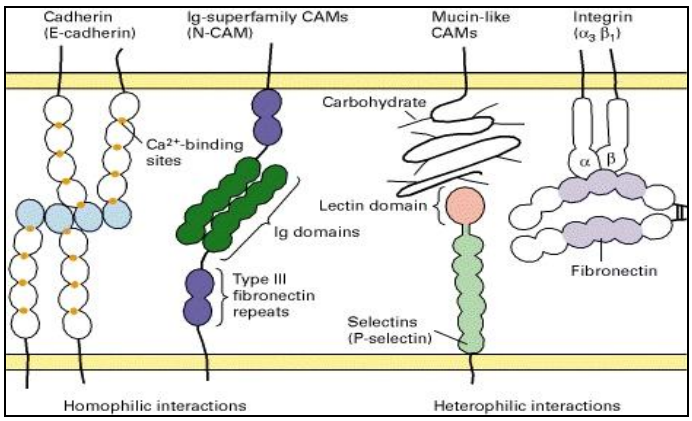

Fig 17- Major families of cell-adhesion molecules (CAMs) [90].

2.10.1 Cell adhesion assay

To evaluate the effect of SDFI isoforms on tumor cell adhesion. 35000 cells (SW480, D05) were seeded in 100 µl RPMI medium supplemented with 10% FBS per well in 96 well plates. Two rows for each SDFI isoforms and control were incubated at 37°C and 5% CO2 for 45 minute. The second row was gently washed 2x with 100µl PBS puffer. To determine cell adhesion activity after incubation luminescence assay was measured. The CellTiter-GLO Luminescent cell viability assay is similar to the luminescence assay in the proliferation assay.

2.11 Definition of migration and invasion

2.11.1 Cellular Migration assay

The most common method used to study cell motility in vitro was first described by Boyden S in 1962 [91]. Trans well® migration assays are one of the modifications of the Boyden Chamber system. Boyden Chamber assays consist of a cylindrical cell culture insert nested in the well of cell culture plate. The insert contains a polycarbonate membrane at the bottom with an 8µm pore size.

To study the effect of SDFI isoforms on the migration of tumor cells, SW480 and D05 were serum-starved for 4 hour. $4x10^4$ cells were seeded in 150µl RPMI medium supplemented with 2 % FCS on to the insert in the upper chamber of trans well culture plates and they migrated in vertical direction through the pores of the membrane into the lower chamber which contains 500µl RPMI medium supplemented with 20% FCS (high serum). Chambers were incubated for 24 hour at 37 °C and 5% CO2. After incubation, the amount of migrated cells in the lower chamber was determined by luminescence. 125 µL CellTiter-GLO was added to each Trans well®, contents were mixed and incubated for 2 minutes. 100 µl per wall were transferred to a 96-well plate, and measured after 12 minutes.

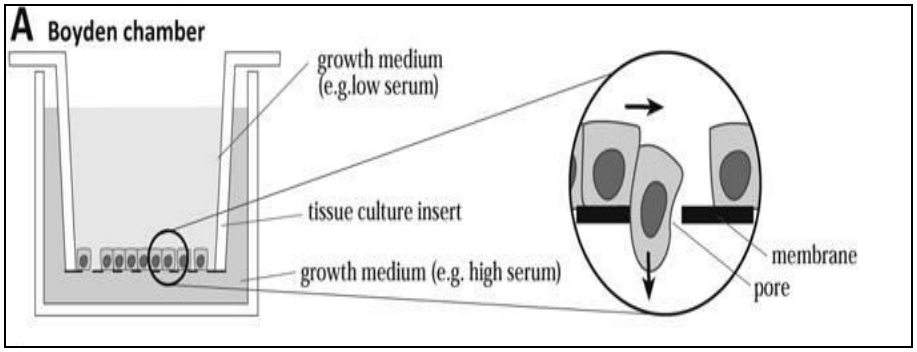

Fig18- Transwell migration assay (Boyden chamber assay). Migration of a cell through a pore in the membrane is depicted [92].

2.11.2 Invasion assay protocol

Cell invasion was quantified applying the Boyden chamber assay [91]. The principal technical setup of the transwell invasion assay is similar to the migration assay. Modifications of the Filter assay including variants where the porous membrane is coated with an extracellular matrix such as Fibronectin [92].

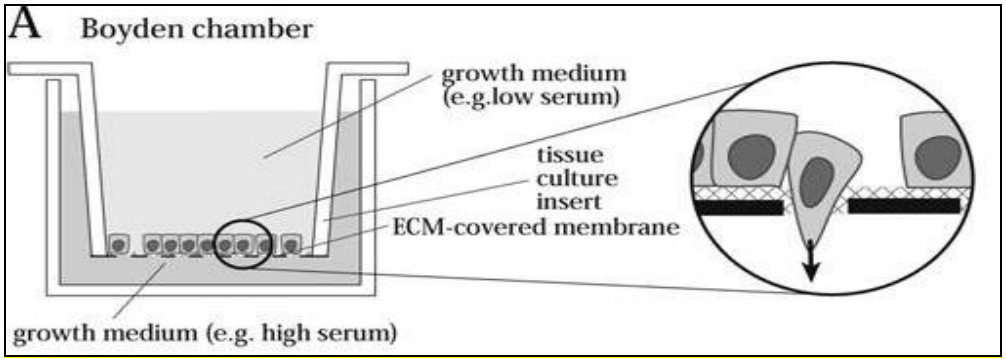

Fig19- Transwell invasion assay (Boyden chamber assay). The thin ECM coating (hatched areas), which occludes the pores of the filter is indicated [92].

Before seeding the cells into the top chamber the filter was coated with 20µg/ml Fibronectin overnight at 4°C.Then $4x10^4$ cells were seeded in 150µl RPMI medium supplemented with 2 % FCS onto the insert in the upper chamber of trans well culture plates and they migrated in vertical direction through the pores of the membrane into the lower chamber, which contains 500µl RPMI medium supplemented with 20% FCS (high serum). Chambers were incubated for 24 hour at 37°C and 5% CO2. After incubation, the amount of migrated cells in the lower chamber was determined by luminescence. 125 µL CellTiter-GLO was added to each lower chamber contents were mixed and incubated for 2 minutes. 100 µl per well were transferred to a 96-well plate, and measured after 12 minutes.

2.12 Animal experiments

2.12.1 Subcutaneous xenograft tumor system

42 animals were divided in 7 groups, SW480 tumor cells (1×10^6 and 3×10^6) were suspended in 0.2 ml pure RPMI 1640 medium and 1× PBS (1:1) and applied by subcutaneous injection into the right and left flank of 7–8-week-old female nod-SCID mice.

Inoculation of animals

SW480-GFP control	6 animals
SW480-SDF1 alpha	6 animals
SW480-SDF1 beta	6 animals
SW480-SDF1 gamma	6 animals
SW480-SDF1 delta	6 animals
SW480-SDF1 epsilon	6 animals
SW480-SDF1 theta	6 animals
Total	42 animals

The size of tumors was measured manually twice weekly. Tumors grew for 5 weeks. Thereafter, tumor nodules were excised and measured manually with a vernier micrometer.

2.13 Statistical Analysis

In order to assess the dependence of the SDF1 isoforms on sex, TNM and R we computed mean, standard deviation, minimum, maximum, median, and quartiles in subgroups. Results are displayed in box plots. Further we performed Wilcoxon tests if the explanatory variable had two levels, and Kruskal-Wallis tests, if there were more than two levels of the explanatory variable.

Associations among age, actin and the isoforms were described by Pearson correlation coefficient and displayed in scatterplot matrices.

All tests were performed with exploratory intention, associations with p-values ≤ 0.05 might warrant further consideration. Statistical analysis was performed using SAS 9.2 (c) 2002-2008 by SAS Institute Inc., (Cary, NC, USA).

3 RESULTS

3.1 CXCL12 Gene polymorphism

3.1.1 Patients characteristics

The CXCL12 gene is located at band q11 on chromosome 10 [93] and encodes for the six isoforms of human CXCL12/(SDF-1) known as SDF-1alpha, SDF-1beta, SDF-1gamma, SDF-1delta, SDF-1epsilon and SDF-1theta, which are the result of alternative splicing events of the same gene.
The present study included 73 CRC patients, comprised of 30 (41%) females and 43 (59%) males with an average age at diagnosis of 66.5 years. All tumors were classified according to the TNM classification.

The aim of this work was to study the CXCL12 coding gene polymorphisms at codon G801A by Restriction fragment length polymorphism (RFLP) assay in CRC patients and to correlate them with the clinical presentation and tumor characteristics Table (24).

We investigated the distribution of CXCL12-3`G801A genotypes in CRC patients. In order to examine the association of the CXCL12 gene variants with CRC, PCR products were cleaved and analysed. A typical agarose gel after the separation of PCR products is shown in Fig 20-A. CXCL12 polymorphism reveal a 302- bp fragment and a genotypic distribution of CXCL12 alleles after RFLP analysis are represented in Fig 20-B.

The GG homozygous genotypes of CXCL12 reveal two fragments of 202-bp and 100-bp size. The AA homozygous genotypes of CXCL12 produce only one band of 302 bp, whereas the GA heterozygous genotypes of CXCL12 produce 3 bands of 302, 202 and 100 bp size.

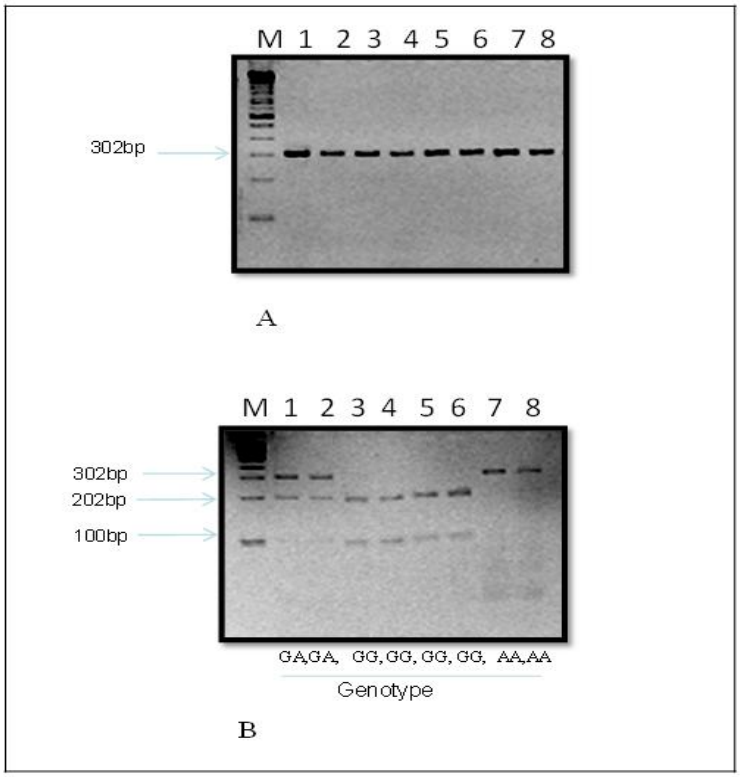

Fig 20- Agrose Gel showing
A-PCR Products for CXCL12 from different CRC patients
Lane M: Molekular Marker 100bp
B-RFLP analysis of CXCL12 gene polymorphism in CRC patients
Lane M: Molekular Marker 100bp
Lanes1, 2: mutated heterozygote GA genotype (100, 202 and 302 bps size)
Lanes 3, 4, 5, 6: wild type homozygote GG genotype (100 and 202 bps size)
Lanes7, 8: mutated homozygte AA genotype (302 bps size)

3.1.2 Genotype frequencies

CXCL12 amplicons were successfully detected in all patients. We compared the CXCL12 **(G/G)** allele with CXCL12 alleles **(G/A, A/A)** regarding gender, age, and clinical presentation. Table (24)

	G/G (%)	G/A A/A (%)	P value
Total number (%)	**50** (68.5%)	**23** (31.5%)	
Median age(y)	**66**	**67**	P= 0.035
Gender			
Male	**27** (54.0%)	**16** (69.5%)	P= 0.579
Female	**23** (46.0%)	**7** (30.5%)	**NS**
T status			
1 + 2	**11** (22.0%)	**7** (30.5%)	P= 0.067
3 + 4	**39** (78.0%)	**16**(69.5%)	
N status			
0	**12** (24.0%)	**6** (26.0%)	P= 0.364
1 + 2 + 3	**37** (76.0%)	**17**(74.0%)	**NS**
M status			
0	**33** (66.0%)	**13** (56.5%)	P= 0.509
+	**17** (34.0%)	**10** (43.5%)	**NS**
R status			
0	**32** (64.0%)	**11** (47.8%)	P= 0.395
+	**18** (36.0%)	**12** (52.2%)	**NS**
T status			
1 + 2 + 3	**39** (78.0%)	**13** (56.5%)	P= 0.214
4	**11**(22.0%)	**10** (43.5%)	**NS**

N-status could not be obtain from one patient

Table 24-Tumor characteristics in relation to CXCL12 genotypes

G/G homozygosity was observed in fifty CRC patients (68.5%) as compared to twenty three patients with G/A and A/A genotype (31.5 %).

Exept for local progression of the primary tumor, we found no correlation of CXCL12 Gene polymorphism rs1801157 with clinicopathological parameters.

CXCL12 Gene polymorphism rs1801157 revealed a trend towards local progression of the primary tumor as indicated by the T status. The frequency of GG genotype was somewhat higher in patients with stage 3 and 4 tumors (78.0%, P=0.067) as compared to GA/AA genotypes (69.5%).

3.2 CXCR4 and CXCL12 expression in colorectal carcinoma cell lines

In order to understand the role of CXCR4 and CXCL12 in the biology of colon cancer, we analysed five human colon cancer cell lines for the expression of CXCR4 and CXCL12. CXCR4 expression and transcription of human colorectal cancer cell lines varied from strong (Caco-2 , SW480, HT29) and intermediate (SW620) to weak (LS174T).

The RT-PCR analysis of CRC cell lines (Fig.21) suggests that CXCL12 is rather weakly expressed in CRC cell lines. This PT-PCR analysis demonstrated CXCL12 expression is present in only one of five CRC cell lines (Caco-2).

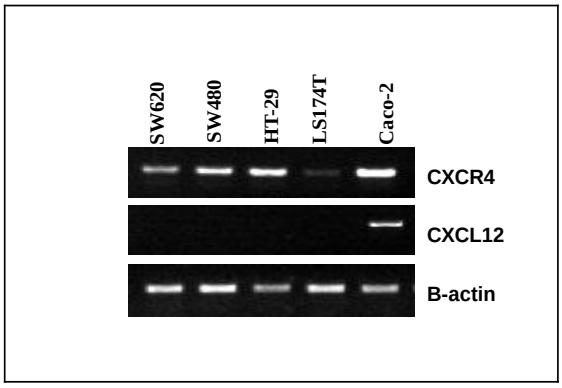

Fig 21- Expression and transcription profile of CXCR4 and CXCL12 in diverse human colorectal cancer cell lines

3.3 Expression and activity of CXCL12 splice variants in human colorectal carcinoma and normal colon mucosa

We first evaluated the expression of novel CXCL12 splice variants **(alpha, beta, gamma, delta, epsilon, and theta)** in 40 established colorectal tumor and 20 colon mucosa specimen. In order to determine the expression patterns of the human SDF-1 isoforms in colorectal tissues and human mucosa tissues, we designed PCR primers that could detect each SDF-1 isoform specifically. The forward primer was located in the 5′-UTR and was the same for all isoforms.

The reverse primer for SDF-1α was located on the third exon of SDF-1α. The reverse primer for SDF-1δ was in the region corresponding to the third intron of SDF-1δ. The reverse primer for SDF-1β and SDF-1γ were located on their respective 3′-UTRs which are unique. The reverse primers for SDF-1ε and SDF-1ϕ bridged the third and fourth exons of each isoforms and were unique to each of them.

RT -PCR analysis showed that the mRNA of these SDF-1 splice variants was expressed in CRC tissues and normal mucosa tissues (Table 25)(Fig 22).

SDF-1α was expressed in 32 of 40 samples (80%). SDF-1 β was expressed in 28 of 40 samples (70%). SDF-1γ was expressed in 20 0f 40 samples (50%). SDF-1δ was expressed in 15 of 40 samples (37.5%). SDF-1ε was expressed in 12 of 40 samples (30%). SDF-1ϕ was expressed in 153 of 40 samples (32.5%).

In contrast, in normal mucosa SDF-1α was expressed in 13 of 20 samples (65%). SDF-1 β was expressed in 10 of 20 samples (50%). SDF-1 γ was expressed in 5 of 20 samples (25%). SDF-1δ was expressed in 8 of 20 samples (40%). SDF-1ε was expressed in 9 of 20 samples (45%). SDF-1ϕ was expressed in 7 of 20 samples (35%)

SDF-1 Isoforms	Expreesion of SDF-1 isoforms in Colon samples 40 (%)	Expreesion of SDF-1 isoforms in Mucosa samples 20(%)
SDF1alpha	**32** (80%)	**13** (65%)
SDF1beta	**28** (70%)	**10** (50%)
SDF1gamma	**20** (50%)	**5** (25%)
SDF1delta	**15** (37.5%)	**8** (40%)
SDF1epsilon	**12** (30%)	**9** (45%)
SDF1theta	**13** (32.5%)	**7** (35%)

Table 25- Expression of SDF-1 isoforms in colorectal carcinoma and normal mucosa tissues

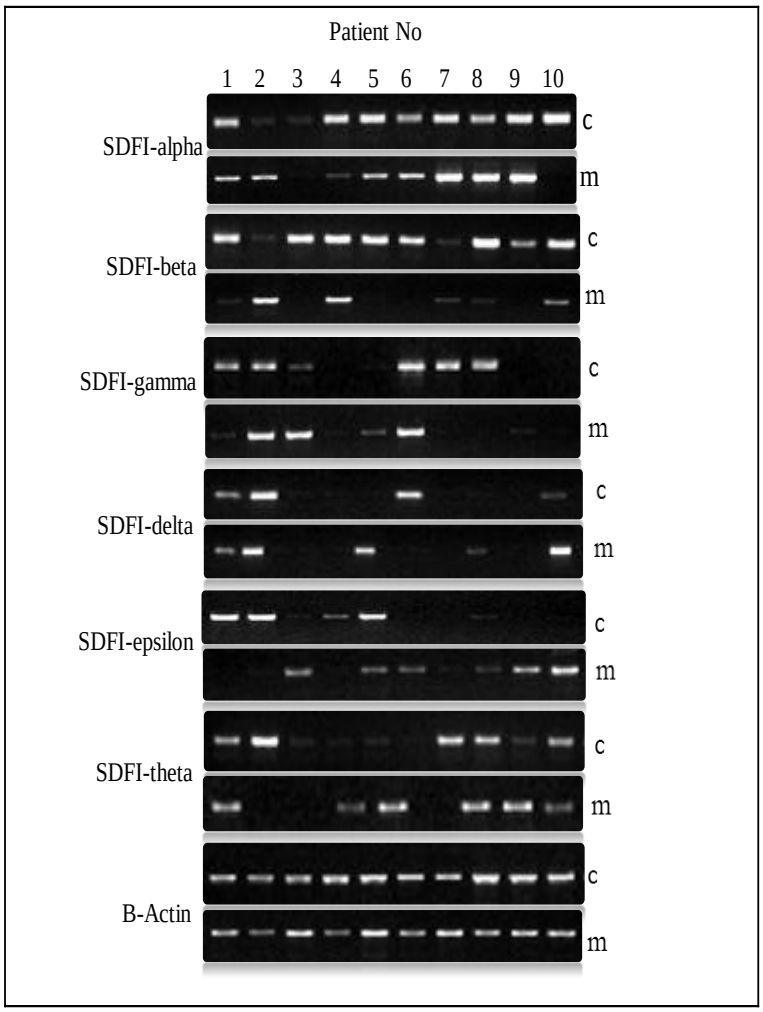

Fig 22- Expression of SDF-1 isoforms in colorectal carcinoma and human normal mucosa tissues. PCR analysis of SDF-1 isoforms in cDNA samples prepared from colon cancer tissues and mucosa normal tissues. (The experiments were repeated twice and identical results were obtained).

3.4 Statistical methods

3.4.1 Correlation of SDF-1 isoforms with clinicopathological parmeters

40 tumors of 39 patients were included in the study. For one on them clinical information was missing. 22 (56%) of the rest were male. The analysed tumors were located in the caecum (n=3, 8%), colon ascendens (n=5; 13%), colon transversum (n=1, 3%), colon descendens (n=2, 5%), sigma (n=13, 33%), rectum (n=15, 38%). Most of the tumors were T3 (n=29, 74%), as comperd to 2 T1 tumors (5%), 5 T2 tumors (13%) and 3 T4 tumors (8%).
The median age was 65.7 (SD=10.7), ranging from 41 to 83. A summary of the distribution of actin and the SDF1 isoforms is given in table 26.

	N	*Mean*	*Std Dev*	*Minimum*	*Lower Quartile*	*Median*	*Upper Quartile*	*Maximum*
Actin	40	280.28	80.66	106.38	234.52	281.64	321.46	537.37
SDFalpha	40	52.62	40.37	0	21.28	45.32	75.71	191.6
SDFbeta	40	38.01	40.59	0	0.17	19.02	82.56	116.51
SDFgamma	40	34.21	51.29	0	0	0	99.7	122.05
SDFdelta	40	36.69	70.58	0	0	0	40.04	316.16
SDFepsilon	40	42.75	51.33	0	0	10.66	93.25	175.41
SDFtheta	40	55.04	45.41	0	0	82.5	92.47	119.72
SDFalpha_percent	40	21.17	21.3	0	7.34	18.39	25.56	121.05
SDFbeta_percent	40	15.12	17.23	0	0.07	6.2	28.44	54.99
SDFgamma_percent	40	16.51	27.9	0	0	0	31.03	108.6
SDFdelta_percent	40	13.11	23.83	0	0	0	14.26	95
SDFepsilon_percent	40	16.56	20.55	0	0	4.54	35.13	74.04
SDFtheta_percent	40	22.22	21.53	0	0	23.05	37.12	90.43

Table 26- Summary measures for the distribution of actin and SDF1 isoforms

There was little association of categorical clinical parameters such as sex, site, TNM and R with actin and the SDF1 isoforms, the only exceptions being an association of SDF β with the presence of metastases and SDF γ with tumor size. The p-values of all associations are shown in table 27.

	Sex	*Site*	*T*	*N*	*M*	*R*
Parameter	*p-value Wilcoxon-Test*	*p-value Kruskall-Wallis-Test*	*p-value Kruskall-Wallis-Test*	*p-value Kruskall-Wallis-Test*	*p-value Wilcoxon-Test*	*p-value Wilcoxon-Test*
Actin	0.9887	0.1286	0.6591	0.3631	0.2958	0.6181
Alter	0.1564	0.9575	0.1410	0.3777	0.4534	0.3674
SDFalpha	0.1975	0.8651	0.2426	0.8603	0.4633	0.7115
SDFalpha_percent	0.3877	0.5311	0.4916	0.8412	0.2679	0.5097
SDFbeta	0.6375	0.5039	0.6006	0.9006	0.0656	0.1535
SDFbeta_percent	0.7643	0.2016	0.2761	0.6571	0.0457	0.1120
SDFdelta	0.8738	0.9815	0.2151	0.5787	0.2409	0.3576
SDFdelta_percent	0.9620	0.9850	0.2900	0.6048	0.1894	0.2873
SDFepsilon	0.1056	0.4253	0.3827	0.8219	0.8746	0.7947
SDFepsilon_percent	0.1119	0.6915	0.3480	0.7572	0.7885	0.8836
SDFgamma	0.4688	0.1407	0.0423	0.1403	0.2412	0.3720
SDFgamma_percent	0.6328	0.0992	0.0423	0.1395	0.2551	0.3911
SDFtheta	0.8744	0.2319	0.9746	0.2725	0.3751	0.2030
SDFtheta_percent	0.4127	0.5595	0.9540	0.2821	0.4193	0.4431

Table 27- p-values for Wilcoxon tests and Kruskal-Wallis tests for association of SDF1 isoforms with clinical parameters

Actin and the SDF1 isoforms did exhibit correlation with age. Further, there was significant association among the SDF1 isoforms. Also SDF γ tends to decrease when actin increases. After standardisation, some correlations are substantially different from zero, in particular SDF1 β and SDF1θ.

SDFIalpha isoform was correlated with isoforms of SDFIbeta (P= 0.0048), SDFIgamma (P= 0.0023), and SDFItheta (P=0.0084). SDFIbeta isoform was correlated with isoforms of SDFI gamma (P= 0.0016), SDFIdelta (P= 0.0001), SDFIepsilon (P= 0.0478) and SDFItheta P= 0.0232), as well as SDFIgamma isoform was correlated SDFItheta (P= 0.0003), and SDFI epsilon was correlated with SDFIbeta (P= 0.0738).

Pearson Correlation Coefficients *p-value for testing H_0: r=0* *Number of Observations*								
	Age	*Actin*	*SDFalpha*	*SDFbeta*	*SDFgamma*	*SDFdelta*	*SDFepsilon*	*SDFtheta*
Age	-	-0.13972 0.3962 39	-0.04777 0.7728 39	-0.02730 0.8690 39	0.19317 0.2387 39	0.07543 0.6481 39	-0.21384 0.1912 39	0.10631 0.5195 39
Actin	-0.13972 0.3962 39	-	-0.01916 0.9066 40	-0.08372 0.6075 40	-0.35767 0.0235 40	0.10351 0.5250 40	-0.05144 0.7526 40	-0.09977 0.5402 40
SDFalpha	-0.02286 0.8902 39	-0.40136 0.0103 40	-	0.23404 0.1461 40	0.16911 0.2969 40	0.21220 0.1887 40	-0.04299 0.7922 40	0.11430 0.4825 40
SDFbeta	0.02145 0.8969 39	-0.32314 0.0420 40	0.43695 0.0048 40	-	0.16463 0.3100 40	0.60533 <.0001 40	0.28580 0.0738 40	0.03862 0.8130 40
SDFgamma	0.13937 0.3974 39	-0.54909 0.0002 40	0.46757 0.0023 40	0.48248 0.0016 40	-	-0.15802 0.3301 40	-0.12948 0.4258 40	0.25850 0.1073 40
SDFdelta	0.07224 0.6621 39	-0.00248 0.9879 40	0.25954 0.1058 40	0.56648 0.0001 40	-0.00486 0.9763 40	-	0.05196 0.7502 40	-0.25492 0.1124 40
SDFepsilon	-0.13369 0.4172 39	-0.22619 0.1605 40	0.05407 0.7404 40	0.31493 0.0478 40	0.14699 0.3654 40	-0.01127 0.9450 40	-	-0.16050 0.3225 40
SDFtheta	0.12114 0.4626 39	-0.42788 0.0059 40	0.41089 0.0084 40	0.35834 0.0232 40	0.53831 0.0003 40	-0.11986 0.4613 40	0.08839 0.5876 40	-

Table 28- Correlation among SDFI isoforms

3.5 Plasmid DNATransfection

3.5.1 CXCL12 splice variants expression in colorectal cell line and melanoma cell line

We tested the expression of CXCL12 variants in multiple colorectal cell lines including SW480, SW620, HT29 and melanoma cell lines D05, D14 in order to to choose the most appropriate cell line to perform our transfection experiment. We selected colon cell line SW480 and melanoma cell line D05, of which both of them were negative for all CXCL12 variants (Fig 23, 24).

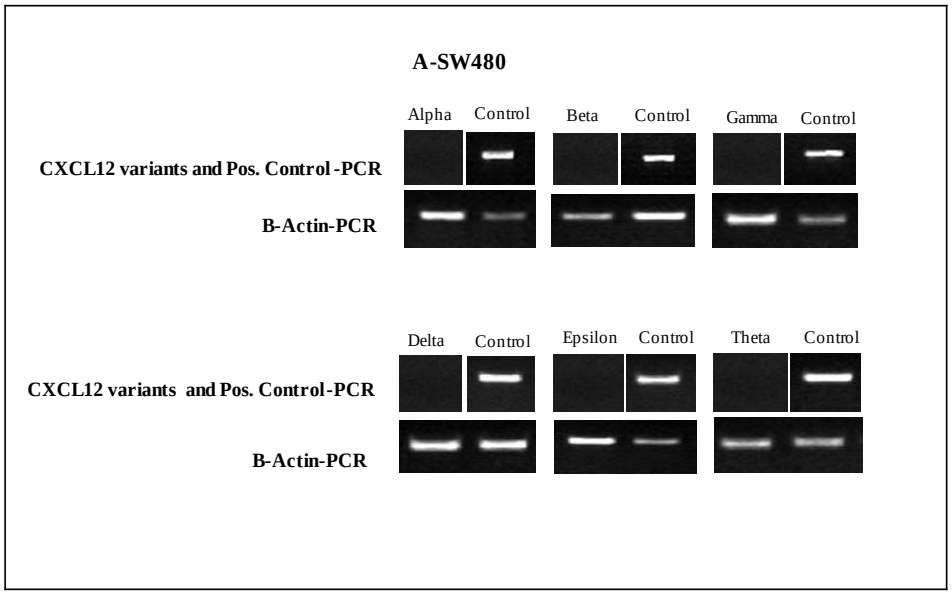

Fig 23- Expression of CXCL12 variants in SW480
Colorectal carcinoma cell line SW480 was negative for all CXCL12 variants. Colon carcinoma samples were used as a positive control

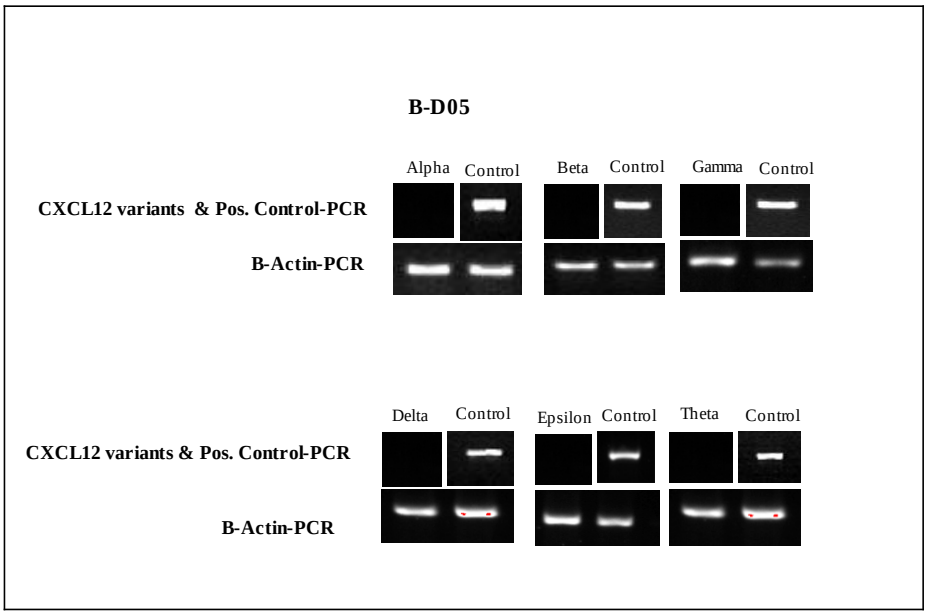

Fig 24- Expression of CXCL12 variants in D05
Melanoma cell line D05 was negative for all CXCL12 variants. Colon carcinoma samples were used as a positive control

3.5.2 Transfection of CXCL12 splice variants in tumor cells

We tested the transfection method in human colon cell lines SW480, SW620 and melanoma cell line D05, D14. We mainly used lipofectamine 2000 as the transfection reagent and a DNA plasmid encoding the green fluorescence protein GFP. Transfection had been successful for all variants of CXCL12 with cell lines SW480 and D05, but did not succeed with any other cell lines.

To compare the transfection efficiencies, total cellular RNAs and mRNA were isolated 48 h after the transfection from tumor cells, Transcription levels were measured by RT-PCR **(**Fig 25).

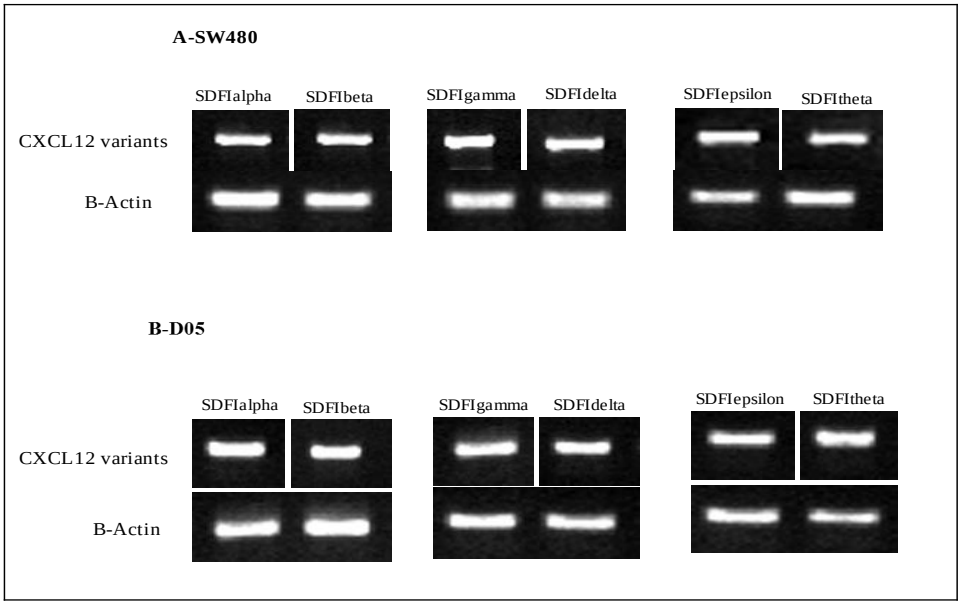

Fig 25- Expression of CXCL12 variants after the transfection in A-colorectal cell line SW480 and B-Melanoma cell line D05, respectively.

SDF1alpha	**89aa**	**270bp**
SDF1beta	**93aa**	**282bp**
SDF1gamma	**119aa**	**361bp**
SDF1delta	**140aa**	**423bp**
SDF1epsilon	**90aa**	**273bp**
SDF1theta	**100aa**	**303bp**

Table 29- CXCL12 splice variants (SDF-I isoforms)

3.5.3 FACS Analysis

3.5.3.1 FACS Analysis of SW480 and D05 in Vitro

To confirm the results, twenty-four hours after the transfection, cells were processed for fluorescence activated cell sorting (FACS) and fluorescence microscopic analysis.

Both cell lines, SW480 and D05 were positive for all six SDFI isoforms after transfection using lipofectamine 2000 with the enhanced GFP expression vector pcDNA3.1/ NT-GFP-TOPO. Fig (26-A, B), (27 A, B) respectively.

3.5.3.2 FACS Analysis of SW480 in Vitro

The results of **FACS analysis** showed that all SDFI isoforms were expressed in the colorectal cell line SW480. We named the stable clones as follows; **SW480-1α, SW480-1β**, **SW480-1γ, SW480-1δ, SW480-1ε**, **SW480 -1θ** and **SW480- GFP** as a negative control.

Stable clones	Expression %
SW480-1α	97.94%
SW480-1β	98.76%
SW480-1γ	97.98%
SW480-1δ	97.88%
SW480-1ε	98.55%
SW480 -1θ	95.22%.
SW480- GFP	93.31%

Table 30- Expression of SDFI isoforms in colorectal cell line SW480

The FACS experience was repeated once a month to ensure the survival of the SDFI gene within the tumor cells

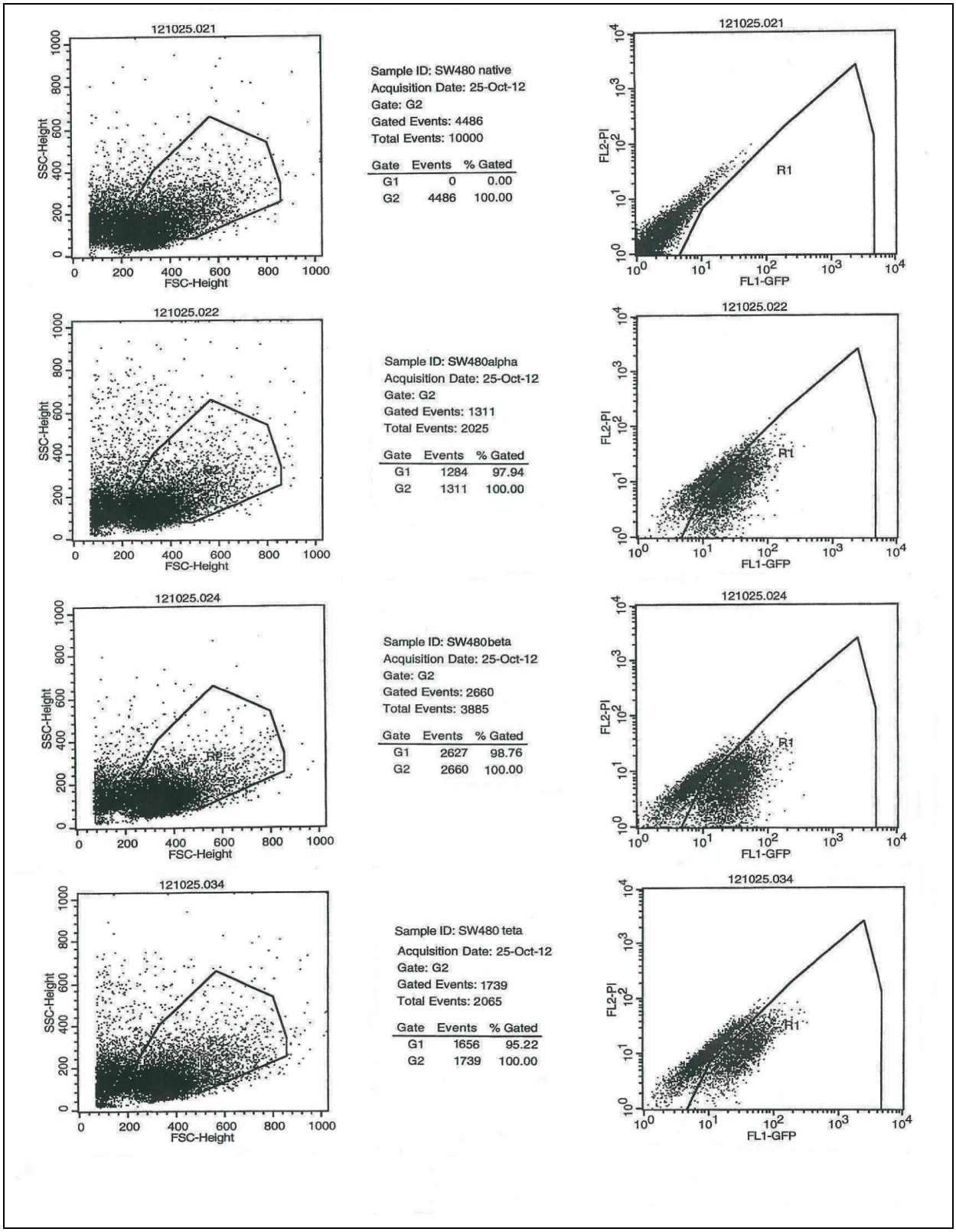

Fig 26- (A) FACS graphs showed a comparable expression of SDFI isoforms in SW480 after transfection.

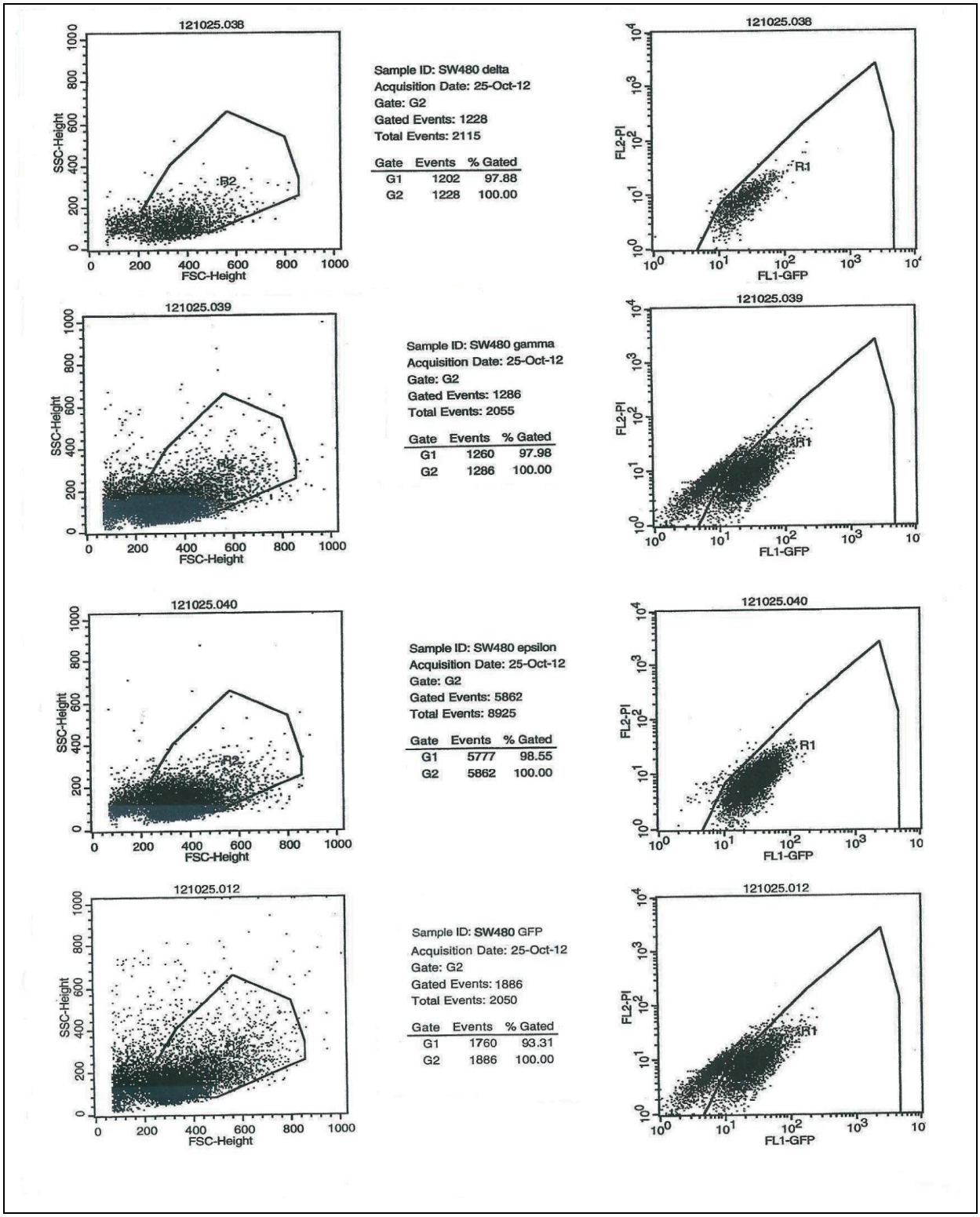

Fig 26- (B) FACS graphs showed a comparable expression of SDFI isoforms in SW480 after transfection.

3.5.3.3 FACS Analysis of D05 in Vitro

The results of **FACS Analysis** showed that all SDFI isoforms were expressed in melanoma cell line D05. We named the stable clones as follows; **DO5 -1α, DO5-1β**, **DO5 -1γ, DO5-1δ, DO5-1ε**, **DO5-1θ, DO5- GFP as a negative control**.

Stable clones	Expression %
DO5-1α	96.53%
DO5-1β	98.36%
DO5-1γ	98.11%
DO5-1δ	97.53%
DO5-1ε	98.82%
DO5-1θ	99.14%.
DO5- GFP	97.94%

Table 31- Expression of SDFI isoforms in melanoma cell line D05

We repeated the FACS experience once a month to ensure the survival of the SDFI gene with-in the tumours cell.

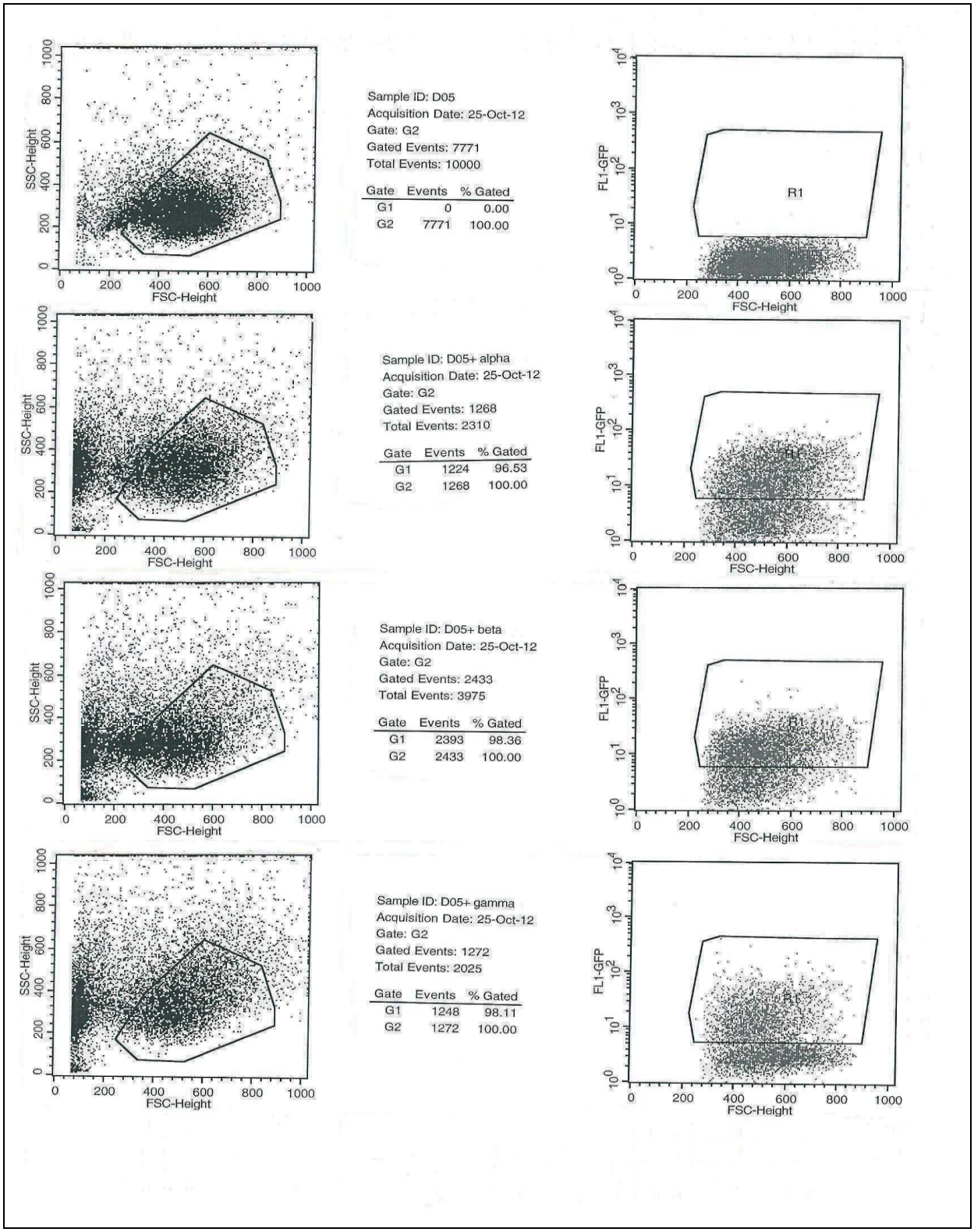

Fig 27- (A) FACS graphs showed a comparable expression of SDFI isoforms in D05 after transfection.

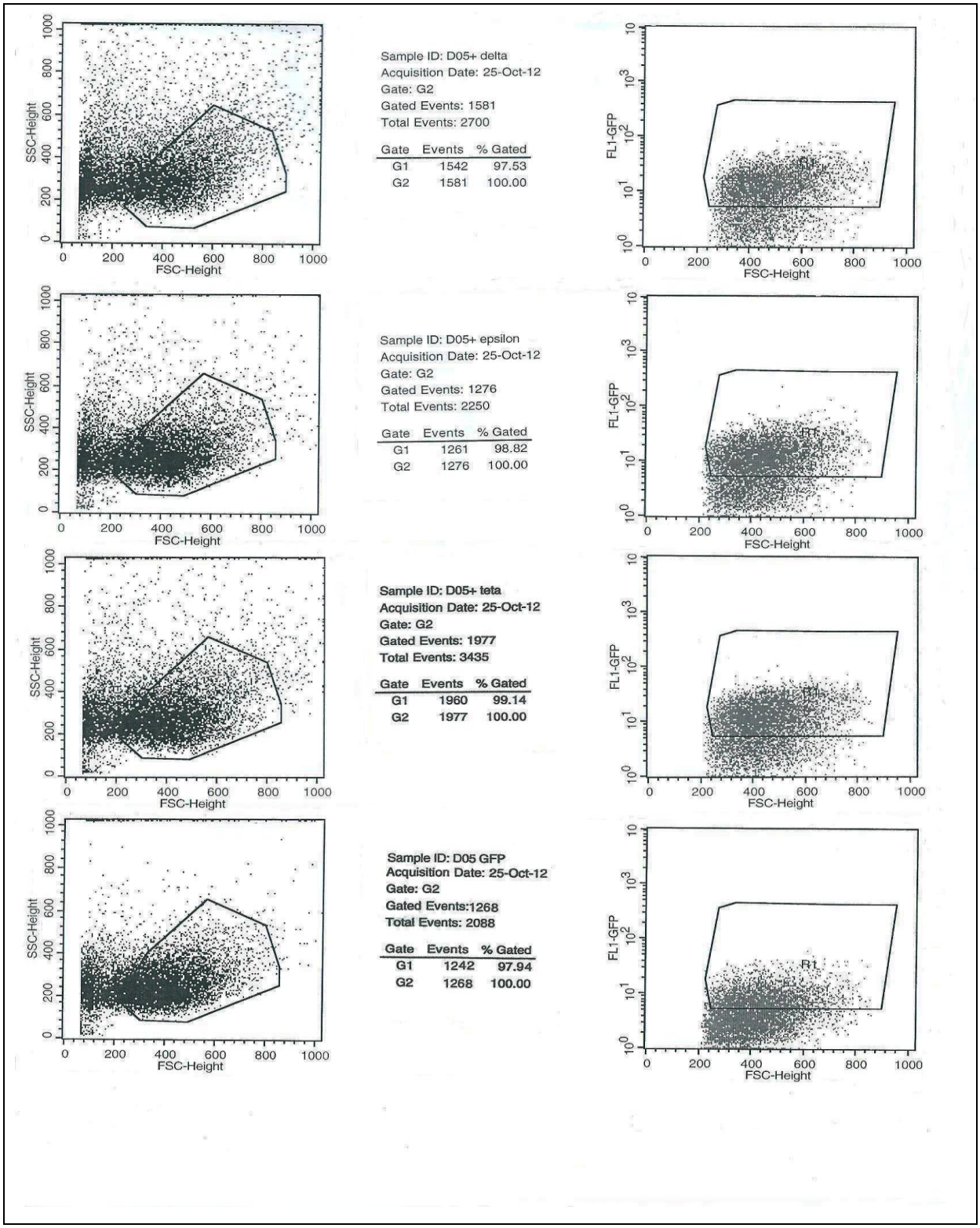

Fig 27 - (B) FACS graphs showed a comparable expression of SDFI isoforms in D05 after transfection.

3.6 Cell Proliferation Assay

3.6.1 Effect of CXCL12 splice variants on cell proliferation of colorectal cancer

Since the activation of CXCR4 by CXCL12 was known to play an important role in cell proliferation in many kinds of cancer cells, we investigated the role of CXCL12 variants on cell proliferation of tumor cells.

Cell proliferation assay was performed in two cell lines, colorectal cell line **SW480** and melanoma cell line **D05**.

Our data show that all CXCL12 variants had effect on cell proliferation through comparing the results with SW480-GFP as a negative control Fig (28-A, 28-B).

The luminescence analysis on day 4 showed that **SW480-1β** had the highest rate of growth (828 %, +/- 26.8%, P=0.000) and **D05-1β** showed the same results (647 %, +/- 25.2%, P=0.000). **SW480-1α** (733 %, +/- 34.6%, P=0.000) and **D05-1α** (697 %, +/- 29.3 P=0.000) were the second most proliferation inducers.

SW480-1γ (630 %, +/- 24.4%, P=0.000) and **D05-1γ** (494 %, +/- 31.8%, P=0.000) were third and similar with **SW480-1δ** (645 %, +/- 33.3%, P=0.000) and **D05-1δ** (437 %, +/- 23.5%, P= 0.000) followed by **SW480-1ε** (608 %, +/- 46.1%, P=0.000) and **D05-1ε** (402 %, +/- 26.4%, P=0.000).

Finally, **SW480-1θ** had the lowest rate of growth (558 %, +/- 46.1%, P=0.005), so was **D05-1 θ** (550 %, +/- 31.2%, P=0.000).

SW480-GFP as a negative control (483 %, +/- 36.3%) and **D05-GFP** (373 %, +/- 24.2%) revealed the weakest proliferation.

The experiments were repeated twice and similar results were obtained.

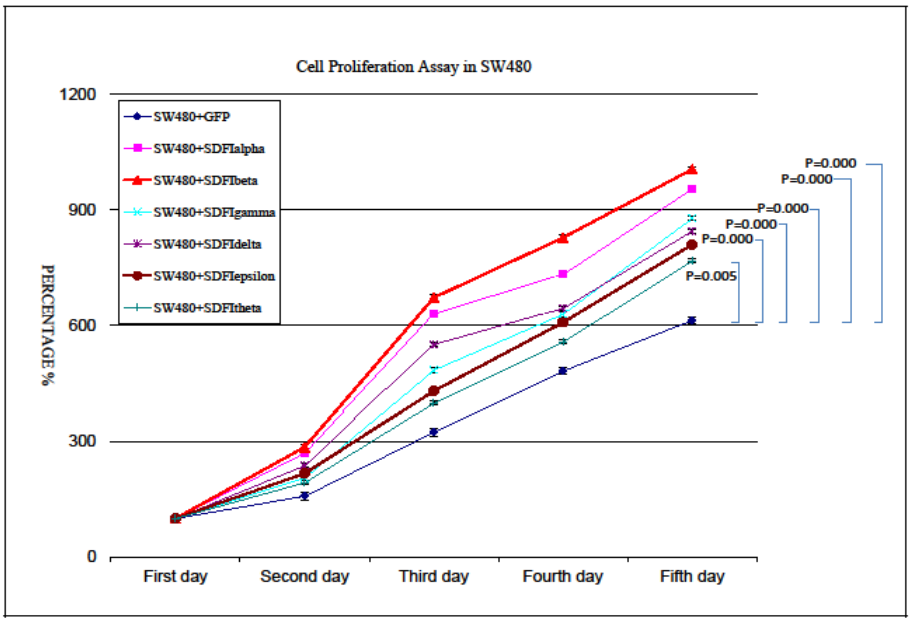

Fig 28-(A) Effect of CXCL12 splice variants on the proliferation of SW480 cells

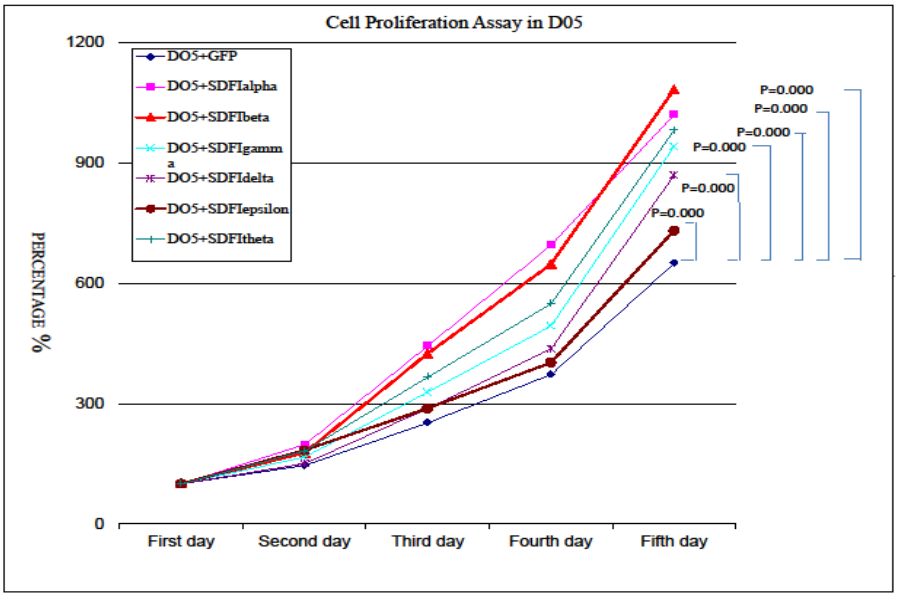

Fig 28-(B) Effect of CXCL12 splice variants on the proliferation of D05 cells

3.7 Cell Migration Assay

3.7.1 Effect of CXCL12 splice variants on cell migration of colorectal cancer

Our result demonstrated that all CXCL12 variants induced the cell migration of SW480 and D05.

The maximum effect was identified in **SW480-1θ** (23.8, +/- 2.07, P=0.010) and in **D05-1θ** (24.4, +/- 1.40, P=0.001) followed by **SW480-1ε** (23.4, +/- 3.32, P= 0.070) and in **D05-1ε** (22.8, +/- 1.20, P=0.009) Fig (29-A, 29-B).

Other CXCL12 variants also enhanced cell migration. Following results were obtained **SW480-1δ** (20.0, +/- 1.43, P=0.041) and **D05-1δ** (21.9, +/- .47, P=0.052) followed by **SW480-1γ** (18.7, +/- 1.6, P=0.032) and **D05-γ** (19.9, +/- 1.34, P=0.066), **SW480-1β** (16.1, +/- 1.6, P=0.020) and **D05-1β** (19.3, +/- 2.20, P=0.066) and finally **SW480-1α** (15.3, +/- 0.89, P=0.011) and **D05-1α** (18.4, +/- 0.36, P=0.045). **SW480-GFP** as a negative control revealed weakest migration (10.8, +/- 0.18) as proven in **D05-GFP** (12.4, +/- 0.36).

The experiments were repeated twice and similar results were obtained.

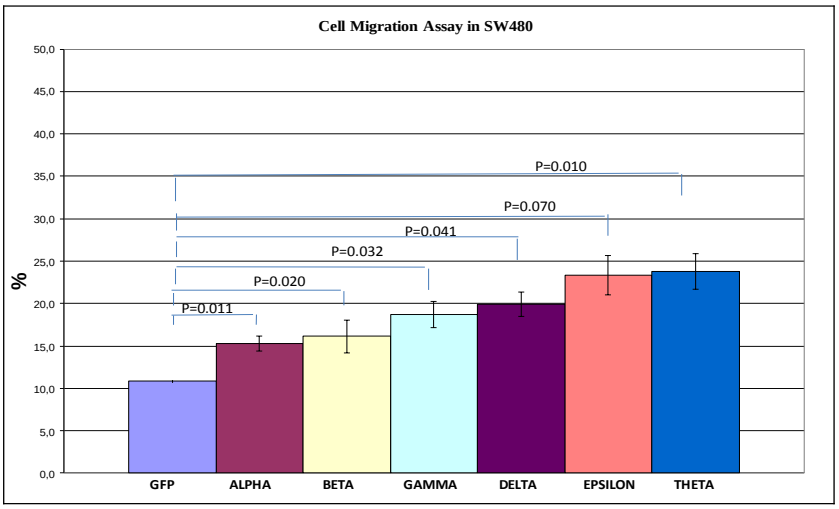

Fig 29-(A) Effect of CXCL12 splice variants on the migration of SW480 cells

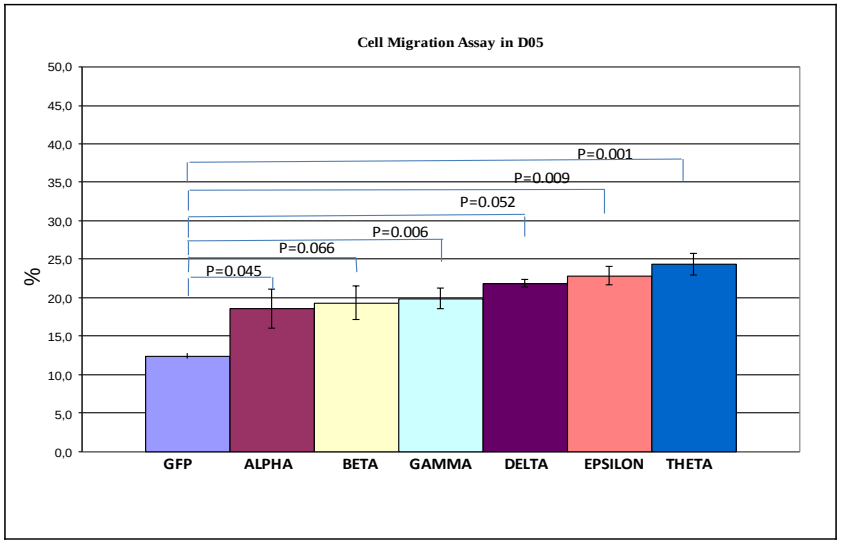

Fig 29-(B) Effect of CXCL12 splice variants on the migration of D05 cells

3.8 Cell Invasion Assay

3.8.1 Effect of CXCL12 splice variants on cell invasion of colorectal cancer

To confirm the mechanism by which CXCL12 splice variants induced invasion more than other variants of colorectal cancer we performed cell invasion assays.

The maximum effect was identified in **SW480-1θ** (12.3, +/- 1.03, P=0.070) and **D05-1θ** (12.6, +/- 1.55, P=0.056) followed by **SW480-1ε** (11.2, +/- 1.19, P= 0.030) and **D05-1ε** (11.8, +/- 0.19, P=0.048) Fig (30-A, 30-B).

Other CXCL12 splice variants also enhanced colorectal cell invasion. **SW480-1δ** (10.6, +/- 0.82, P=n.s.) and **D05-1δ** (10.7, +/- 2.08, P= n.s.) followed by **SW480-1γ** (10.5, +/- 1.69, P= n.s.) and **D05-1γ** (9.8, +/- 0.9, P= n.s.), **SW480-1β** (9.8, +/- 1.52, P= n.s) and **D05-1β** (10.2, +/- 0.43, P=0.006). Finally **SW480-1α** (8.6, +/- 1.34, P= n.s.) and **D05-1α** (9.3, +/- 0.87, P= n.s.)

SW480-GFP as a negative control revealed weakest invasion (5.5, +/- 0.65) as did **D05-GFP** (6.1, +/- 1.23).

The experiments were repeated twice and similar results were obtained.

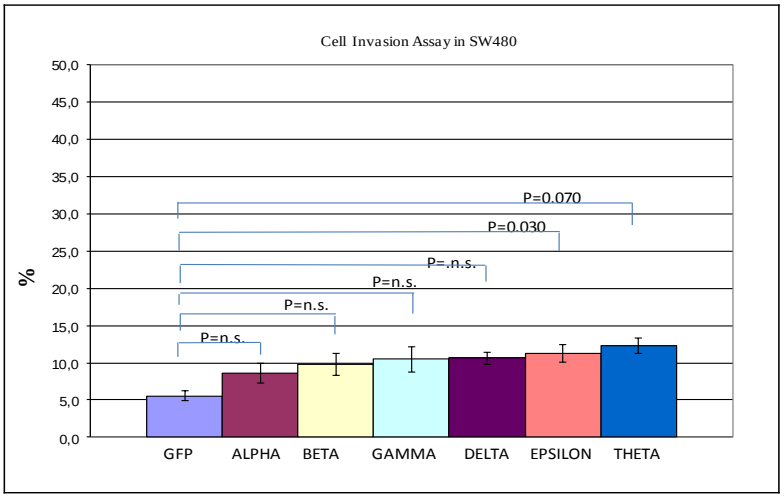

Fig 30-(A) Effect of CXCL12 splice variants on the invasion of SW480 cells

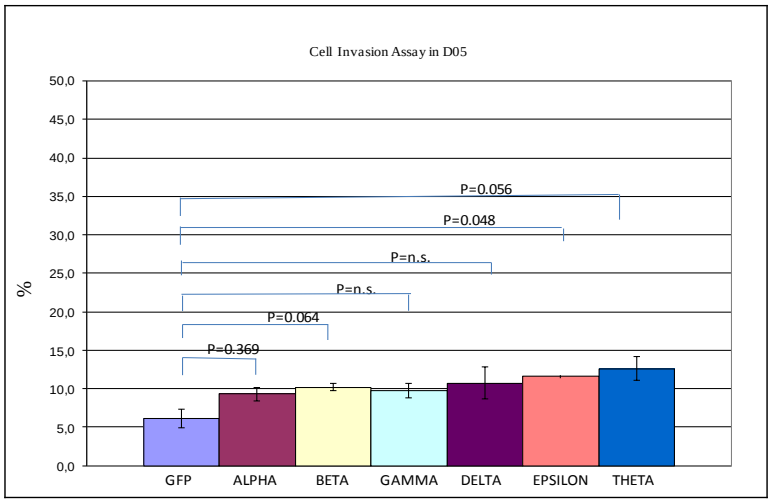

Fig 30-(B) Effect of CXCL12 splice variants on the invasion of D05 cells

3.9-Cell Adhesion Assay

3.9.1 Effect of CXCL12 splice variants on cell adhesion of colorectal cancer

By comparing the results with **SW480-GFP** as a negative control we found that, CXCL12 splice variants significantly enhanced adhesion of SW480 and D05 cells. In contrast **CXCL12-1β** promotes tumor cell adhesion more than other splice variants Fig (31-A, 31-B).

The results were in **SW480-1β** (71.8, +/- 2.8, P=0.003) and **D05-1β** (69.1, +/- 2.5, P=0.000) followed by **SW480-1α** (70.2, +/- 4.5, P=0.009) and **D05-1α** (66.6, +/- 3.2, P=0.000) followed by **SW480-1γ** (67.9, +/- 3.5, P=0.009) and **D05-1γ** (63.8, +/- 3.2, P=0.000), **SW480-1δ** (66.3, +/- 2.5, P=0.033) and **D05-1δ** (63.3, +/- 3.2, P=0.000) and **SW480-1ε** (64.3, +/- 4.0, P=0.033) and as well as **D05-1ε** (61.4, +/- 3.5, P=0.000). Finally **SW480-1θ** (61.4, +/- 4.5, P=n.s.) and **D05-1 θ** (57.6, +/- 2.0, P=0.000).

SW480-GFP as a negative control showed the weakest results (58.4 %, +/- 5.0) and **D05-GFP** (50.0 %, +/- 3.3).

The experiments were repeated twice and similar results were obtained.

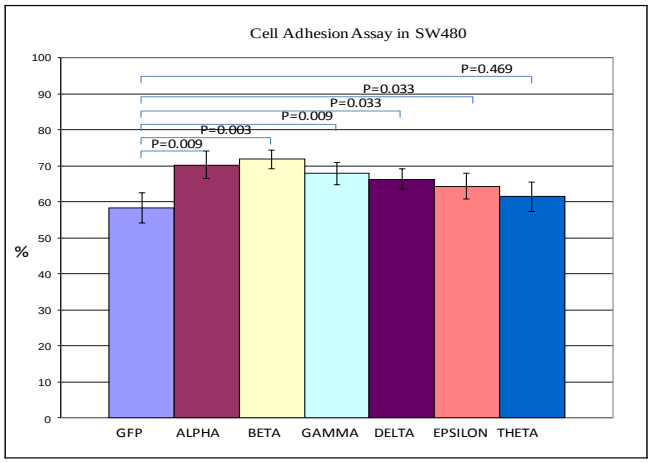

Fig 31-A Effect of CXCL12 splice variants on the adhesion of SW480 cells

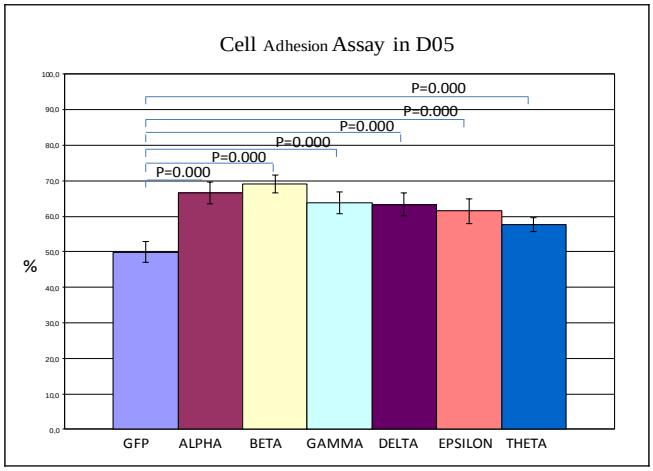

Fig 31-B Effect of CXCL12 splice variants on the adhesion of D05 cells

3.10 The effect of CXCL12 splice variants on cell proliferation of colorectal carcinoma and melanoma cell lines after treatment with different concentration of AMD3100

3.10-1 Effect of CXCL12 splice variants on cell proliferation activity after treatment with 0µg\ml AMD3100

Tumor growth induced by CXCL12 variants was inhibited through different concentration of AMD3100. Our result showed that there is no significant inhibition of tumor growth with the concentration of 0µg\ml AMD3100.

The luminescence analyses on day 4 showed that **SW480-1β** had the highest rate of growth when compared with others variants (777 %, +/- 26.7%, P= 0.000). In Melanoma cell lines **D05-1β** showed the same results (662 %, +/- 17.6%, P= 0.000). **SW480-1α** (749 %, +/- 35.2%, P= 0.000) and **D05-1α** (636%, +/- 27.3, P= 0.000) revealed the second strongest induction of proliferation.

Followed by **SW480-1γ** (710 %, +/- 34.5%, P= 0.078) and **D05-1γ** (655 %, +/- 51.8%, P= 0.000) then **SW480-1δ** (694 %, +/- 39.5%, P= 0.000) and **D05-1δ** (615%,+/- 17.8%, P= 0.000), then **SW480-1θ** (694 %, +/- 11.9%, P= 0.023) and **D05-1θ** (572 %, +/- 21.4%, P= 0.000).

Finally **SW480-1ε** had the lowest rate of growth (625 %, +/- 44.6%, P= 0.000) and as proven in **D05-1ε** (546 %, +/- 30.2%, P= 0.000).

SW480-GFP as a negative control showed the weakest results (571 %, +/- 15.3%) and **D05-GFP** (454 %, +/- 15.5 %).

The experiments were repeated twice and similar results were obtained

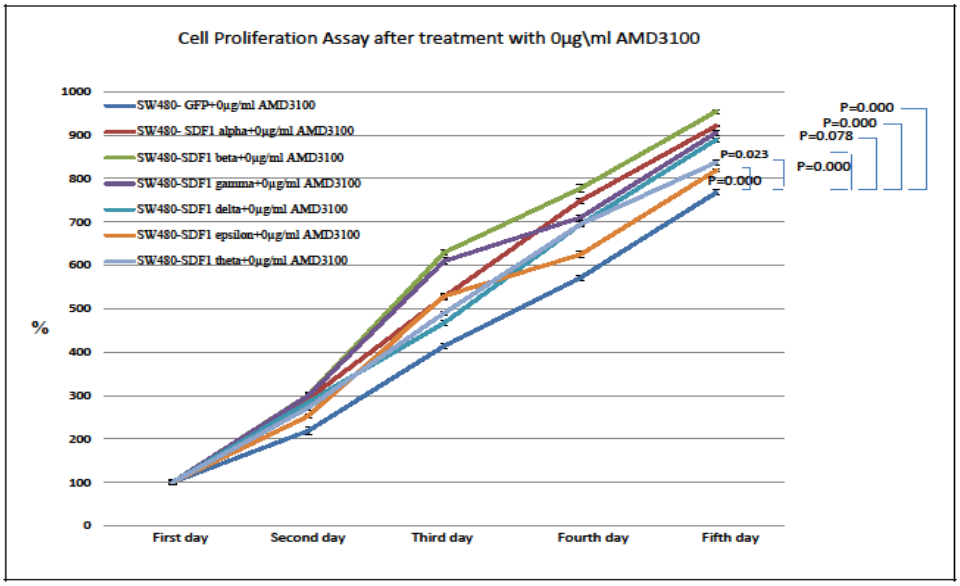

Fig 32-A Effect of CXCL12 splice variants on the cell proliferation of SW480 cells after treatment with 0µg\ml AMD3100

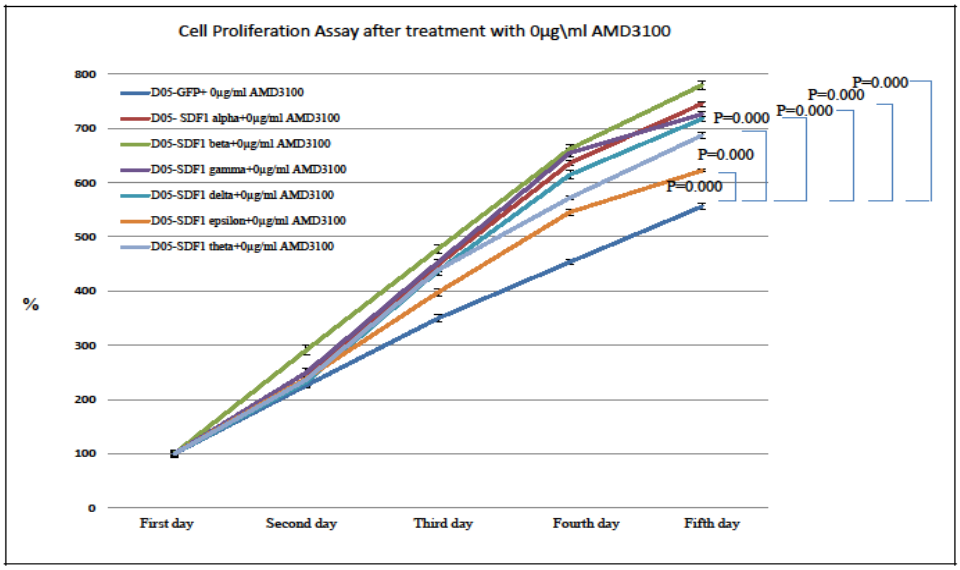

Fig 32-B Effect of CXCL12 splice variants on the cell proliferation of D05 cells after treatment with 0µg\ml AMD3100

3.10.2 The effect of CXCL12 splice variants on cell proliferation activity after treatment with 5µg\ml AMD3100

To study the effect of AMD3100 on CXCL12 splice variants induced cell proliferation in tumor cells, cells were treated over night with 5µg\ ml AMD3100.

Our results showed that the enhancing effect of CXCL12 on cell proliferation was inhibited by treatment with 5µg\ ml AMD3100.

The luminescence analyses on day 4 showed that **SW480-1β** had the highest rate of growth (626 %, +/- 41.3%, P= 0.098) and **D05-1β** showed identical results (604 %, +/- 33.6%, P= 0.098). **SW480-1α** (615 %, +/- 40.6%, P= n.s.) and **D05-1α** (575%, +/- 18.3, P= 0.015) revealed the second strongest induction of proliferation.
Followed by **SW480-1γ** (518 %, +/- 14.5%, P= 0.000) and **D05-1γ** (518 %, +/- 19.8%, P= 0.000). **SW480-1δ** (490 %, +/- 30.8%, P= 0.006) and **D05-1δ** (588 %, +/- 18.5,P= 0.000), followed by **SW480-1θ** (518 %, +/- 16.4%, P= 0.000) and **D05-1θ** (471 %, +/- 27.6.%, P= 0.132) which revealed weaker proliferation induction.
Finally, **SW480-1ε** had the lowest rate of growth (401 %, +/- 15.6%, P= 0.019) as also shown in **D05-1ε** (420 %, +/- 15.2%, P= 0.031).
SW480-GFP as a negative control showed following results (596 %, +/- 22.3%, P= 0.000) as did **D05-GFP** (502 %, +/- 15.8%, P= 0.000).

The experiments were repeated twice and similar results were obtained

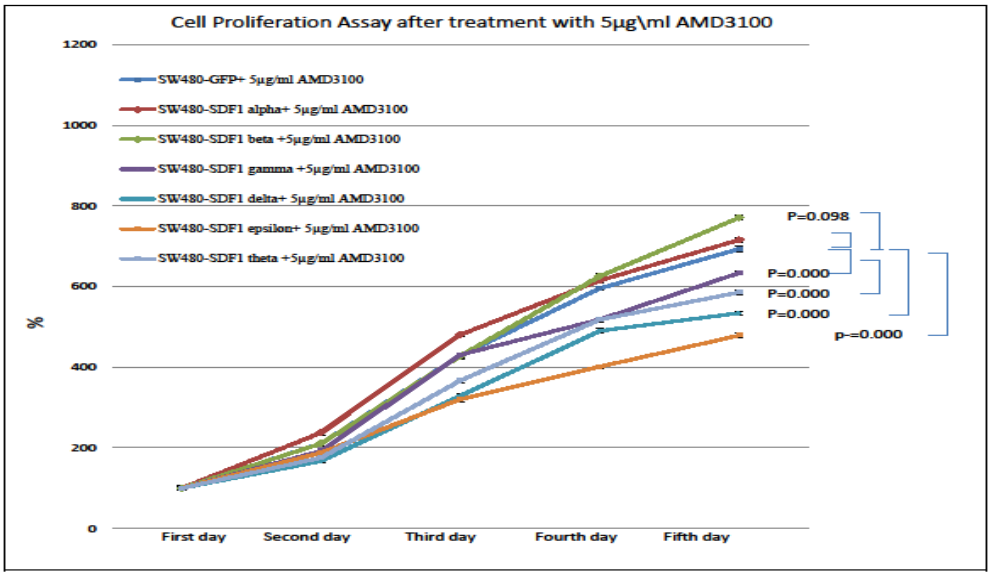

Fig 33-A Effect of CXCL12 splice variants on the cell proliferation of SW480 cells after treatment with 5µg\ml AMD310

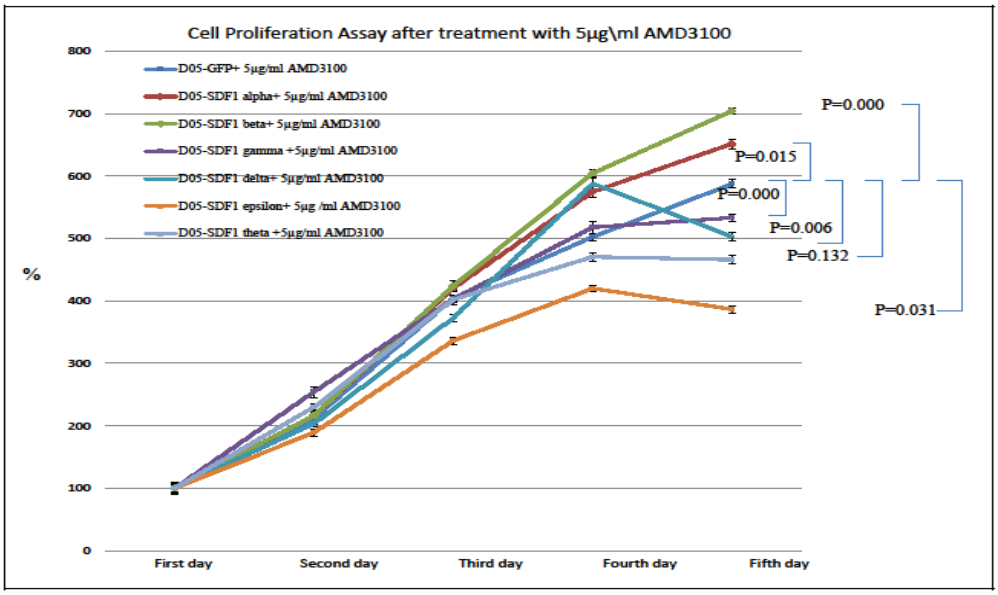

Fig 33-B Effect of CXCL12 splice variants on the cell proliferation of D05 cells after treatment with 5µg\ml AMD310

3.10.3 Effect of CXCL12 splice variants on cell proliferation activity after treatment with 10µg\ml AMD3100

The effect of CXCL12 on tumor cell proliferation has been described under optimal culture conditions. Treatment with AMD3100 has greatly inhibited spontaneous proliferation.

Our results showed that the enhancing effect of CXCL12 on cell proliferation was strongly inhibited by treatment with 10µg\ ml AMD3100.
The luminescence analyses on day 4 showed that **SW480-1β** had the highest rate of growth (489%, +/- 29.7%, P= 0.000) and **D05-1β** showed identical results (497%, +/- 41.5%, P= 0.047). **SW480-1α** (498%, +/- 31.2%, P= 0.000) and **D05-1α** (457%,+/- 14.6, P= 0.047) revealed the second strongest induction of proliferation.
Followed by **SW480-1γ** (333%, +/- 15.5%, P= 0.098) and **D05-1γ** (454 %, +/- 42.8%, P= 0.142). **SW480-1δ** (473%, +/- 23.7%, P= 0.000) and **D05-1δ** (433%, +/- 22.3%, P= 0.004) then **SW480-1θ** (419 %, +/- 35.5%, P= 0.000) and **D05-1θ** (422 %, +/- 39.1%, P= n.s.) which revealed wearker proliferation induction.
Finally **SW480-1ε** had the lowest rate of growth (374 %, +/- 25.7%, P= 0.000) as also shown in **D05-1ε** (382%, +/- 32.2%, P= 0.031).
SW480-GFP as a negative control showed following results (406%, +/- 18.1%) as did **D05-GFP** (422 %, +/- 39.4%).

The experiments were repeated twice and similar results were obtained

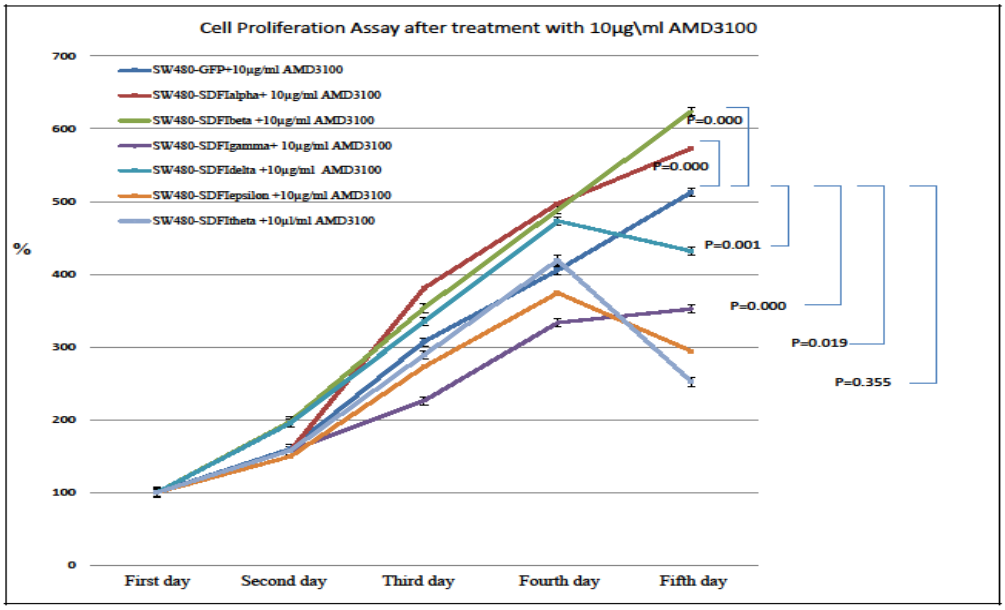

Fig 34-A Effect of CXCL12 splice variants on the cell proliferation of SW480 cells after treatment with 10µg\ml AMD3100

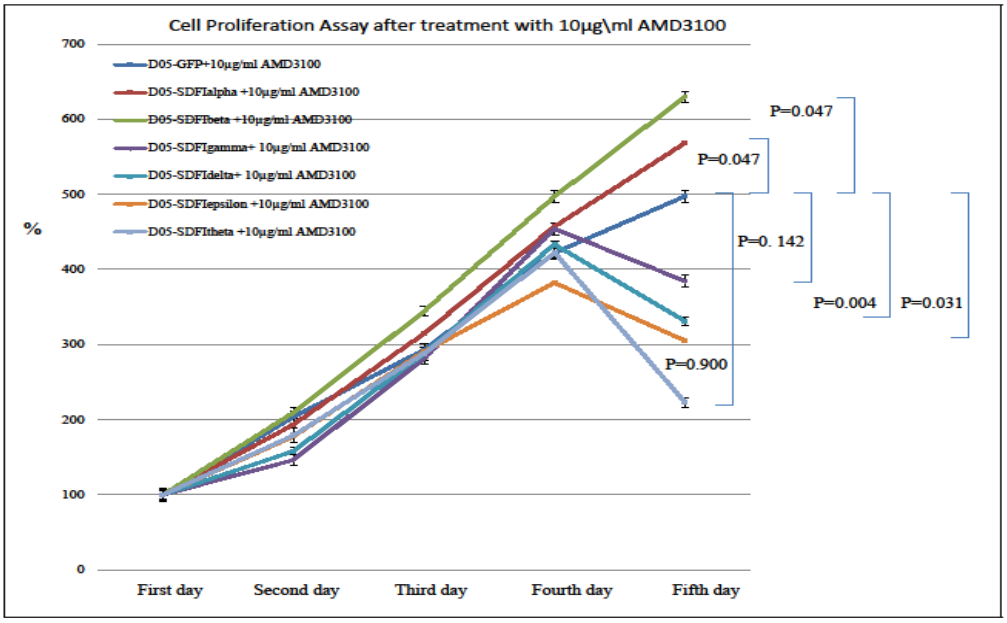

Fig 34-B Effect of CXCL12 splice variants on the cell proliferation of D05 cells after treatment with 10µg\ml AMD3100

3.11 The Akt and MAPK signalling pathways in colorectal cancer

3.11.1 The effect of CXCL12 splice variants on the phosphorylation of AKT MKE ½, SAPK/JNK and p38 in colorectal cancer

To test if CXCL12 splice variants expression in CRC cells is functional, and any of these splice variants play a fundamental role in colon tumorigenesis we analysed major signalling pathways after transfection with CXCL12 splice variants in colorectal carcinoma cell line (SW480) and melanoma cell line (D05).

Our results showed that all CXCL12 splice variants activate AKT kinase and MAP kinase as compared to the control in both cell lines. Activation and expression of phospho-AKT, phospho-MKE ½, phospho-SAPK/JNK and phosoho-p38 were assessed by Western Blot (Fig 35-A, 35-B).

All six CXCL12 splice variants activated and expressed phospho- AKT. CXCL12-beta has the strongest expression followed by CXCL12-alpha as compared to other variants and the control.

Concerning activation and expression of MAP kinases, our results showed in all six CXCL12 splice variants an induced a transient activation of phospho-MEK-1/2 which varied from strong (Delta, Epsilon and Theta) and intermediate (Gamma) to weak (Alpha and Beta) in both cell lines.

Similarly, SAPK/JNK kinases were phosphorylated after stimulation by CXCL12 variants. while no p38 MAP kinase activation was observed (Fig 35-A, 35-B).

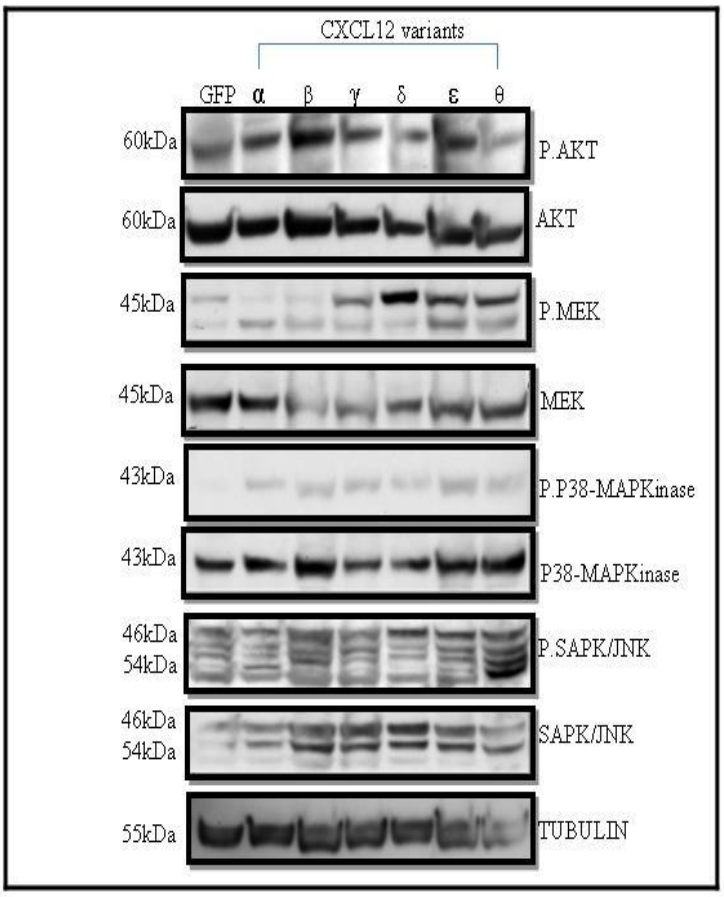

Fig 35- (A) Western Blot analysis of AKT and MAPKinase in SW480 cell line. CXCL12 variants activated AKT, MEK, and SAPK/JNK phosphorylation. No activation of P38 MAPKinase was observed

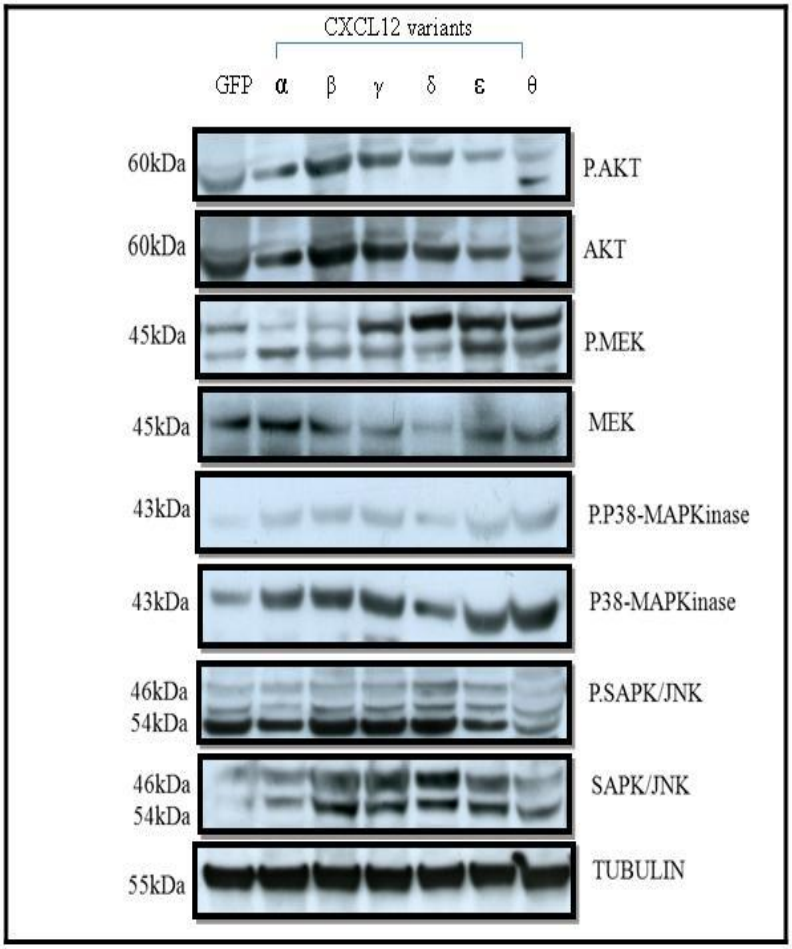

Fig 35- (B) Western Blot analysis of AKT and MAPKinase in D05 cell line. CXCL12 variants activated AKT, MEK, and SAPK/JNK phosphorylation. No activation of P38 MAPKinase was observed

3.11.2 Effect of CXCL12 splice variants on the AKT& MEK-1/2 in colorectal cancer after treatment with AMD3100

The ability of AMD3100 to decrease the effect of CXCL12 variants on inducing phosphorylation of AKT&MEK-1/2 was assessed. SW480 and D05 cells were treated with different concentration of AMD3100 (0µg\ml, 5µg\ml and 10µg\ml) and collected after 18-24 hours. Then AKT and MEK-1/2 phosphorylation was determined by Western Blot as described.

3.11.3 The effect of CXCL12 splice variants on the phosphorylation of AKT after treatment with AMD3100

Our findings indicated that CXCL12 splice variants activate AKT. Here the induction of CXCL12 was inhibited by AMD3100 in both cell lines Fig (36-A) (36-B).

AMD3100 inhibit phosphorylation of AKT strongest in **SW480-1δ, SW480-1ε**, **SW480-1θ** and weakest in **SW480-1γ.**

Thus, there was no significant inhibition of AKT phosphorylation in **SW480-1*α*, SW480-1β**.

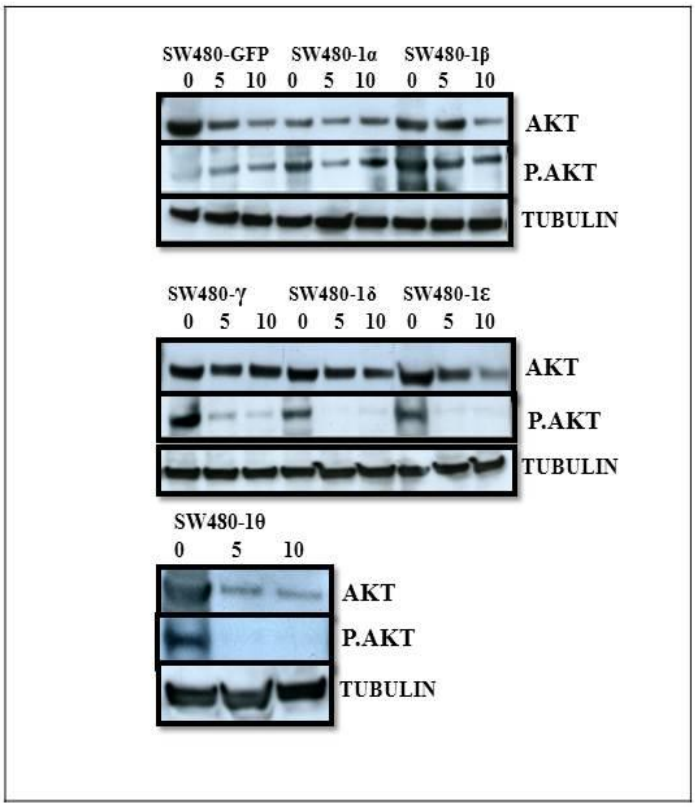

Fig 36-(A) Effect of AMD3100 on CXCL12 splice variants induced phosphorylation of AKT in SW480 Cells that were treated with different concentrations of AMD3100, 0µg\ml, 5µg\ml and 10µg\ml

We tested the ability of AMD3100 to decrease the effect of CXCL12 to induced phosphorylation of AKT in melanoma cell line D05 and obtained identical results.

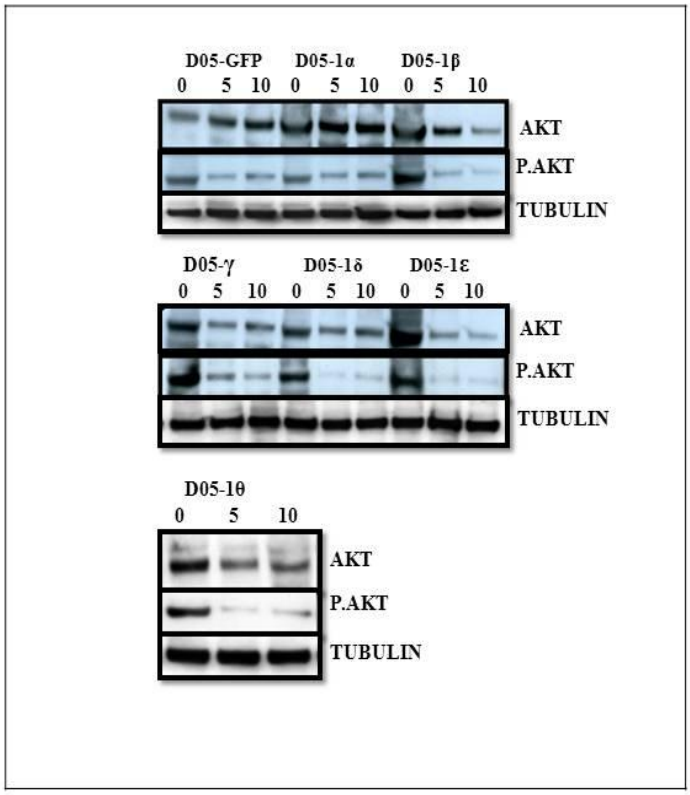

Fig 36-(B) Effect of AMD3100 on CXCL12 splice variants induced phosphorylation of AKT in D05 Cells that were treated with different concentrations from AMD3100 with 0µg\ml, 5µg\ml and 10µg\ml.

3.11.4 The effect of CXCL12 splice variants on the phosphorylation of MEK-1/2 after treatment with AMD3100

We studied the ability of AMD3100 to decrease the effect of CXCL12 induced phosphorylation of MEK-1/2 in SW480 and D05 cell lines Fig 37-A, 37-B).

Our results showed that the inhibitor AMD3100 suppressed phosphorylation of MEK-1/2 strongest in **SW480-1δ, SW480-1ε**, **SW480-1θ** and weakest in **SW480-1γ.**

Thus, there was no significant inhibition of MEK-1/2 phosphorylation with **SW480-1α, SW480-1β.**

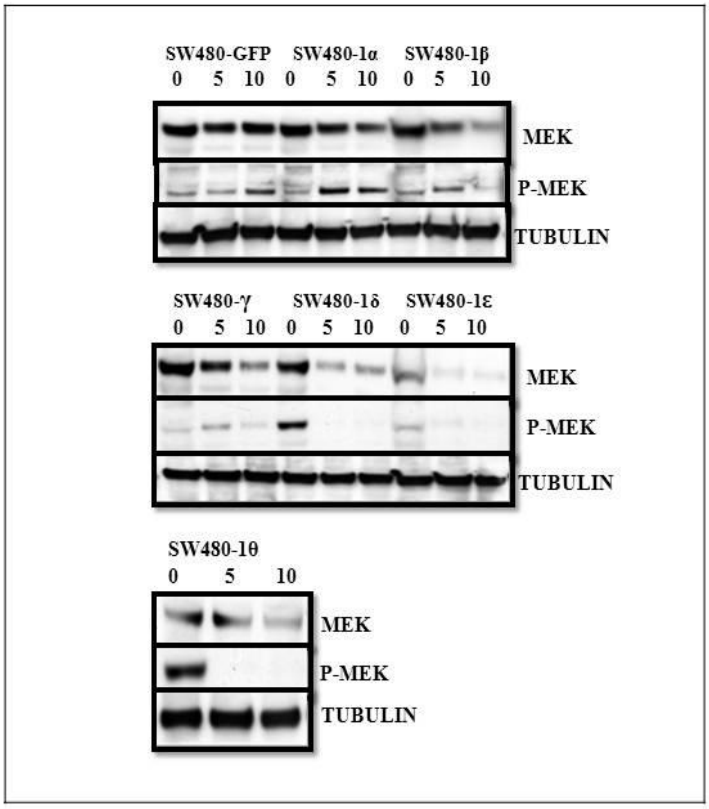

Fig 37-(A) Effect of AMD3100 on CXCL12 splice variants induced phosphorylation of MEK in SW480 Cells were treated with different concentrations of AMD3100 0µg\ml,5µg\ml, 10µg\ml

Identical results were obtained in D05.

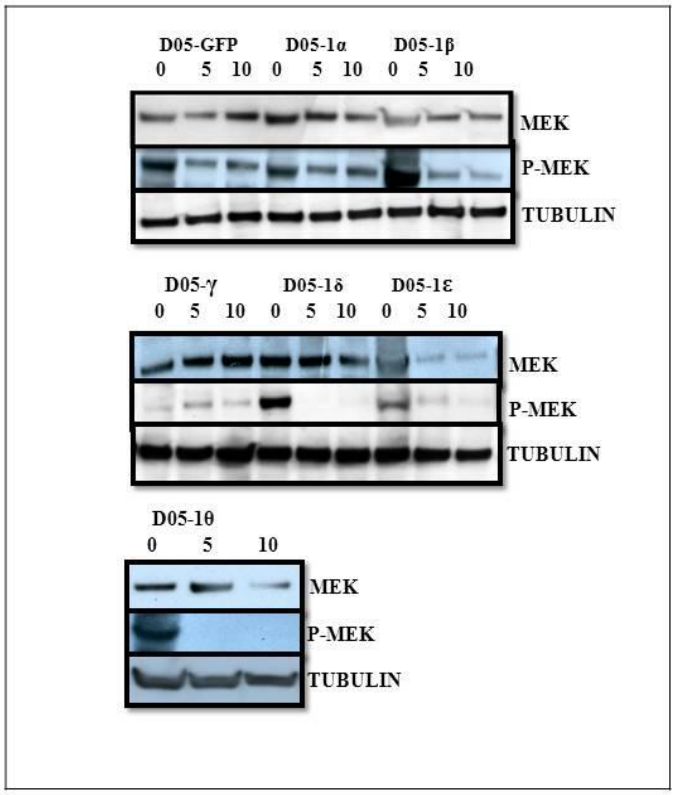

Fig 37-(B) Effect of AMD3100 on CXCL12 splice variants induced phosphorylation of MEK in D05 Cells were treated with different concentrations of AMD3100 0µg\ml,5µg\ml, 10µg\ml

3-12 Animal experiments

3-12-1 In vivo xenograft model

3-12-2 Macroscopic examination of the mouse situs

After sacrificing the mice, the situs was opened and examined macroscopically for tumor infiltra-tion and metastasis. Some organs, such as the intestinum, liver and stomach were removed and inspected. Subsequently, the size of the tumor was determined by a vernier micrometer Fig (38, 39).

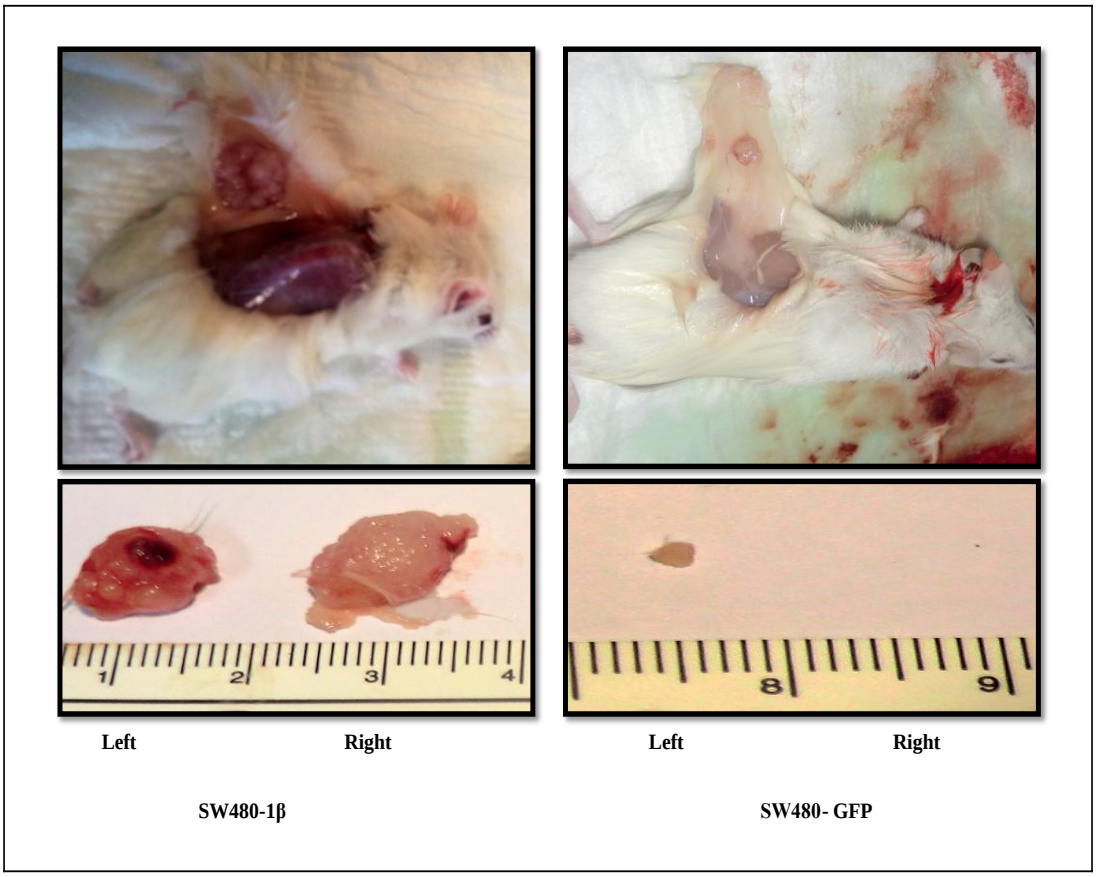

Fig 38- Comparison between tumor infiltration in the positive clone (**SW480-1β**) and control (**SW480- GFP**) .The tumor infiltrated the peritoneum.

Ex vivo analyses of tumor size indicated that compared to SW480-GFP as a negative control all transfected cells (SW480-1α, SW480-1β, SW480-1γ, SW480-1δ, SW480-1ε and SW480-1θ) revealed increased tumor growth. Particular SW480-1β has been associated with high rates of tumor size Fig (39).

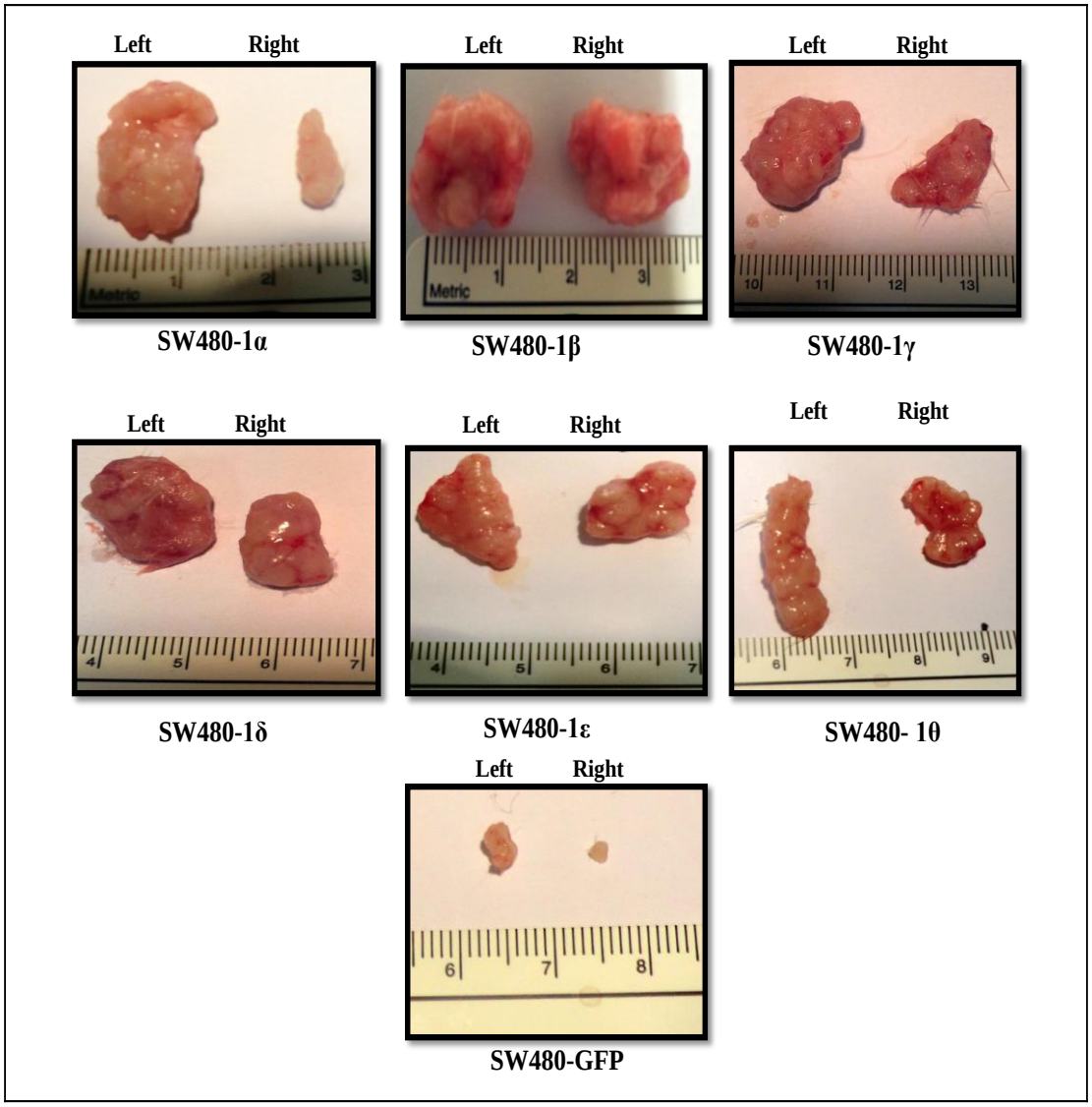

Fig 39- Comparison between tumor size and SDF1 isoforms of animals on the right &left side

We examined the relationship between tumor weight and tumor area with SDF-1 isoforms (Table 32)

gene	N Obs	Variable	Label	N	Mean	Std Dev	Mini-mum	Lower Quar-tile	Medi-an	Upper Quar-tile	Maxi-mum
alpha	6	Weight	Weight	6	25.73	2.13	22.30	24.40	26.30	26.60	28.50
		AreaLeft		6	115.5	51.45	24.00	91.00	132.5	144.00	169.00
		TumorWeight-Right	TumorWeight-Right	6	0	0.20	0.19	0.20	0	0.50	0.73
		AreaRight		6	0.40	50.27	35.00	48.00	0.39	112.00	170.00
					82.50				65.00		
beta	6	Weight	Weight	6	22.78	0.84	21.86	22.00	22.70	23.43	24.00
		AreaLeft		6	146.6	42.02	96.00	120.00	140.0	168.00	216.00
		TumorWeight-Right	TumorWeight-Right	6	7	0.18	0.51	0.53	0	0.87	0.90
		AreaRight		6	0.67	37.04	45.00	48.00	0.61	78.00	140.00
					68.50				50.00		
control	6	Weight	Weight	6	24.42	1.11	23.40	23.60	24.22	24.60	26.50
		AreaLeft		3	2.00	1.73	1.00	1.00	1.00	4.00	4.00
		TumorWeight-Right	TumorWeight-Right	1	0.01	.	0.01	0.01	0.01	0.01	0.01
		AreaRight		1	1.00	.	1.00	1.00	1.00	1.00	1.00
delta	6	Weight	Weight	6	24.15	0.96	22.40	23.77	24.45	24.85	25.00
		AreaLeft		6	74.50	73.60	20.00	25.00	48.00	90.00	216.00
		TumorWeight-Right	TumorWeight-Right	6	0.39	0.20	0.16	0.30	0.33	0.46	0.75
		AreaRight		6	42.83	18.61	25.00	25.00	42.00	60.00	63.00
epsilon	6	Weight	Weight	6	23.73	1.20	22.15	22.90	23.60	24.80	25.30
		AreaLeft		6	59.83	32.68	20.00	25.00	62.00	90.00	100.00
		TumorWeight-Right	TumorWeight-Right	6	0.47	0.14	0.33	0.38	0.44	0.50	0.74
		AreaRight		6	44.83	30.45	28.00	28.00	30.00	48.00	105.00
gamma	6	Weight	Weight	6	23.07	1.23	22.10	22.60	22.70	22.80	25.53
		AreaLeft		6	97.50	51.68	28.00	70.00	88.50	140.00	170.00
		TumorWeight-Right	TumorWeight-Right	6	0.36	0.08	0.28	0.30	0.35	0.43	0.45
		AreaRight		6	41.00	24.84	24.00	25.00	30.50	48.00	88.00
theta	6	Weight	Weight	6	24.85	1.11	23.90	23.90	24.60	25.50	26.60
		AreaLeft		6	80.83	48.31	25.00	30.00	86.00	108.00	150.00
		TumorWeight-Right	TumorWeight-Right	6	0.43	0.14	0.20	0.38	0.44	0.55	0.60
		AreaRight		6	84.50	53.61	40.00	48.00	61.50	120.00	176.00

Table 32- Summary measures for the distribution of tumor weight and tumor area with SDF 1 isoforms

Our results demonstrate that there is a significant difference between the SDF-1 isoforms for tumor weight and tumor area of animals on the left & right side. However SDF1 beta followed by SDF1 alpha showed the highest rate of tumor weight and tumor area of animals as compared with other SDF-1 isoforms Fig (40, 41).

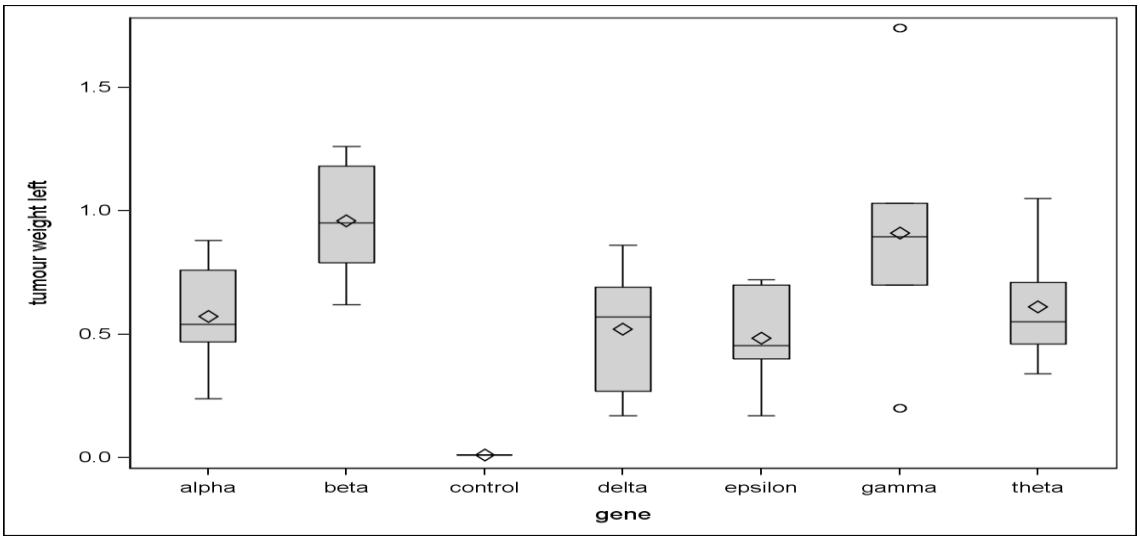

Fig 40-(A) Comparison of the average tumor weight with SDF-1 isoforms of animals on the left side

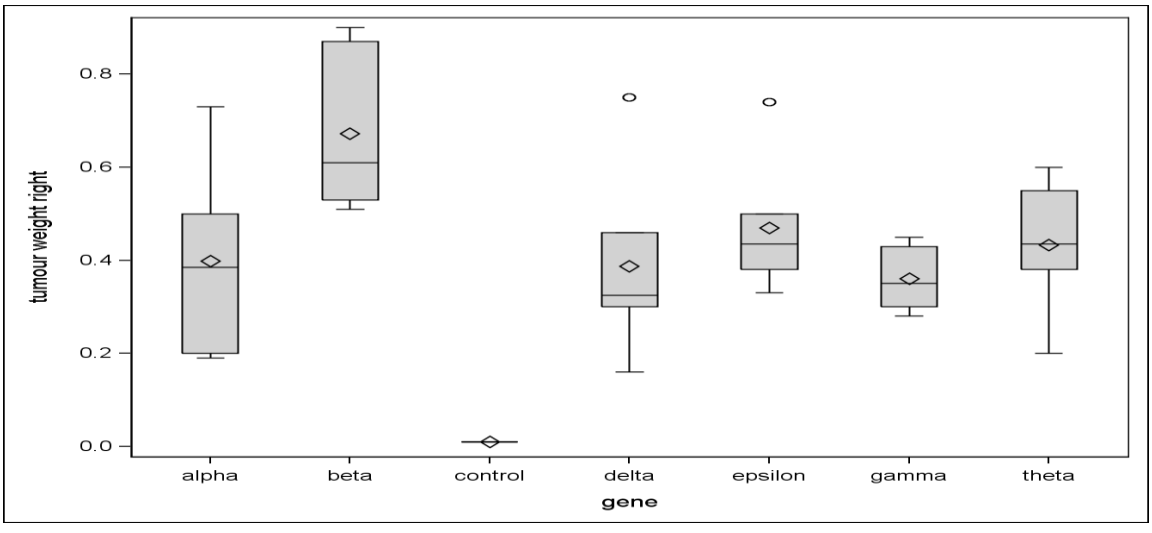

Fig 40-(B) Comparison of the average tumor weight with SDF-1 isoforms of animals on the right side

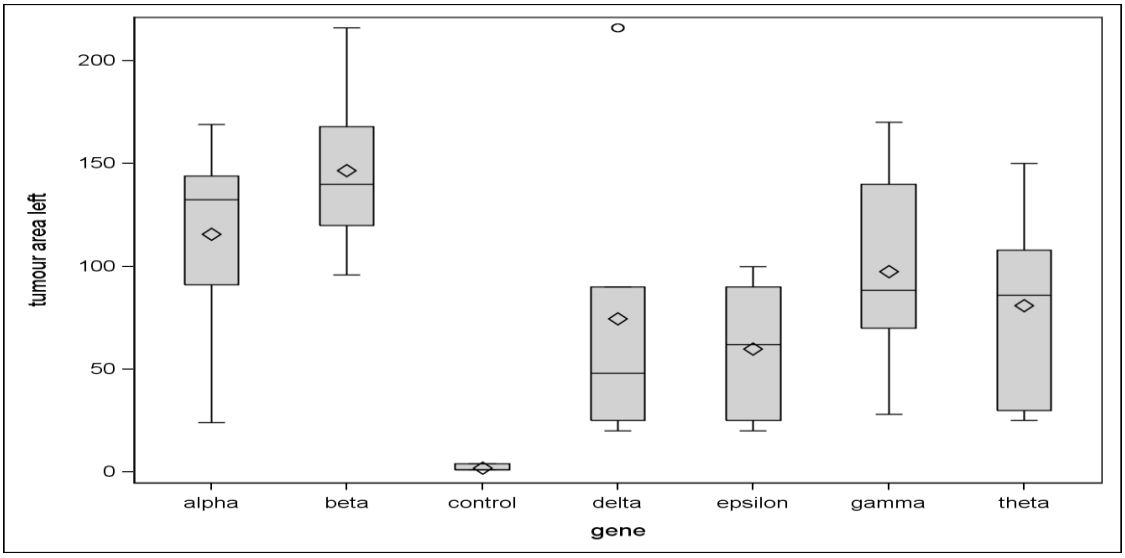

Fig 41-(A) Comparison of the average tumor area with SDF-1 isoforms of animals on the left side

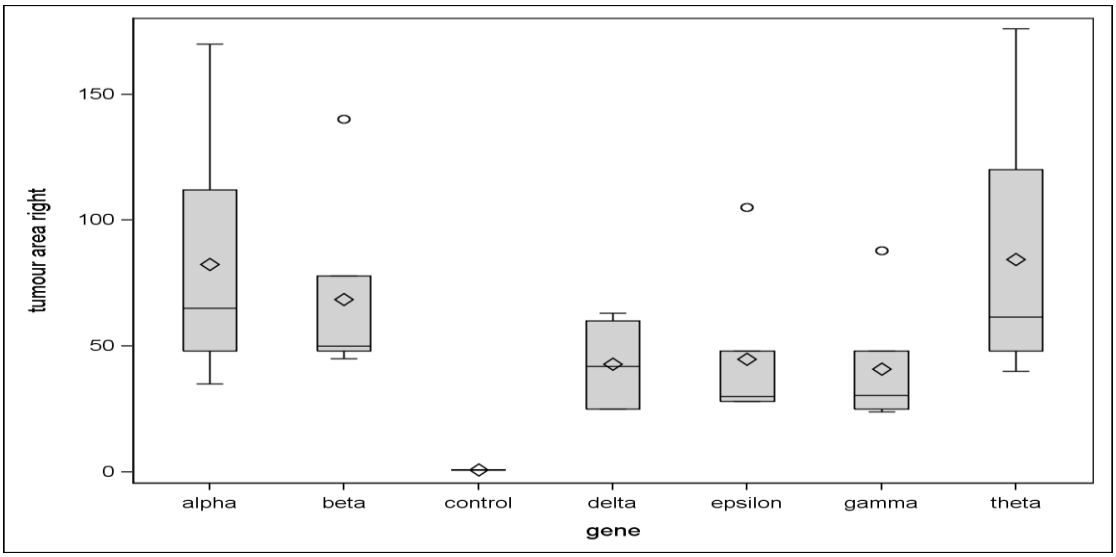

Fig 41-(B) Comparison of the average tumor area with SDF-1 isoforms of animals on the right side

4 DISCUSSIONS

4.1 CXCL12 Gene polymorphism

The novel human CXCL12 (SDF-1) isoforms, known as SDF-1alpha, SDF-1beta, SDF-1gamma, SDF-1delta, SDF-1epsilon and SDF-1theta derived from alternatively splicing events of the same gene [73].

A single-nucleotide polymorphism (SNP), designated CXCL12-G801A (rs1801157), was identified in the 3` untranslated region (3`UTR) of the CXCL12b gene transcript and involved a G-to-A transition at nucleotide position p801 relative to the start codon. The functions of SDF-1 are thought to be important for the pathogenesis of certain diseases [93, 94].

Several studies have been carried out to examine an association between disease susceptibility and CXCL12-3`G801A polymorphism. These studies suggested that CXCL12-3`G801A polymorphism was associated with an increased risk of HIV infection [95], lung cancer [96] breast cancer [97], acute leukemia [98], prostate cancer [99], non- Hodgkins lymphoma [100] and oral squamous cell carcinoma [101,102]. However, only a few studies concern the CXCL12-3`G801A polymorphism in CRC patients to clarify whether the CXCL12-3`G801A polymorphism is associated with disease susceptibility and clinical characteristics in colorectal cancer.

A total of 73 patients were included in our study group, the frequency of G/G homozygote was observed in fifty (68.5%) CRC patients as compared to twenty three (31.5%) patients with G/A and A/A genotypes. it is of interest to compare the results that we obtained by CXCL12 gene polymorphism in human colorectal cancer with those obtained previously. The results of the present study were nearly similar to the results of Dimberg et al., 2007, who studied the CXCL12 Gene polymorphism in 151 CRC patients and 141 controls and reported that the frequency of (GG) (GA) (AA) genotypes were 55.6 (84%), 41.1 (62%) and 3.3 (5%) for their CRC patients respectively, there was no significant difference in genotype distribution between CRC patients and controls [80].

Also our results were nearly similar to the results of Van Rii. et al., 1998, who analyzed the effect of SDFI-gene in 344 participants of the Amsterdam cohort on ADIS-free survival and survival after ADIS diagnosis and reported that 12 (3.5%) subjects were homozygous (AA)

and 95 (27.6%) subjects were heterozygous (GA). The remaining 237 (68.9%) subjects were wild homozygous (GG) [103].

In present study we attempted to determine whether an association existed between the CXCL12 gene polymorphism and CRC, the data in this report showed that the genotype distribution was significantly associated with CRC.

Previous publications further reported that the influence of the CXCL12 gene polymorphism may contribute differentially between colon and rectal cancer in mediating tumor progression, angiogenesis, metastasis and leukocyte migration [80].

Dimberg. et al., 2007 [80] and Hidalgo-Pascual. et al., 2007 [104] could not elicit a significant correlation between CXCL12-A and different prognostic markers such as metastasis development or disease-free survival time in CRC in their studies. Our data were in line with their publication, we only found a trend towards larger primary tumor.

Our results were in disagreement with the study of Chang SC. et al., 2009, who compared the frequency of 6 SDF1alpha single-nucleotide polymorphisms (SNPs) in 424 patients with primary T3 stage CRC. He reported that SDF1alpha-G801A polymorphism was associated with LN metastasis. The frequency of GA/AA genotypes was significantly higher (54.8%) in a group of patients with lymph node metastasis than in patients without LN metastasis (40.7%). In the latter group, disease-free survival was shorter in patients with the GA/AA genotype (74%) than in patients with the GG genotype (87.6%). His conclusion of the experiment was that the SDF1alpha-G801A polymorphism could increase expression of SDF-1alpha mRNA and be a predictive marker of lymph node metastasis in colorectal cancer [105].

To assess the association between the CXCL12 G801A polymorphism and cancer risk, Gong H. et al., 2012, reported that a meta-analysis of 17 studies with 3048 cancer patients and 4522 controls was conducted to evaluate the strength of the association using odds ratio (OR) with 95% confidence interval (CI). The results showed that the variant genotypes were associated with a significantly increased risk of all cancer types (OR=1.38, 95% CI=1.18-1.61 for GA versus GG, and OR=1.36, 95% CI=1.17-1.59 for GA/AA versus GG). This meta-analysis indicated that the CXCL12 G801A polymorphism is a low-penetrance risk factor for cancer development [106].

CXCL12 played an important role in two non related diseases, HIV and cancer, as its receptor (CXCR4) is the co-receptor used by HIV T-tropic strains [94]. The CXCL12 G801A polymorphism was first described in HIV-infected patients [95, 107].

About the role of CXCL12 G801A (rs1801157) polymorphism in other tumors such as breast cancer, Shen W. et al., 2012, reported that the CXCL12 G801A polymorphism had been implicated in breast cancer risk and it may be a low-penetrate risk factor for developing breast cancer [108].

To investigate the effect of the CXCL12 G801A polymorphism in prostate cancer, Hirata H. et al., reported that the frequency of CXCL12 AA genotype was significantly higher in a group of patients with lymph node metastasis (23%) compared with those without metastasis (7%). The frequency of CXCL12 expression in AA + GA genotype carriers was significantly higher than that in GG genotype carriers. This study suggests that CXCL12 G801A polymorphism can be an important marker for detecting micro invasion and PC metastasis [99].

Other studies demonstrated that there was no relationship between the CXCL12 G801A (rs1801157) polymorphism and cervical carcinoma [109] and bladder carcinoma [110].

4.2 Expression and activity of CXCL12 splice variants in Human Colorectal carcinoma and normal colon mucosa

This is the first study analyzing the expression profiles of the chemokine CXCL12 (SDF-1) splice variants in a larger series of human colorectal cancer tissues and normal human mucosa.

It would be interesting to investigate the expression of novel CXCL12 splice variants and to understand the potential pathophysiological relevance under different conditions. Different splice variants in some cases may display similar functions but are active in different tissues or physiological conditions. A better understanding of the functional diversity of SDFI splicing variants may lead to novel therapies that target these variants, which may delay or inhibit the metastatic process in cancer cells.

Previous studies demonstrated that CXCL12 is widely expressed in various organs including heart, liver, brain, kidney, skeletal muscle and lymphoid organs, vascular endothelial cells,

stromal fibroblasts, and osteoblasts are the major cellular source for CXCL12 in these organs [111, 112, 113, 114, 115].

Subsequent studies have confirmed that chemokine CXCL12 is also expressed constitutively in ovarian cancer [116, 117], breast cancer [118, 119], prostate cancer [120, 121], pancreatic cancer [122,123], thyroid cancer [124], Glioblastoma [125] and colorectal cancer [126, 127]. CXCL12 is also expressed in many other human tumors such as renal cell carcinoma, gastric cancer, cervical cancer, kidney cancer, lung cancer and hepatocellular carcinoma [69].

In recent study we have found the expression of the novel splice variants of CXCL12 in colon cancer and mucosa tissues, so we were not surprised to identify the frequent expression of CXCL12 variants in CRC. SDF1alpha was the most predominant splicing variant in both colon and mucosa tissues followed by SDFIbeta, whereas the other splice variants gamma, delta, epsilon and theta were expressed less abundantly. Our findings were consistent with previous data in the literature of Yu, L. et al., 2006, Altenburg, J. et al., 2007, Janowski, M., 2009, that demonstrated that SDFIalpha was a ubiquitously expressed splicing variant in all organs and it played different roles (motogen, mitogen, neuromodulator) in various tissues. SDFIbeta isoform was more limited, his activity in the blood seemed to be designed for inter-organ communication via blood-mediated gradients as well as for supporting angiogenesis [73, 71, 70]. Davis, DA et al., 2005, reported in his study that SDF-1alpha was the most widespread splicing variant. It played important roles in many physiological processes: It was an essential regulator of haematopoiesis, lymphocyte homing, pre-B-cell growth, angiogenesis [128], the management of the HSC population in bone marrow [129], the guidance of primordial germ cells during development [130]. It played a part in the CNS as neuro-modulator [131].

In contrast SDF-1β was less prevalent than SDF-1α and seemed to be related to the vascular system [128]. SDF-1β was more resistant to blood-dependent degradation stimulated angiogenesis and was present in highly vascularized organs such as the liver, spleen, bone marrow and kidneys, with absence in the brain [40, 73, 132].

SDF-1γ -mRNA was expressed at higher levels in adulthood [133]. It was found mainly in the heart, brain and bone marrow [134].

SDF-1δ, SDF-1ε and SDF-1φ splicing variants were all abundant in the pancreas. SDF-1δ was detected in the spleen, fetal liver and lungs whereas SDF-1φ and SDF-1ε were found in the heart and liver, fetal and adult kidneys [70, 73].

4.3 Effect of CXCL12 splice variants on proliferation of colorectal cancer cells

4.3.1 CXCL12 splice variants induced tumor cell proliferation

The effect of CXCL12 splice variants in two cell lines SW480 and D05 was tested ***in vitro*** by using cell proliferation assays. Our findings provided interesting data on CXCL12 (SDF-1) splice variants promoting proliferation of colon cancer cells.

In the present study, we were able to detect functional differences of novel CXCL12 splice variants in their ability to induce tumor cell proliferation. All SDF-1 splice variants had effects on cell proliferation of tumor cells, However SDFI beta and SDFI alpha showed the highest rate of growth as compared with other SDF-1 splice variants.

Numerous studies demonstrated that ligand receptor binding of CXCL12 to CXCR4 axis was involved in several aspects of tumor progression including angiogenesis, cell proliferation, adhesion, and directional migration [52,135,136, 137,138].

Sehgal et al. provided the first evidence that CXCL12 could modulates tumor cell proliferation and survival [139] for mitotic CXCL12 activity in human tumors, where as transfection of an antisense RNA that blocks CXCR4 translation inhibited glioma cell proliferation. After that, Barbero et al. confirmed that glioma cell proliferation can be induced by exogenous CXCL12 [140].

Subsequent studies reported that CXCL12 can induce proliferation of several tumor cell lines, in addition to glioma cells, including ovarian carcinoma [55], small cell lung cancer [54], prostate cancer [141], neck squamous cell carcinoma [142] and pancreatic cancer [143].

CXCL12-dependent proliferation correlated with the activation of ERK1/2 and AKT pathways. Both pathways were known to be involved with the transduction of proliferative signals in normal and tumor glial cells [144].

AKT was known to play a pivotal role in tumor cell survival and possible proliferation [140]. Also P38 and ERK1/2 have been implicated in tumor cell survival; therefore AKT may not be the only player in cell survival signaling [145].

CXCL12 could promote cell survival through the PI3-kinase- and MAP-kinase cascades without cell cycle progression. BAD is a pro-apoptotic protein of the Bcl-2 family that could be inactivated by the CXCL12-mediated activation of MAPK extracellular signal regulated kinases (MEK), extracellular signal-regulated kinase-ribosomal S6 kinases, and PI3K-pathways. Genes associated with cell survival could be up-regulated upon CXCL12 exposure. Thus, CXCL12 promoted cell survival by two mechanisms 1- post-translational inactivation of the cell death machinery 2- an increased transcription of cell survival-related genes [146].

The ERK MAPK pathway was one of the most important mechanisms for cell proliferation in tumor cells [147], CXCL12-dependent cell proliferation was linked to ERK activation [54, 55, 141, 148, 149].

In this experimental study, comparing the results of cell proliferation assay with the results of signal transduction experiments, we showed that SDF-1 beta activated AKT strongly, and AKT could enable proliferation and survival of cells that have sustained a potentially mutagenic impact. Therefore, it could contribute to acquisition of mutations in other genes (As noted above).

4.3.2 Role of AKT in cell proliferation

AKT is a 57 kD Ser/Thr kinase also known as **PKB** (Protein kinase B), that plays a key role in multiple cellular processes including glucose metabolism, apoptosis, transcription, cell migration and cell proliferation.

The function of numerous substrates related to the regulation of cell proliferation, such as glycogen synthase kinase-3 **(GSK-3)** membrane translocation of the glucose transporter **GLUT4**, Cyclin-dependent kinase inhibitors, **P21/Waf1/Cip1** and **P27/Kip2**, mammalian target of rapamycin **(mTOR),** and tuberous sclerosis complex 2 **(TSC2)** modulates by activated Akt protein (Fig 42) [150].

Several factors are directly phosphorylated by AKT. Cross et al., provided the first evidence of kinases regulating GSK3 in insulin, and the inhibition of GSK3 activity by Akt leading to direct phosphorylation of an N-terminal regulatory serine residue downstream of insulin-activated PI3K. They also reported that the inhibition of GSK3 by Akt prevented the phosphorylation of the cytoplasmic signaling molecule β-catenin, which impeded its degradation; hence it was translocated to the nucleus. Once in the nucleus, β-catenin combined with different transcription factors like TCF/LEF-1, to induce the expression of several genes, such as Cyclin D1, which induced cell cycle progression via regulation of RB hyper phosphorylation and inactivation. [151].

AKT phosphorylated both of P21/Waf1/Cip1 and P27/Kip2, and inhibited their anti-proliferative effects by retaining them in the cytoplasm [150].

mTOR is also phosphorylated by Akt, which promotes translation of Cyclin D mRNA. P70 ribosomal protein S6 kinase (P70S6K1) is also activated and eukaryotic initiation factor 4E-binding protein 1 (4EBP1) is inhibited by mTOR [152,153].

Finally Phosphorylation of TSC2 by Akt to inhibited its growth suppressor functions. Phosphorylated TSC2 failed to form a complex with TSC1, which inhibited P70S6K1 (an activator of translation) and activated 4E-BP1 (an inhibitor of translation) [152,154].

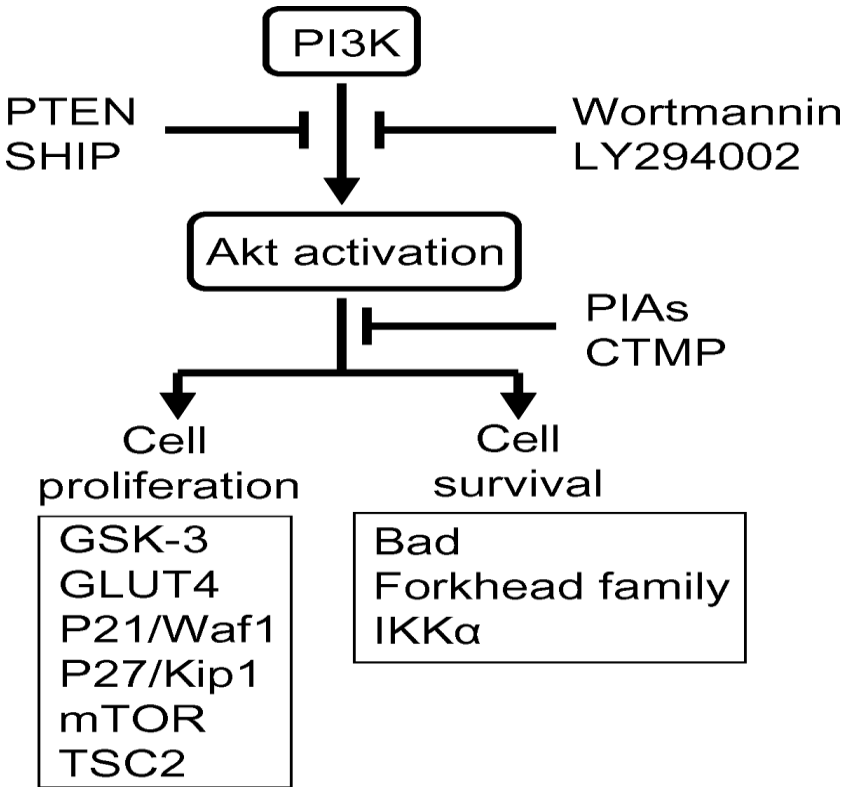

Fig 42- Regulation of cell proliferation and survival by PI3KAkt signalling [150].

4.3.3 Role of MAPK in cell proliferation

The carcinogenesis of colorectal cancer is a complex multistep process involving progressive disruption of intestinal epithelial-cell proliferation, apoptosis, differentiation, and survival mechanisms [155]. The cell cycle is regulated by external signals. Several growth factors trigger signal transduction cascades through binding to membrane receptors and internal cell signalling including Ras mutations and SRC1 activation [156]. Dysregulation of the cell cycle is common and contributes to tumorigenesis in colorectal cancer and other malignant disorders [156]. Several studies demonstrated that the ERK MAPK pathway, but not the JNK pathway or the p38 MAPK pathway, was a major regulator of cell proliferation in colorectal cancer [156].

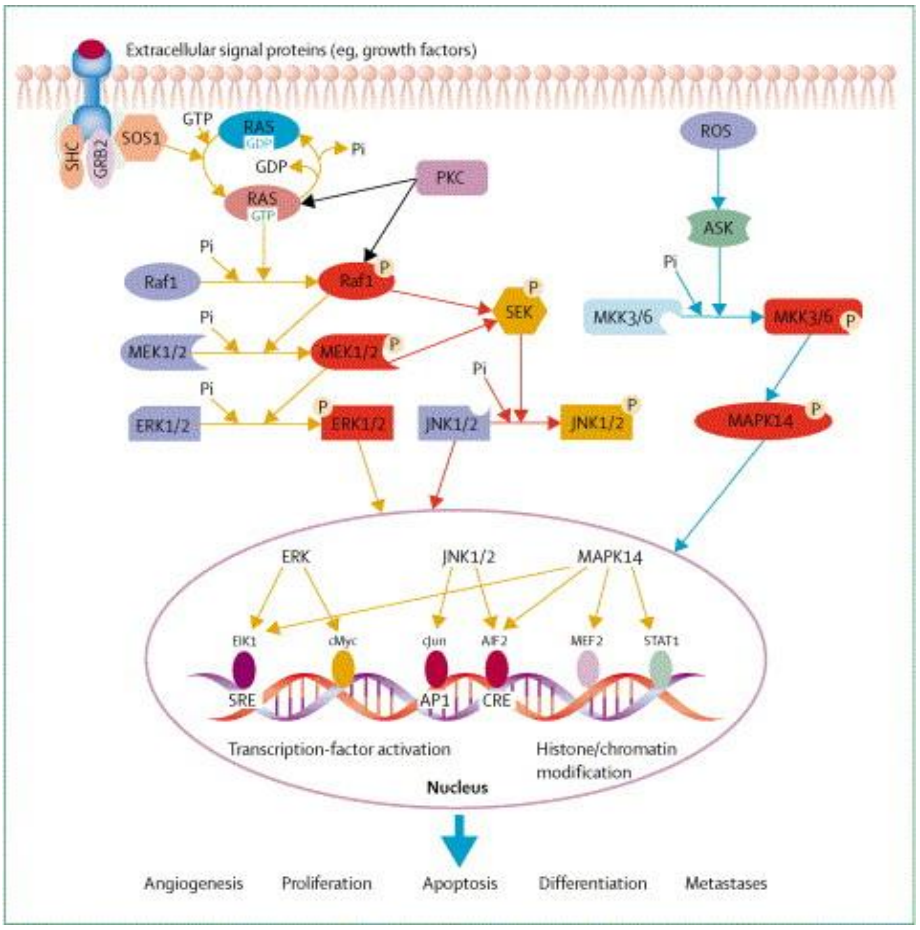

Fig 43- MAPK signalling in pathogenesis [156].

There are three major subfamilies of MAPK: the extracellular-signal-regulated kinases (ERK MAPK, Ras/Raf1/MEK/ERK); the c-Jun N-terminal or stress-activated protein kinases (JNK or SAPK) and MAPK14 also known as P38. That these signalling cascades cause altered gene expression is well established in human beings [157]. The ERK MAPK pathway is one of the most important for cell proliferation [158].

There is an increasing amount of evidence suggesting that the activation of the ERK MAPK pathway is involved in the pathogenesis, progression, and oncogenic behaviour of human colorectal cancer [159].

4.4 Effect of CXCL12 splice variants on migration and invasion of colorectal cancer cells

4.4.1 CXCL12 splice variants stimulate tumor cell migration and invasion

The effect of CXCL12 splice variants in two cell lines SW480 and D05 was tested ***in vitro*** by using cell migration and cell invasion assays.

The major findings of the present study were that all SDF-1/CXCL12 splice variants promoted cell migration and invasion of colorectal cancer cells. SDF-1 theta and SDF-1 epsilon induced migration and invasion more than other splice variants of colorectal cancer.

The functional role of the CXCL12/CXCR4 axis in tumor progression and metastasis has been emphasized. Several lines of evidence suggested that the CXCL12/CXCR4 system was involved in the progression and metastasis of CRC ligand receptor binding of CXCL12 to CXCR4 [160, 161, 162].

The CXCL12/CXCR4 pathway could mediate cancer cells homing to specific secondary sites, thereby promoting organ-specific metastasis. The first evidence provided by Muller et al. 2001 showed that the CXCL12/CXCR4 pathway mediated human breast cancer metastasis. The blocking of CXCR4 in vivo with the use of a specific antibody or selective synthetic polypeptide or siRNA resulted in significant inhibition of breast cancer metastasis to regional lymph nodes as well as in the lung [163].

The blocking of CXCR4 expression on the cell surface greatly reduced the ability of colon cancer cells to metastasize to liver and lungs [164].

Many studies demonstrated that high levels of CXCL12 are found in different organs such as lymph nodes, lung, liver, and bone marrow, where tumors frequently metastasize [163,165,166]. In addition to what we have mentioned above, Hypoxia induced expression of CXCR4 on tumor cells [167]. This would sensitize tumor cells to CXCL12 signals and promote tumor metastasis. Yet, hypoxia stimulates both CXCR4 and CXCL12 expression [62]. Human cancer cells express CXCL12 such as neuroblastoma [168], glioblastoma [140], Ovarian [55,62], Breast [118, 119, 163], Colon [167], Prostate [121] and Pancreas [122].

The pathway Ras/Raf/MEK/ERK included several proto-oncogenes and was deregulated in about 30% of all cancers. This cascade was involved in the control of growth signals, cell survival, and invasion in cancer. During the process of oncogenic transformation, colorectal cancer cells escaped from normal growth and differentiation control and acquired the ability to invade surrounding tissues and organs [156].

In this present experimental study, we compared the results of cell migration and invasion assay with the results of signal transduction experiments and could show that the stimulation of CXCL12/CXCR4 played an important role in colon cell migration and invasion by the induction of MEK1/2 and AKT signal transductions. SDF-1 theta and SDF-1 epsilon activated MEK1/2 strongly and MEK1/2 could enable cell migration and invasion in tumor cells (As noted above).

Our findings tested also that CXCL12 and its splice variants played an important role in the invasion as well as the metastasis in colon cancer. These results were consistent with the previous studies that demonstrated the activation of ERK and AKT signalling after stimulation of cancer cells with CXCL12 [169-171]. A high level of actin polymerization was a key for the formation of pseudopodia in cancer cells, which in turn were implicated in the enhancement of cancer cell migration and invasion [172, 173]. Brand, S., 2005, reported that CXCL12 could activate ERK-1/2, SAPK/JNK kinases, AKT and matrix metalloproteinase-9 (MMP-9). These CXCL12-induced signals mediated reorganization of the actin cytoskeleton, resulting in increased colon cell migration and invasion. [171].

Bonacchi, A. et al., 2001, observed that the activation of MAP kinases such as ERK-1/2 and the activation of AKT have been linked to cell migration [174].
Sotsios, Y.et al., 1999, indicated that CXCL12 predominantly activated MEK-ERK MAP kinase and Akt signalling. Interestingly, the activation of ERK-MAP kinases and Akt has been implicated in cell migration [175]. Finally several studies have demonstrated the persistent localization of matrix metalloproteinase (MMP) expression to the interface between invading CRC cells and surrounding stroma, supporting a role for MMP secretion in CRC invasion and metastasis [176].

4.5 Effect of CXCL12 splice variants on adhesion of colorectal cancer cells

4.5.1 CXCL12 splice variants promote tumor cell adhesion

The effect of CXCL12 splice variants in two cell lines SW480 and D05 was tested ***in vitro*** by using cell adhesion assay.

Our experiments demonstrated that all SDF-1/CXCL12 splice variants induced cell adhesion of colorectal cancer cells in vitro. SDFIbeta and SDFIalpha promoted colorectal cell adhesion more than other splice variants.

Metalloproteases (MMPs) are a family of enzymes involved in the degradation of extracellular matrix in the surrounding normal tissue and mediated cancer invasion and metastases [177]. Activation of Metalloproteases broke down the physical barriers of metastasis, thus promoting invasion by cancer cells [178]. CXCL12 may modulate the expression and function of cell surface integrin molecules and promoted tumor cell adhesion. Integrins are a large family of heterodimeric transmembrane glycoproteins that attached cells to extracellular matrix proteins of the basement membrane or to ligands on other cells. CXCL12 induced adhesion of SCLCs to VCAM-1, fibronectin, and collagen [179,180].

In support of this observation numerous studies have documented that the chemokine CXCL12 induced MMP synthesis in different cell types and facilitated tumor cell adhesion and colonization [181-185].

The CXCL12/CXCR4 pathway was implicated in the mechanic process of tumor metastasis including tumor cell adhesion and migration [69].

4.6 AKT and MAPK signalling pathways involving in colorectal cancer

4.6.1 Effect of CXCL12 splice variants on the phosphorylation of AKT in colorectal cancer

Signal transduction experiments indicated that CXCR4/CXCL12 pathway was functional in human CRC cells mediating specific functions such as CRC proliferation, migration and invasion [171]. Therefore, the importance of AKT and its signalling pathway in colorectal carcinogenesis was the topic of this work.

Here the major research goal was to understand the function of AKT and oncogenic activity in colon cancer. A recent study found that all six CXCL12 splice variants activated and expressed phospho-AKT. CXCL12-beta has the strongest expression followed by CXCL12-alpha. and CXCL12-theta has the weakest expression as compared to other variants.

Understanding AKT kinase and its downstream signaling pathway was important to exploit Akt as a target for therapeutic intervention for cancer.

Akt was involved in the pathway PI3K/AKT/mTOR and PI3K/AKT which activated human cancer [186].

AKT was a major downstream effector of PI3K and played pivotal roles in protein synthesis, cellular metabolism, survival, and proliferation. [187]. Baba et al., 2011, examined the role of activated AKT expression in 717 patients with colorectal cancer. They reported that p-AKT expression was related with early stage disease and good prognosis. P-AKT expression might serve as positive prognostic marker in colorectal cancer patients [187].

Previous studies indicated that Akt / protein kinase B was related with various cellular responses, including tumor cell survival, proliferation, and invasiveness. The activation of Akt was also one of the most frequent alterations observed in human cancer. Tumor cells that had constantly active Akt could depend on Akt for survival [188,189].

Huang X.F., Chen J.Z,. 2009, demonstrated that the PI3K/Akt signal pathway activated numerous signals for cell survival, cell growth and cell cycle leading to carcinogenesis [190].

Two main intracellular pathways, the mitogen-activated protein kinase (MAPK) pathway and the phosphatidylinositol 3-kinase- (PI3K-) protein kinase B (AKT), were activated by the epidermal growth factor receptor (EGFR). These pathways led to the activation of numerous transcription factors, which then impact cellular responses including proliferation, migration, differentiation, and apoptosis [191].

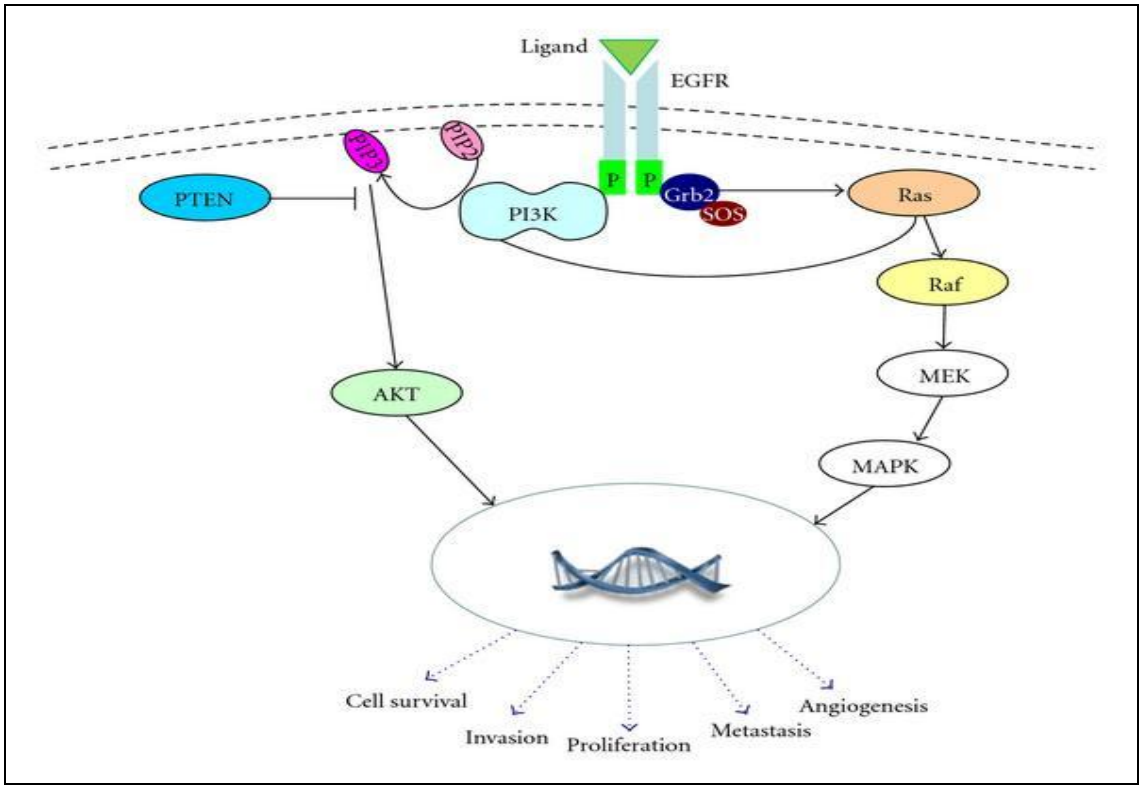

Fig 44- EGFR regulates AKT and MAPK signalling pathway [188]. Signalling through the EGFR pathway is a complex process that may contribute to tumor progression through increased, cell survival, invasion, cell proliferation metastasis and angiogenesis.

4.6.2 Effect of CXCL12 splice variants on the phosphorylation of MAPK in colorectal cancer

Our findings reinforced the concept of a critical role for the CXCL12 splice variants axis in colorectal cancer pathogenesis. One of the most important results of the current study was that all six CXCL12 splice variants activated and expressed phospho-MEK 1/2 in colorectal cancer cells which varied from strong (Delta, Epsilon and Theta) and intermediate (Gamma) to weak (Alpha and Beta).

Similarly, all six CXCL12 splice variants activated and expressed phospho-SAPK/JNK in colorectal cancer cells, while no p38 MAP kinase activation was observed.

It was of interest to compare the results that we obtained of MAPK pathway in human colorectal cancer cells with those obtained previously. Brand, S., 2005, reported in his study that CXCL12 induced a transient activation of ERK-1/2 and SAPK/JNK, whereas no p38 MAP kinase activation was observed in cell line HT-29. He reported that similar observation was obtained in colorectal cell line SW480 cells [171]. Wang Y. K. et al., 2010, indicated that the kinase activities of Akt and extracellular signal-regulated kinase (Erk) 1/2 were significantly upregulated in primary colon cancer cells CD133 (+) [192].

Mitogen-activated protein kinases (**MAPkinases)** are serine/threonine-specific protein kinases which belong to the **CMGC** (**C**DK/**M**APK/**G**SK3/**C**LK) kinase group.
There are three major subfamilies of MAPK: [192,193]

The extracellular signal–regulated kinases (ERKs) are widely expressed and are involved in the control of cell division, and inhibitors of these enzymes are being explored as anticancer agents.

The c-Jun amino-terminal kinases (JNKs) are regulated several important cellular functions including cell growth, differentiation, survival and apoptosis and are responsive to stress stimuli, such as cytokines, ultraviolet irradiation, heat shock, and osmotic shock. [193].

P38 mitogen-activated protein kinases are activated by a variety of cellular stresses stimuli including hormones, ligands for G protein–coupled receptors and stresses such as osmotic shock, ultraviolet light, irradiation, and heat shock. The p38 MAPKs are key regulators of inflammatory cytokine expression, they appear to contribute to human diseases like asthma and autoimmunity [193].

The MAPK is one of the most important signalling pathways regulate diverse cellular processes such as proliferation, gene expression, differentiation, mitosis, movement, metabolism, cell survival and apoptosis. MAPKs signalling are involved in directing cellular responses to a numerous array of stimuli, including mitogens, osmotic stress, heat shock and pro-inflammatory cytokines [193, 194]. It is de-regulated in various diseases, ranging from cancer to immunological, inflammatory and degenerative syndromes [195].

Focusing on the ERK MAPK pathway (Fig 45), the Raf-MEK-ERK pathway was a key downstream effector of the Ras small GTPase, the most frequently mutated oncogene in different human cancers. Ras was a key downstream effector of the epidermal growth factor receptor (EGFR), which was mutationally activated and/or overexpressed in a wide variety of human cancers. ERK was a downstream signalling module that was activated by the Raf serine/threonine kinases. Raf activated the MAPK/ERK kinase (MEK)1/2 dual-specificity protein kinases, which then activated ERK1/2. The mutational activation of Raf in human cancers supports the important role of this pathway in human oncogenesis [196].

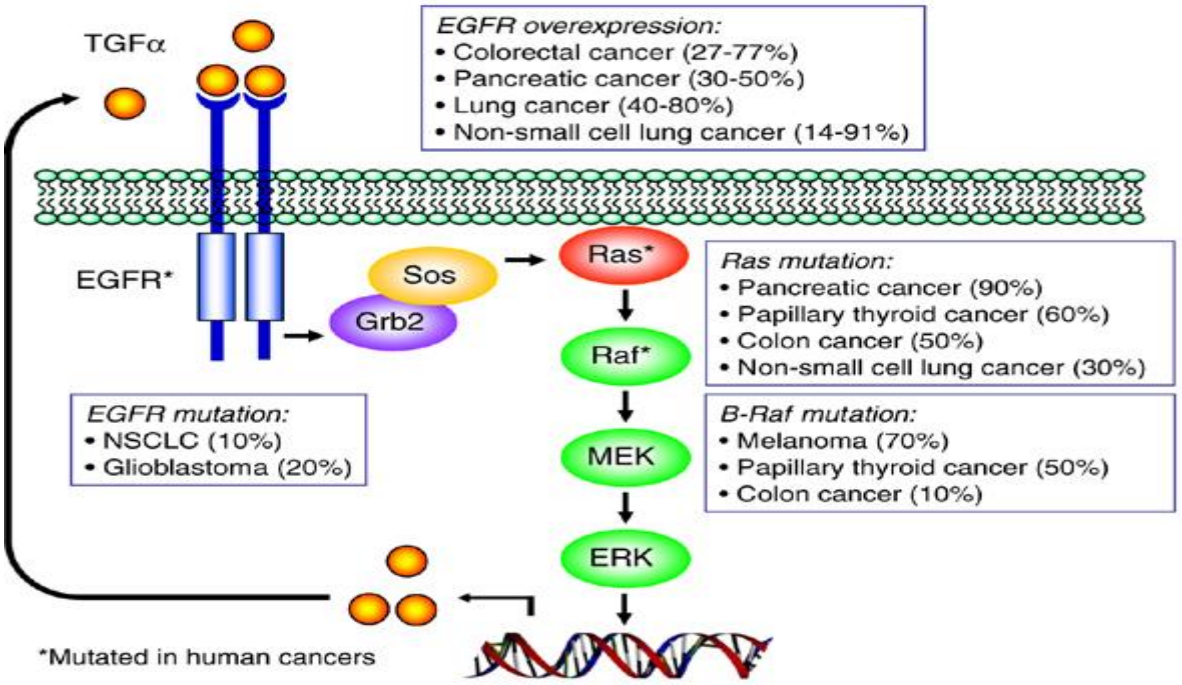

Fig 45- Activation of the ERK MAPK cascade by mutated oncogene in human cancers [196]. Activated Ras activates the protein kinase activity of RAF kinase. RAF kinase phosphorylates and activates MEK, MEK phosphorylates and activates a mitogen-activated protein kinase (MAPK) (also known as ERK).

4.7 AMD3100 inhibits cell Proliferation of colon cancer

The treatment with AMD3100 (antagonists of CXCR4) markedly reduced cell viability of tumor cells in vitro.

We have shown that AMD3100 significantly inhibited the proliferation ability of SW480 and D05 cells with concentration 5µg/ml and 10µg/ml, especially with CXCL12 variants (gamma, delta, epsilon and theta), but not with CXCL12 (alpha and beta). These results were consistent with the studies by Li, J. K., 2008, who reported that the AMD3100 could inhibit proliferation, invasion and metastasis activity of the colorectal cell line SW480 through down-regulation of VEGF and MMP-9 expression [197].

4.7.1 AMD3100 exclusively inhibits CXCL12/CXCR4-mediated colorectal cancer

The inhibition of CXCL12/CXCR4 and its pathway by AMD3100 may represent one of the potential approaches in colon cancer therapy.

To evaluate whether AMD3100 (antagonists of CXCR4) activation on CRC cells led to new therapeutic avenues for CRC patients, we have demonstrated the potent antagonistic activity of AMD3100 against CXCL12 splice variants in colorectal cell line and melanoma cell line after treatment with AMD3100 at different concentrations (0µg/ml-5µg/ml -10µg/ml).

AKT and MAPK pathways were representing an important drug target for many diseases; here in the present study we gave an overview of the role of AMD3100 as a therapeutic potential for treatment of colon cancer by targeting AKT and MEK pathways. Our findings showed that the inhibition of CXCL12 splice variants by AMD3100 suppressed the phosphorylation of MEK1/2 and AKT from strong with CXCL12 (delta, epsilon and theta) to weak with CXCL12 gamma, whereas it had no significant effect on CXCL12(alpha and beta). As we have mentioned above, AMD3100 inhibited the Proliferative properties of CXCL12 splice variants (gamma, delta, epsilon and theta), but not with CXCL12 (alpha and beta) in colon cancer cells. These results were consistent with the previous studies that demonstrated the inhibition of CXCR4 by AMD3100 and supressed the phosphorylation of MEK1/2 and AKT [173].

Ganju et al. reported that in both, in vitro and in vivo mouse models, several CXCR4/CXCL12 antagonists have been shown to have potential therapeutic effects to inhibit tumor growth and metastasis of various cancers [198].

The bicyclam derivative plerixafor hydrochloride (AMD-3100) has been described as a highly therapeutic potential for the treatment of HIV infection, inflammatory diseases, cancer and stem cell mobilization [87,88,199].

5. SUMMARY

5.1 Summary

The chemokine CXCL12, also known as stromal cell-derived factor-1 (SDF-1) is a small protein (8-14 KDa), which is expressed in six isoforms (SDF-1α, SDF-1β, SDF-1γ, SDF-1δ**,** SDF-1ε and SDF-1θ) from a single gene. This gene regulates leukocyte trafficking and is variably expressed in a number of normal and cancer tissues.

In addition to that, literature evidence suggests that CXCL12 plays multiple roles in tumor pathogenesis**:** it promotes tumor growth and malignancy, enhances tumor angiogenesis, participates in tumor metastasis, and contributes to immunosuppressive networks within the tumor microenvironment.

To shed light on the role of the chemokine CXCL12 splice variants in the development of cancer and to understand the potential physiological relevance and their possible functional differences in colorectal cancer, we transfected and expressed all CXCL12 splice variants (alpha, beta, gamma, delta, epsilon and theta) in colorectal cell line SW480 and melanoma cell line D05.

The study outlined in this thesis was designed to address the following aims:

- To investigate the roles of CXCL12 splice variants in mediating tumor progression, adhesion, migration, invasion and metastasis of colorectal cancer.
- To investigate whether the CXCL12 variants pathways represent an important target for developing cancer therapies.
- To develop an in vivo mouse model to investigate the role of the CXCL12 variants in the increased of tumor growth in colorectal cancer.

Our findings demonstrate that:

- The CXCL12 G801A polymorphism is a low-penetrance risk factor for the development of colorectal cancer. CXCL12 gene polymorphism rs1801157 is correlated with local progression of the primary tumor as indicated by the T status (tumor-node-metastasis). Whereas there is no relation between CXCL12 Gene polymorphism rs1801157 and distant or nodal metastisis.

- All six CXCL12 splice variants are expressed in colon cancer and healty colon mucosa. A high rate of expression was significantly associated with SDF-1alpha then SDF-1 beta.
- All six CXCL12 variants enhanced tumor cell proliferation in vitro. SDF-1beta then SDF-1alpha showed the greatest activity in proliferation assay.
- All six CXCL12 variants induced tumor cell adhesion in vitro, SDF-1beta then SDF-1alpha showed the greatest activity in the adhesion assay.
- All six CXCL12 variants enhanced cell migration and invasion in tumor cells in vitro. SDF-1epsilon and SDF-1theta showed the greatest activity and the weakest activity was observed with SDF-1alpha and SDF-1beta.
- All six CXCL12 variants activated Akt and (MAPK) mitogen activated protein kinase pathways, thus regulating many essential processes in tumor cells, cell survival, proliferation, migration, invasion and adhesion.
- It is interesting to note that, AMD3100 was shown to inhibit CXCL12 splice variants which induced AKT & MEK-1/2 phosphorylation.
- The inhibitor AMD3100 suppressed strongly CXCL12 variants, -delta, -epsilon and -theta and suppressed weakly CXCL12-gamma, whereas it had no significant effect on CXCL12- alpha and beta. It may affect several major signaling pathways related to proliferation, migration and invasion.

- It is important to note that the Inhibition of CXCL12 variants and its pathway by AMD3100 may represent one of the potential approaches in cancer therapy.
- We propose that in further studies we need to clearly understand the biological activities of these novels CXCL12 variants in different types of cancers.

5.2 ZUSAMMENFASSUNG

Das Chemokin CXCL12 (auch bekannt als SDF-1) ist ein kleines Protein (8-14) KDa, das in sechs Isoformen exprimiert wird (SDF-1α, SDF-1β, SDF-1γ, SDF- 1δ, SDF-1ε und SDF-1θ) von einem einzigen Gen, dass die Leukozyten-Wanderung regelt und variabel in einer Reihe von normalen und Krebsgeweben exprimiert wird.

CXCL12 spielt verschiedene Rollen in der Tumorpathogenese. Es wurde nachgewiesen, dass CXCL12 das Tumorwachstum und die Malignität fördert, die Tumorangiogenese stärkt, sich an der Metastasierung beteiligt und zu immunsuppressiven Netzwerken innerhalb des Tumormikromilieus beiträgt. Daher liegt es nahe, dass der CXCL12/CXCR4-Signalweg ein wichtiges Ziel ist für die Entwicklung von neuartigen Krebstherapien.

Um Licht auf die Rolle der Chemokin CXCL12 Splicevarianten in der Entwicklung von Krebs zu werfen und die mögliche physiologische Relevanz und ihre möglichen funktionellen Unterschiede bei Darmkrebs zu verstehen, haben wir alle CXCL12 Splicevarianten (alpha, beta, gamma, delta, epsilon und theta) in die kolorektalen Zelllinie SW480 und die Melanomzellinie D05 transfiziert und exprimiert.

Diese Arbeit wurde erstellt, um die folgenden Ziele zu erreichen.

- Untersuchung der Rolle von CXCL12 Splicevarianten bei der Vermittlung von Tumorprogression, Adhäsion, Migration, Invasion und Metastasierung von Darmkrebs.
- Untersuchung, ob die CXCL12 Variantenwege ein wichtiges Ziel für die Entwicklung von Krebstherapien darstellen.
- Um eine in vivo Mausmodell zu entwickeln, um die Rolle der CXCL12 Varianten im Rahmen des Tumorwachstums zu verstehen.

Unsere Ergebnisse zeigen, dass:

- Der CXCL12 G801A Polymorphismus ist ein Low-Penetranz Risikofaktor für die Entwicklung von Darmkrebs. Der CXCL12-Gen-Polymorphismus rs1801157 ist mit dem T-Status (Tumor-node-Metastasen) assoziiert. Es gab keine Beziehung zwischen CXCL12-Gen-Polymorphismus rs1801157 und Fernmetastisen oder LN metastasen.

• Alle sechs CXCL12 Splicevarianten werden im Darmkrebs und in gesunder Kolon mucosa exprimiert. Die höchste Expression wird bei SDF-1alpha, dann SDF-1 beta gefunden.

• Alle sechs CXCL12 Varianten zeigen erhöhte Tumorzellproliferation in vitro. SDF-1beta, gefolgt von SDF-1alpha zeigte die größte Aktivität im Proliferationsassay.

• Alle sechs CXCL12 Varianten induzieren die Tumorzelladhäsion.SDF-1beta dann SDF-1alpha zeigte die größte Aktivität im Rahmen des Adhäsionsassay.

• Alle sechs CXCL12 Varianten erhöhten die Zellmigration und Invasion von Tumorzellen in vitro. SDF-1theta und SDF-1epsilon 1theta zeigten die größte Aktivität, während die schwächste Aktivität mit SDF-1alpha und SDF-1beta beobachtet wurde.

• Alle sechs CXCL12 Varianten aktivieren Akt und (MAPK) Mitogen- acktivatedierte Protein kinase Wege und damit die Regulierung viele essentieller Prozesse in Tumorzellen, wie Proliferation, Migration, Invasion und Adhäsion.

• Es ist interessant festzustellen, dass AMD3100 die CXCL12 Splicevarianten inhibriert, die AKT-MEK-1/2-Phosphorylierung induzieren.

Der Inhibitor AMD3100 unterdrückt stark die CXCL12 Varianten -delta, -epsilon und theta- und unterdrückt schwach CXCL12-gamma. während es keine signifikante Wirkung auf CXCL12-alpha und beta hatte. Es hat möglicherweise Auswirkungen auf mehrere große Signalwage in Bezug auf Proliferation, Migration und Invasions.

• Es ist wichtig anzumerken, dass die Hemmung von CXCL12-Varianten durch AMD3100 einen der möglichen Ansaätze in der Krebstherapie darstellen kann.

• Wir schlagen vor, dass weitere Studien erwogen werden, die wir brauchen, um die biologische Aktivität dieser neuen CXCL12 Varianten bei verschiedenen Arten von Krebs klar zu verstehen.

6 REFERENCES

[1] Germ Cancer Research Center Heidelberg. The Most Frequent Causes of Death in Germany in 2010: In: ***https://www.dkfz.de/en/krebsatlas/total/mort_2_e.html.*** Last updated 26.10.12 (date of access 5.11.12).

[2] Jemal A., et al., Global cancer statistics. CA Cancer J Clin 2011: 61:69-90.

[3] Robert Koch Institute and the Society of Epidemiologcal Cancer Registries in Germany: cancer in Germany. 2007/2008.8 Issue. Berlin 2012.

[4] Germ Cancer Research Center Heidelberg. Trend graph for the five leading groups of cause's death in Germany.In: ***https://www.dkfz.de/en/krebsatlas/total/mort_6_e.html .*** Last updated 26.10.12 (date of access 5.11.12).

[5] World Health Organization. The global burden of disease: 2004 update. Geneva: World Health Organisation; 2008.

[6] American Cancer Society. What is cancer? In: ***http://www.cancer.org/Cancer/CancerBasics/what-is-cancer.***

[7] Germ Cancer Research Center Heidelberg. The 20 most frequent causes of cancer death in Germany. In: ***https://www.dkfz.de/en/krebsatlas/total/organ_e.html.*** Last updated 25.09.12 (date of access 5.11.12).

[8] Cancer Research .UK. How many different types of cancer are there? In: ***http://www.cancerresearchuk.org/cancer-help/about-cancer/cancer-questions/how-many-different-types-of-cancer-are-there.***

[9] National Cancer institute. Understanding Cancer Series Posted: 01/28/2005 Reviewed: 09/30/2009. In: ***http://www.cancer.gov/cancertopics/understandingcancer/cancer/page4***

[10] National Cancer institute. Understanding Cancer Series Posted: 01/28/2005 Reviewed: 09/30/2009**.** In: ***http://www.cancer.gov/cancertopics/understandingcancer/cancer/page9***

[11] National Cancer institute. Understanding Cancer Series Posted: 01/28/2005 Reviewed: 09/30/2009**.** In: ***http://www.cancer.gov/cancertopics/understandingcancer/cancer/page2***

[12] Kuma V., Robbins SL., Robbins basic pathology. 8th ed. Philadelphia, PA: Saunders/Elsevier; 2007.

[13]American Cancer Society. Cancerfacts and figures 2011. In: http://***www.cancer.org/.../cancerfactsfigures/cancerfact.***

[14] Birgisson H., Cancer of the Colon and Rectum, PHD thesis submitted to faculty of medicine, Uppsala University, Swedisch, 2006.

[15] American Society of Colon & Rectal Surgeons, 2012 In: ***http://www.fascrs.org/patients/conditions/colorectal_cancer/.***

[16] Chan A.T., Giovannucci E.L., Primary prevention of colorectal cancer.Gastroenterology 2010, 138(6):2029-2043.

[17] Yeatman T., Colon cancer .secondary article .University of South Florida, Tampa, Florida, USA, 2001.

[18] Fearon E.R., Vogelstein B. A., genetic model for colorectal tumorigenesis .Cell.1990,61 (5):759-67.

[19] Vogelstein B., et al., Genetic alterations during colorectal-tumor development.N Engl J Med. 1988, 319 (9):525-32.

[20] Vogelstein B., Kinzler K.W., Cancer genes and the pathways they control. Nat Med. 2004 ,10(8):789-99.

[21] Andreyev H.J., et al., Kirsten ras mutations in patients with colorectal cancer: the multicenter "RASCAL" study. J Natl Cancer Inst. 1998, 90(9):675-684.

[22] Kahlenberg M.S., et al., p53 tumor suppressor gene status and the degree of genomic instability in sporadic colorectal cancers. J Natl Cancer Inst .1996, 88(22):1665-1670.

[23] Cho K.R., Fearon E.R., DCC: linking tumour suppressor genes and altered cell surface interactions in cancer? Eur J Cancer .1995, 31A (7-8):1055-1060.

[24] Markowitz S.D., Bertagnolli M.M., Molecular origins of cancer: Molecular basis of colorectal cancer. N. Engl. J. Med.2009, 361(25): 2449-2460.

[25] Haubrich W.S., Dukes of the Dukes classification. Gastroenterology .2000,118 (5):828.

[26] Sobin L.H., TNM: evolution and relation to other prognostic factors. Semin Surg Oncol 2003, 21(1):3-7.

[27] Sobin L.H., Gospodarowicz M.K., Wittekind Ch., TNM classification of malignant tumours. ebrary, Inc. In. 7th ed. Chichester, West Sussex, UK ; Hoboken, NJ: Wiley-Blackwell; 2009.

[28] Baird PN., D'Andrea RJ., Goodall GJ., Cytokine receptor genes: structure chromosomal location, and involvement in human disease. Leuk Lymph .1995,18(5-6): 373-83.

[29] Cohen M.C., Cohen S., Cytokine function. A study in biologic diversity. Am J Clin Pathol. 1996, 105(5): 589-98.

[30] Germano G., Allavena P., Mantovani A., Cytokines as a key component of cancer-related inflammation. Cytokine. 2008, 43(3): 374-9.

[31] Bajetto A., et al., Chemokines and their receptors in the central nervous system. Front Neuroendocrinol. 2001, 22(3): 147-84.

[32] Charo I.F., Ransohoff R.M., The many roles of chemokines and chemokine receptors in inflammation. N Engl J Med. 2006, 354(6): 610-21.

[33] Viola A., Luster A.D., Chemokines and their receptors: drug targets in immunity and inflammation. Annu Rev Pharmacol Toxicol. 2008, 48: 171-97.

[34] Fernandez E.J., Lolis E., Structure, function, and inhibition of chemokines. Annu Rev Pharmacol Toxicol.2002, 42: 469-99.

[35] Vandercappellen J., Van Damme J., Struyf S., The role of CXC chemokines and their receptors in cancer. 2008, 267(2):226-44.

[36] Raman D., et al., Role of chemokines in tumor growth.Cancer Lett.2007, 256(2):137-65.

[37] Zlotnik A., Yoshie O., Chemokines: a new classification system and their role in immunity. Immunity .2000 , 12(2):121-7.

[38] Murphy PM., et al., International union of pharmacology. XXII. Nomenclature for chemokine receptors. Pharmacol Rev. 2000, 52(1): 145-176.

[39] Arya M., The role of the CXCL12 – CXCR4 chemokine ligand – receptor interaction in the metastasis of prostate cancer 2010.PHD thesis. Division of Surgery and Interventional Science, University College London.

[40] Sun X., et al., CXCL12/CXCR4/CXCR7 Chemokine Axis and Cancer Progression. Cancer Metastasis Rev. 2010, 29(4): 709–722.

[41] Drury L.J., Wendt M.K., Dwinell M.B., CXCL12 chemokine expression and secretion regulates colorectal carcinoma cell anoikis through Bim-mediated intrinsic apoptosis. PLoS One. 2010, 22: 5(9):e12895.

[42] Ganju R.K., et al., The alpha-chemokine, stromal cell-derived factor-1alpha, binds to the transmembrane G-protein-coupled CXCR-4 receptor and activates multiple signal transduction pathways. J. Biol. Chem. 1998, 273(36): 23169-23175.

[43] Zlotnik A., Chemokines and cancer.Int. J. Cancer .2006, 119(9): 2026-2029.

[44] Moyer R.A., et al., Rho activation regulates CXCL12 chemokine stimulated actin rearrangement and restitution in model intestinal epithelia. Lab. Invest.2007, 87(8):807-817.

[45] Haribabu B., et al., Regulation of human chemokine receptors CXCR4. Role of phosphorylation in desensitization and internalization. J. Biol.Chem.1997, 272(45): 28726-28731.

[46] Neel N.F., et al., Chemokine receptor internalization and intracellular trafficking. Cytokine Growth Factor. Rev. 2005,16(6):637-658.

[47] Nibbs R.J., et al., Cloning and characterization of a novel promiscuous human beta-chemokine receptor D6. J. Biol.Chem.1997, 272(51): 32078-32083.

[48] Horuk R., et al., Identification and characterization of a promiscuous chemokine-binding protein in a human erythroleukemic cell line. J. Biol. Chem.1994, 269(26): 17730-17733.

[49] Borroni E.M., Bonecchi R., Shaping the gradient by nonchemotactic chemokine receptors. Cell. Adh Migr.2009, 3(2):146-147.

[50] Teicher B.A., Fricker S.P., CXCL12 (SDF-1)/CXCR4 Pathway in Cancer. Clin Cancer Res. 2010 ,16(11):2927-31.

[51] Nagasawa T., et al., Molecular cloning and characterization of a murine pre-B-cell growth-stimulating factor/stromal cell-derived factor 1 receptor, a murine homolog of the human immunodeficiency virus 1 entry coreceptor fusin. Proc Natl Acad Sci U S.1996, A93 (25): 14726-14729.

[52] Balkwill F., Cancer and the chemokine network. Nat Rev Cancer. 2004,4(7): 540–50.

[53] Smith M.C., et al., CXCR4 regulates growth of both primary and metastatic breast cancer, Cancer Res.2004, 64(23):8604–8612.

[54] Phillips R.J., et al., The stromal derived factor-1/CXCL12-CXC chemokine receptor 4 biological axis in non-small cell lung cancer metastases, Am. J. Respir. Crit.Care Med. 2003,167(12):1676–1686.

[55] Scotton C.J., et al., Multiple actions of the chemokine CXCL12 on epithelial tumor cells in human ovarian cancer, Cancer Res. 2002,62(20):5930–5938.

[56] Pan J., et al., Stromal derived factor-1 (SDF-1/CXCL12) and CXCR4 in renal cell carcinoma metastasis, Mol. Cancer. 2006,5: 56.

[57] Taichman R.S.,et al., Use of the stromal cell-derived factor-1/CXCR4 pathway in prostate cancer metastasis to bone, Cancer Res.2002, 62(6):1832–1837.

[58] Geminder H., et al., A possible role for CXCR4 and its ligand, the CXC chemokine stromal cellderived factor-1, in the development of bone marrow metastases in neuroblastoma, J. Immunol. 2001,167(8):4747–4757.

[59] Vandercappellen J., Van Damme J., Struyf S.,The role of CXC chemokine and their receptors in cancer.2008.Cancer letters 2008, 267(2):226-244.

[60] Szlosarek P.W., et al., Aberrant regulation of argininosuccinate synthetase by TNF-alpha in human epithelial ovarian cancer, Int. J. Cancer 2007,121(1): 6-11.

[61] Kulbe H., et al., The inflammatory cytokine tumor necrosis factor-alpha regulates chemokine receptor expression on ovarian cancer cells, Cancer Res. 2005,65(22):10355–10362.

[62] Kryczek I., et al., CXCL12 and vascular endothelial growth factor synergistically induce neoangiogenesis in human ovarian cancers, Cancer Res.2005, 65(2):465–472.

[63] Ratajczak M. Z., et al., The pleiotropic effects of the SDF-1-CXCR4 axis in organogenesis, regeneration and tumorigenesis.Leukemia 2006, 20(11): 1915-1924.

[64] Barbieri F., et al., CXC receptor and chemokine expression in human meningioma: SDF1/CXCR4 signaling activates ERK1/2 and stimulates meningioma cell proliferation, Ann. N.Y. Acad. Sci. 2006, 1090 :332–343.

[65] Hattori K., et al., Plasma elevation of stromal cell derived factor-1 induces mobilization of mature andimmature hematopoietic progenitor and stem cells, Blood 2001, 97(11):3354–3360.

[66] Lane W.J., et al., Stromal-derived factor 1-induced megakaryocyte migration and platelet production is dependent on matrix metalloproteinases, Blood 2000, 96 (13):4152–4159.

[67] Petit I., Jin D., Rafii S., The SDF-1-CXCR4 signaling pathway: a molecular hub modulating neo-angiogenesis,Trends Immunol. 2007, 28 (7):299–307.

[68] Ma Q ., et al., Impaired B-lymphopoiesis, myelopoiesis, and derailed cerebellar neuron migration in CXCR4- and SDF-1-deficient mice, Proc. Natl. Acad. Sci. USA .1998, 95(16) : 9448–9453.

[69] Kryczek I., et al., Stroma-derived factor (SDF-1/CXCL12) and human tumor pathogenesis. Am J Physiol Cell Physiol 2007, 292(3): C987–C995.

[70] Janowski M., Functional diversity of SDF-1 splicing variants. Cell Adh Migr. 2009, 3(3): 243–249.

[71] Altenburg JD., et al., A naturally occurring splice variant of CXCL12/stromal cell-derived factor 1 is a potent human immunodeficiency virus type 1 inhibitor with weak chemotaxis and cell survival activities. J Virol. 2007, 81(15): 8140–8148.

[72] Altenburg JD., Structure function analysis of the CXCL12 chemokine. PHDThesis, February, 2008. Submitted to the faculty of the University Graduate School.

[73] Yu L., et al., Identification and expression of novel isoforms of human stromal cell-derived factor 1. Gene. 2006, 374:174–179.

[74] Shirozu M., et al., Structure and chromosomal localization of the human stromal cell-derived factor 1 (SDF1) gene.Genomics. 1995, 28(3): 495-500.

[75] Gleichmann M., et al., Cloning and characterization of SDF-1gamma, a novel SDF-1 chemokine transcript with developmentally regulated expression in the nervous system. Eur J Neurosci. 2000, 12(6):1857-66.

[76] Santhosh K.G., Cardiomyocyte specific deletion of stromal cell derived factor-1 (SDF-1/CXCL12) protects the heart from hypertrophic and ischemic damage. PHD thesis. December 2010 .university of berlin.

[77] Bartlett J. M., Stirling D. A., Short History of the Polymerase Chain Reaction. Methods Mol Biol. 2003, 226:3-6.

[78] Rychlik W., Spencer W., Rhoads R.E., Optimization of the annealing temperature for DNA amplification in vitro". Nucl Acids Res .1990,18(21):6409-12.

[79] PCR Diagrams and Images .2011.http://missionpcr.blogspot.de/p/pcr-diagrams-and-images.html

[80] Dimberg J., et al., Polymorphism and circulating levels of the chemokine CXCL12 in colorectal cancer patients. Int J Mol Med. 2007,19(1): 11-5.

[81] Schmittgen T.D., et al., Quantitative reverse transcription-polymerase chain reaction to study mRNA decay: comparison of endpoint and real-time methods. Anal. Biochem.2000, 285(2): 194–204.

[82] Joyce C., Quantitative RT-PCR. A review of current methodologies. Methods Mol. Biol. 2002,193: 83–92 .

[83] Groskreutz D., Schenborn E.T., Reporter systems. In: Methods in Molecular Biology . R. Tuan, Humana Press, NJ. 1997,63: 11ed.

[84] Sarver N.P., et al., Bovine papilloma virus deoxyribonucleic acid: A novel eucaryotic cloning vector. Mol. Cell. Biol. 1981,1(6): 486–96.

[85] Towbin H., Staehelin T., Gordon J., Electrophoretic transfer of proteins from poly-acrylamide gels to nitrocellulose sheets: procedure and some applications. Proceedings of the National Academy of Sciences USA .1979,76 (9): 4350–54.

[86] Western blot antibody. exactantigen.com. http://www.exactantigen.com/review/western-blot-antibody.html. Retrieved 2009-01-29.

[87] Davies S. L., et al., Plerixafor Hydrochloride. Drugs of the Future .2007, 32 (2): 123.

[88] Fricker Simon P., et al., Characterization of the molecular pharmacology of AMD3100: A specific antagonist of the G-protein coupled chemokine receptor, CXCR4. Biochemical Pharmacology. 2006, 72(5): 588–596.

[89] Bast RC Jr., et al., Cancer Medicine .5th edition.2000.

[90] Lodish H., et al., Molecular Cell Biology. 4th edition.2000.New York. From: Section 22.1, Cell-Cell Adhesion and Communication.

[91] Boyden S., The chemotactic effect of mixtures of antibody and antigen on polymorpho-nuclear leucocytes. J Exp Med 1962, 1 (115):453-66.

[92] Kramer N., et al., In vitro cell migration and invasion assays. Mutat Res. Jan-Mar 2013, 752(1):10-24.

[93] Manetti M., et al., Association between a stromal cell derived factor1 (SDF-1/cxcl12) gene polymorphism and microvascular disease in systemic sclerosis.Ann Rheum Dis 2009, 68(3): 408-411.

[94] Liu W., et al., CXCL12 G801A polymorphism is associated with an increased risk of benign salivary gland tumors in the Chinese population .Med Oncol. 2012, 29(2): 677-681.

[95] Winkler C., et al., Genetic restriction of AIDS pathogenesis by an SDF-1 chemokine gene variant. Science.1998, 279(5349): 389–393.

[96] Razmkhah M., et al., Stromal cell-derived factor-1 (SDF-1) gene and susceptibility of Iranian patients with lung cancer. Lung Cancer.2005, 49(3): 311–5.

[97] Razmkhah M., et al., Stromal cell-derived factor-1 (SDF-1) alleles and susceptibility to breast carcinoma. Cancer Lett. 2005, 225(2): 261–6.

[98] Dommange F., et al., CXCL12 polymorphism and malignant cell dissemination/tissue infiltration in acute myeloid leukemia. Faseb J. 2006, 20(11): 1913–5.

[99] Hirata H., et al., CXCL12 G801A polymorphism is a risk factor for sporadic prostate cancer susceptibility. Clin Cancer Res. 2007, 13(17): 5056–62.

[100] de Oliveira KB., et al., CXCL12 rs1801157 polymorphism in patients with breast cancer, Hodgkin's lymphoma, and non-Hodgkin's lymphoma. J Clin Lab Anal. 2009, 23(6): 387–93.

[101] Teng Y.H., et al., Contribution of genetic polymorphisms of stromal cell-derived factor-1 and its receptor, CXCR4, to the susceptibility and clinicopathologic development of oral cancer. Head Neck. 2009, 31(31): 1282–8.

[102] Vairaktaris E., et al., A DNA polymorphism of stromal-derived factor-1 is associated with advanced stages of oral cancer. Anticancer Res. 2008, 28(1A):271–5.

[103] van Rij RP., et al., The role of a stromal cell derived factor-1 chemokine gene variant in the clinical course of HIV-1 infection. 1998, 12(9): F85-F90.

[104] Hidalgo-Pascual M., et al., Analysis of CXCL12 3'UTR G>A polymorphism in colorectal cancer. Oncol Rep. 2007: 18 (6):1583-7.

[105] Chang S.C., et al., SDF-1alpha G801A polymorphism predicts lymph node metastasis in stage T3 colorectal cancer .Ann Surg Oncol. 2009 Aug, 16(8):2323-30.

[106] Gong H., et al., The CXCL12 G801A polymorphism and cancer risk: evidence from 17 case-control studies. Gene. 2012 Nov 10, 509(2):228-31.

[107] Su B., et al., An HIV-resistant allele is exceptionally frequent in New Guinean highlanders. Jama.1998, 280:1830.

[108] Shen W., et al., CXCL12 G801A polymorphism and breast cancer risk: a meta-analysis Molecular Biology Reports. 2012 Feb, 39(2): 2039.

[109] Maley S.N., et al., Genetic varation in CXCL12 and risk of cervical carcinoma: a population-based case –control study.In J Immunogenet.2009, 36(6): 367-375.

[110] Vazquez-Lavista., et al., Genetic association of monocyte chemoattractant protein 1 (MCP-1)-2518 polymorphism in Mexican patients with transitional cell carcinoma of the bladder.Urology.2009,74:414-418.

[111] Grunewald M., et al., VEGF-induced adult neovascularization: recruitment, retention, and role of accessory cells. Cell.2006, 124(1): 175–189.

[112] Katayama Y., et al., Signals from the sympathetic nervous system regulate hematopoietic stem cell egress from bone marrow. Cell.2006, 124(2): 407–421.

[113] Petit I., et al., G-CSF induces stem cell mobilization by decreasing bone marrow SDF-1 and up-regulating CXCR4. Nat Immunol.2002, 3(7): 687–694.

[114] Ponomaryov T., et al., Induction of the chemokine stromal-derived factor-1 following DNA damage improves human stem cell function. J Clin Invest.2000, 106(11): 1331–1339.

[115] Zou YR., et al., Function of the chemokine receptor CXCR4 in haematopoiesis and in cerebellar development. Nature.1998, 393(6685): 595–599.

[116] Machelon V., et al., CXCL12 expression by healthy and malignant ovarian epithelial cells. BMC Cancer .2011, 11: 97.

[117] Kryczek I., et al., Accumulation of CD45RO(+) cells in peritoneal carcinomatous fluid favours survival of ovarian carcinoma patients. Cancer Immunol Immunother .2002, 51(9): 513–519.

[118] Mirisola V., et al., CXCL12/SDF1 expression by breast cancers is an independent prognostic marker of disease-free and overall survival. Eur J Cancer. 2009 Sep; 45(14):2579-87.

[119] Kang H., et al., Stromal cell derived factor-1: its influence on invasiveness and migration of breast cancer cells in vitro, and its association with prognosis and survival in human breast cancer. Breast Cancer Res .2005, 7(4): R402–R410.

[120] Taichman R.S., et al., Use of the stromal cell-derived factor-1/CXCR4 pathway in prostate cancer metastasis to bone. Cancer Res.2002, 62(6) :1832–1837.

[121] Sun Y., et al**.,** Expression of CXCR4 and CXCL12 (SDF-1) in Human Prostate Cancers (PCa) In Vivo. Journal of Cellular Biochemistry.2003, 89(3): 462–473.

[122] Koshiba T., et al., Expression of stromal cell-derived factor 1 and CXCR4 ligand receptor system in pancreatic cancer: a possible role for tumor progression. Clin Cancer Res.2000, 6(9): 3530–3535.

[123] Marchesi F., et al., Increased survival, proliferation, and migration in metastatic human pancreatic tumor cells expressing functional CXCR4. Cancer Res.2004, 64(22): 8420–8427.

[124] Hwang J.H., et al., CXC chemokine receptor 4 expression and function in human anaplastic thyroid cancer cells. J Clin Endocrinol Metab.2003, 88(1): 408–416.

[125] Rempel S.A., et al., Identification and localization of the cytokine SDF1 and its receptor, CXC chemokine receptor 4, to regions of necrosis and angiogenesis in human glioblastoma. Clin Cancer Res .2000, 6(1): 102–111.

[126] Schimanski C.C., et al., Effect of chemokine receptors CXCR4 and CCR7 on the metastatic behavior of human colorectal cancer. Clin Cancer Res.2005, 11(5): 1743–1750.

[127] Akishima-Fukasawa Y., et al., Prognostic Significance of CXCL12 Expression in Patients with Colorectal Carcinoma. American Journal of Clinical Pathology. 2009 132(2): 202-210.

[128] Davis D.A., et al., Identification of carboxypeptidase N as an enzyme responsible for C-terminal cleavage of stromal cell-derived factor-1alpha in the circulation. Blood .2005, 105(12): 4561-8.

[129] Weidt C., et al., Stem cell migration: a quintessential stepping stone to successful therapy. Curr Stem Cell Res Ther .2007, 2(1): 89-103.

[130] Boldajipour B., et al., Control of chemokine-guided cell migration by ligand sequestration. Cell .2008, 132(30: 463-73.

[131] Limatola C., et al., SDF-1alpha-mediated modulation of synaptic transmission in rat cerebellum. Eur J Neurosci.2000, 12(7): 2497-504.

[132] Colobran R., et al., The chemokine network II. On how polymorphisms and alternative splicing increase the number of molecular species and configure intricate patterns of disease susceptibility. Clin Exp Immunol .2007, 150(1): 1-12.

[133] Gleichmann M., Gillen C., Czardybon M., Cloning and characterization of SDF-1gamma, a novel SDF-1 chemokine transcript with developmentally regulated expression in the nervous system. Eur J Neurosci. 2000 Jun, 12(6): 1857-66.

[134] Rueda P., et al., The CXCL12gamma chemokine displays unprecedented structural and functional properties that make it a paradigm of chemoattractant proteins. PLoS ONE. 2008, 3(7): 2543.

[135] Fricker S.P., A novel CXCR4 antagonist for hematopoietic stem cell mobilization. Expert Opin Investig Drugs. 2008, 17(11): 1749–60.

[136] Murdoch C., Finn A., Chemokine receptors and their role in inflammation and infectious diseases. Blood. 2000, 95(10): 3032–3043.

[137] Luster AD., Chemokines: chemotactic cytokines that mediate inflammation. N Engl J Med. 1998, 338(7): 436–445.

[138] Ganju R.K., et al., The α-chemokine, stromal cell-derived factor-1α, binds to the transmembrane G-protein-coupled CXCR-4 receptor and activates multiple signal transduction pathways. J Biol Chem. 1998, 273(36):23169–23175.

[139] Sehgal A., et al., CXCR-4,a chemokine receptor, is overexpressed in and required for proliferationof glioblastoma tumor cells. J Surg Oncol.1998, 69(2): 99–104.

[140] Barbero S., et al., Stromal cell-derivedfactor 1α stimulates human glioblastoma cell growth through the activationof both extracellular signal-regulated kinases 1/2 and Akt. CancerRes.2003, 63(8): 1969–1974.

[141] Darash-Yahana M., et al., Role of high expression levels of CXCR4 in tumor growth, vascularization, and metastasis. FASEB J 2004, 18(11): 1240–1242.

[142] Katayama A., et al., Expression of CXCR4 and its down-regulation by IFN-gamma in head and neck squamous cell carcinoma. Clin Cancer Res 2005, 11(8): 2937–2946.

[143] Marchesi F., et al., Increased survival, proliferation, and migration in metastatic human pancreatic tumor cells expressing functional CXCR4. Cancer Res 2004, 64(22): 8420–8427.

[144] Sonoda Y., et al., Akt pathway activation converts anaplastic astrocytoma to glioblastoma multiforme in a human astrocyte model of glioma. Cancer Res 2001, 61(18):6674–6678.

[145] Vlahakis S.R., et al., G protein-coupled chemokine receptors induce both survival and apoptotic signaling pathways. J Immunol 2002, 169(10): 5546–54.

[146] Suzuki Y., Rahman M., Mitsuya H., Diverse transcriptional response of CD4+ T cells to stromal cell-derived factor (SDF)-1: cell survival promotion and priming effects of SDF-1 on CD4+ t cells. J Immunol 2001, 167(60: 3064–73.

[147] Troppmair J., et al., Mitogen-activated protein kinase extracellular signal-regulated protein kinase activation by oncogenes, serum, and 12-O-tetradecanoylphorbol-13-acetate requires Raf and is necessary for transformation. J Biol Chem1994, 269(9): 7030–35.

[148] Marchesi F., et al., Increased survival, proliferation, and migration in metastatic human pancreatic tumor cells expressing functional CXCR4. Cancer Res 2004, 64(22): 8420–8427.

[149] Kijima T., et al., Regulation of cellular proliferation, cytoskeletal function, and signal transduction through CXCR4 and c-Kit in small cell lung cancer cells. Cancer Res 2002,62(21): 6304–6311.

[150] Osaki M., Oshimura M., Ito H., PI3K-Akt pathway: Its functions and alterations in human cancer. Apoptosis 2004, 9(6): 667–676.

[151] Cross D., et al., Inhibition of glycogen synthase kinase-3 by insulin mediated by protein kinase B. Nature 1995, 378(6559): 785-9.

[152] Inoki K., et al., TSC2 is phosphorylated and inhibited by Akt and suppresses mTOR signalling. Nat Cell Biol 2002,4(9): 648–657.

[153] Tee AR., et al., Tuberous sclerosis complex-1 and -2 gene products function together to inhibit mammalian target of rapamycin (mTOR)-mediated downstream signaling. ProcNatl Acad Sci USA 2002, 99(21): 13571–13576.

[154] Potter CJ., Pedraza LG., Xu T., Akt regulates growth by directly phosphorylating Tsc2. Nat Cell Biol 2002,4(9): 658–665.

[155] Calvert P.M., Frucht H., The genetics of colorectal cancer. Ann InternMed 2002, 137(7): 603–12.

[156] Fang J., Richardson B., The MAPK signalling pathways and colorectal cancer. LancetOncol 2005, 695): 322-27.

[157] Hommes D.W., Peppelenbosch M.P., van Deventer SJ.H., Mitogen activated protein (MAP) kinase signal transduction pathways and novel anti-inflammatory targets. Gut 2003, 52(1): 144–51.

[158] Troppmair J., et al., Mitogen-activated protein kinase extracellular signal-regulated protein kinase activation by oncogenes, serum, and 12-O-tetradecanoylphorbol-13-acetate requires Raf and is necessary for transformation. J Biol Chem1994, 269(9): 7030–35.

[159] Wang X., et al., Regulation of phorbol estermediated TRAF1 induction in human colon cancer cells through a PKC/RAF/ERK/ NF-kappaB-dependent pathway. Oncogene 2004; 23(10): 1885–95.

[160] Kim J., et al., Chemokine receptor CXCR4 expression in colorectal cancer patients increases the risk for recurrence and for poor survival. J Clin Oncol 2005, 23(12): 2744-2753.

[161] Ingold B., et al., The role of vascular CXCR4 expression in colorectal carcinoma. Histopathology 2009, 55(5): 576-586.

[162] Saigusa S., et al., Stromal CXCR4 and CXCL12 expression is associated with distant recurrence and poor prognosis in rectal cancer after chemoradiotherapy. Ann Surg Oncol 2010, 17(8): 2051-2058.

[163] Muller A., et al., Involvement of chemokine receptors in breast cancer metastasis. Nature 2001, 410(6824): 50–56.

[164] Zeelenberg I.S., et al., The chemokine receptor CXCR4 is required for outgrowth of colon carcinoma micrometastases. Cancer Res 2003,63(13): 3833–3839.

[165] Phillips R.J.,et al., Epidermal growth factor and hypoxia-induced expression of CXC chemokine receptor 4 on non-small cell lung cancer cells is regulated by the phosphatidylinositol 3-kinase/PTEN/AKT/mammalian target of rapamycin signaling pathway and activation of hypoxia inducible factor-1α. J Biol Chem 2005,280(23): 22473–22481.

[166] Sun Y.X., et al., Skeletal localization and neutralization of the SDF-1(CXCL12) /CXCR4 axis blocks prostate cancer metastasis and growth in osseous sites in vivo. J Bone Miner Res 2005, 20(20: 318–329.

[167] Jordan N.J., et al., Expression of functional CXCR4 chemokine receptors on human colonic epithelial cells. J Clin Invest 1999, 104(8): 1061–1069.

[168] Geminder H**.,** et al**.,** A possible role for CXCR4 and its ligand, the CXC chemokine stromal cell-derived factor-1, in the development of bone marrow metastases in neuroblastoma. J Immunol 2001.167(80): 4747–4757.

[169] Mori T., et al., CXCR4 antagonist inhibits stromal cell-derived factor 1-induced migration and invasion of human pancreatic cancer. Mol Cancer Ther 2004,3(1): 29-37.

[170] Chinni S.R., et al., CXCL12/CXCR4 signaling activates Akt-1 and MMP-9 expression in prostate cancer cells: the role of bone microenvironment-associated CXCL12. Prostate 2006, 66(1): 32-48.

[171] Brand S., et al., CXCR4 and CXCL12 are inversely expressed in colorectal cancer cells and modulate cancer cell migration, invasion and MMP-9 activation. Exp Cell Res 2005, 310(1): 117-130.

[172] Lambrechts A., Van Troys M., Ampe C., The actin cytoskeleton in normal and pathological cell motility. *Int J Biochem Cell Biol* 2004; 36(100: 1890-1909.

[173] Leelawat K., et al., Roles of the MEK1/2 and AKT pathways in CXCL12/CXCR4 induced cholangiocarcinoma cell invasion. World J Gastroenterol 2007, 13(10): 1561-1568.

[174] Bonacchi A., et al., Signal transduction by the chemokine receptor CXCR3: activation of Ras/ERK, Src, and phosphatidylinositol 3-kinase/Akt controls cell migration and proliferation proliferation in human vascular pericytes, J. Biol. Chem. 2001, 276(13): 9945– 9954.

[175] Sotsios Y., et al., The CXC chemokine stromal cell-derived factor activates a Gi-coupled phosphoinositide 3-kinase in T lymphocytes, J. Immunol. 1999, 163(11): 5954–5963.

[176] McDonnell S., et al., Metastatic and non-metastatic colorectal cancer (CRC) cells induce host metalloproteinase production in vivo, Clin. Exp. Metastasis 1999,17(4): 341– 349.

[177] Egeblad M., Werb Z., New functions for the metalloproteinases in cancer progression. Nat Rev Cancer 2002, 2(3): 161–174.

[178] Hojilla C.V., Mohammed F.F., Khokha R., Matrix metalloproteinases and their tissue inhibitors direct cell fate during cancer development. Br J Cancer 2003, 89(10): 1817–1821.

[179] Hartmann TN., et al., CXCR4 chemokine receptor and integrin signaling co-operate in mediating adhesion and chemoresistance in small cell lung cancer (SCLC) cells. Oncogene 2005, 24(27): 4462–4471.

[180] Burger M., et al., Functional expression of CXCR4 (CD184) on small-cell lung cancer cells mediates migration, integrin activation, and adhesion to stromal cells. Oncogene 2003, 22(50): 8093–8101.

[181] Klier CM., et al., Chemokine-induced secretion of gelatinase B in primary human monocytes. Biol Chem 2001, 382(9): 1405–1410.

[182] Marchesi F., et al., Increased survival, proliferation, and migration in metastatic human pancreatic tumor cells expressing functional CXCR4. Cancer Res 2004, 64(22): 8420–8427.

[183] Libura J., et al., CXCR4-SDF-1 signaling is active in rhabdomyosarcoma cells and regulates locomotion, chemotaxis, and adhesion. Blood 2002, 100(7): 2597–2606.

[184] Singh S., et al., CXCL12-CXCR4 interactions modulate prostate cancer cell migration, metalloproteinase expression and invasion. Lab Invest 2004, 84(12): 1666–1676.

[185] Yu X., Collin-Osdoby P., Osdoby P., SDF-1 increases recruitment of osteoclast precursors by upregulation of matrix metalloproteinase-9 activity. Connect Tissue Res 2003, 44 Suppl 1:79-84.

[186] Freeman-Cook KD., et al., Design of Selective, ATP-Competitive Inhibitors of Akt. J Med Chem. 2010 , 53(12): 4615-22.

[187] Baba Y., et al., Phosphorylated AKT expression is associated with PIK3CA mutation, low stage, and favorable outcome in 717 colorectal cancers. Cancer. 2011 , 117(7): 1399-408.

[188] Krasinskas AM., EGFR Signaling in Colorectal Carcinoma. Patholog Res Int. 2011 14; 2011: 932932.

[189] Joseph R. Testa., Tumor Genetics; AKT Function and Oncogenic Activity . Scientific report. Fox Chase Cancer Center. 2005. http://www.fccc.edu/docs/sci_report2005/Testa.pdf.

[190] Huang X.F., Chen J.Z., Obesity, the PI3K/Akt signal pathway and colon cancer. Obes Rev. 2009 , 10 (6): 610-6.

[191] Citri A., Yarden Y., EGF-ERBB signalling: towards the systems level. Nat Rev Mol Cell Biol. 2006 , 7(7): 505-516.

[192] Wang YK., et al., Activation of Akt and MAPK pathways enhances the tumorigenicity of CD133+ primary colon cancer cells.2010. Oxford Journals Life Sciences & Medicine Carcinogenesis. 2010, 31(8): 1376-1380.

[193] Johnson G.L., Lapadat R., Mitogen-Activated Protein Kinase Pathways Mediated by ERK, JNK, and p38 Protein Kinases Science 2002, 298 (5600) : 1911-1912.

[194] Pearson G., et al., Mitogen-activated protein (MAP) kinase pathways: regulation and physiological functions. Endocr Rev 2001 Apr, 22(2): 153-83.

[195] Orton R.J., et al., Computational modelling of the receptor-tyrosine-kinase-activated MAPK pathway. Biochem J 2005 December 1, 392(2): 249–261.

[196] Roberts P.J., Der C.J., Targeting the Raf-MEK-ERK mitogen-activated protein kinase cascade for the treatment of cancer. Oncogene 2007, 26(22): 3291–3310.

[197] Li J.K., et al., Inhibition of CXCR4 activity with AMD3100 decreases invasion of human colorectal cancer cells in vitro. World J Gastroenterol. 2008 ,14(15): 2308-13.

[198] Ganju R.K., et al., Role of CXCL12 and CXCR4 in tumor biology and metastasis.signaling pathways and molecular mediators in metastasis.2012: 221-243.

[199] De Clercq E., The bicyclam AMD3100 story. Nat Rev Drug Discov. 2003 Jul; 2(7): 581-7.

7. Appendix

7.1 Tumor characteristics in relation to SDF-I isoforms

40 tumors of 39 patients were included in the study. In order to assess dependence of the SDF1 isoforms on sex, TNM and R we computed mean, standard deviation, minimum, maximum, median, and quartiles in subgroups.

7.2 Correlation of SDFI isoforms with clinical parameter T

Analysis Variable : value											
Parameter	*T*	*N Obs*	*N*	*N Miss*	*Mean*	*Std Dev*	*Minimum*	*Lower Quartile*	*Median*	*Upper Quartile*	*Maximum*
Actin	1	2	2	0	218.64	158.76	106.38	106.38	218.64	330.91	330.91
	2	5	5	0	318.74	98.62	200.74	238.40	332.82	384.83	436.90
	3	29	29	0	270.21	60.80	146.67	233.55	274.76	307.91	416.96
	4	3	3	0	351.57	162.57	235.49	235.49	281.84	537.37	537.37
Alter	1	2	2	0	74.50	0.71	74.00	74.00	74.50	75.00	75.00
	2	5	5	0	73.20	2.95	71.00	71.00	72.00	74.00	78.00
	3	29	29	0	64.31	10.49	44.00	58.00	64.00	72.00	83.00
	4	3	3	0	61.33	17.95	41.00	41.00	68.00	75.00	75.00
SDFalpha	1	2	2	0	45.13	29.96	23.94	23.94	45.13	66.31	66.31
	2	5	5	0	33.97	39.24	0.00	0.00	17.68	71.81	80.39
	3	29	29	0	53.31	40.89	2.36	21.70	41.95	75.69	191.60
	4	3	3	0	90.05	38.97	57.04	57.04	80.07	133.05	133.05
SDFalph_ percent	1	2	2	0	34.78	38.96	7.24	7.24	34.78	62.33	62.33
	2	5	5	0	12.79	16.29	0.00	0.00	4.05	24.15	35.77
	3	29	29	0	21.10	21.53	0.71	10.58	18.56	24.60	121.05
	4	3	3	0	30.54	22.63	14.90	14.90	20.24	56.50	56.50
SDFbeta	1	2	2	0	37.76	20.98	22.93	22.93	37.76	52.59	52.59
	2	5	5	0	20.11	42.52	0.00	0.00	0.00	4.48	96.09
	3	29	29	0	40.65	41.54	0.00	2.05	19.33	85.31	116.51
	4	3	3	0	29.43	48.41	0.34	0.34	2.63	85.31	85.31
SDFbeta _percent	1	2	2	0	28.18	30.06	6.93	6.93	28.18	49.44	49.44
	2	5	5	0	6.15	12.73	0.00	0.00	0.00	1.88	28.87
	3	29	29	0	15.87	17.39	0.00	0.88	6.26	28.00	54.99
	4	3	3	0	10.30	17.29	0.15	0.15	0.49	30.27	30.27
SDFdelta	1	2	2	0	0.00	0.00	0.00	0.00	0.00	0.00	0.00
	2	5	5	0	63.23	141.39	0.00	0.00	0.00	0.00	316.16
	3	29	29	0	28.11	50.31	0.00	0.00	0.00	36.78	186.24

Analysis Variable : value											
Parameter	*T*	*N Obs*	*N*	*N Miss*	*Mean*	*Std Dev*	*Mini-mum*	*Lower Quartile*	*Median*	*Upper Quartile*	*Maxi-mum*
	4	3	3	0	40.55	40.89	0.50	0.50	38.92	82.23	82.23
SDFdel-ta_percent	1	2	2	0	0.00	0.00	0.00	0.00	0.00	0.00	0.00
	2	5	5	0	19.00	42.48	0.00	0.00	0.00	0.00	95.00
	3	29	29	0	10.98	18.97	0.00	0.00	0.00	13.90	60.10
	4	3	3	0	12.21	15.11	0.21	0.21	7.24	29.17	29.17
SDFepsilon	1	2	2	0	39.39	55.70	0.00	0.00	39.39	78.77	78.77
	2	5	5	0	10.84	18.93	0.00	0.00	0.00	10.51	43.72
	3	29	29	0	50.11	54.59	0.00	3.05	27.77	106.68	175.41
	4	3	3	0	38.90	58.27	0.00	0.00	10.81	105.89	105.89
SDFepsi-lon_percent	1	2	2	0	37.02	52.36	0.00	0.00	37.02	74.04	74.04
	2	5	5	0	3.17	5.69	0.00	0.00	0.00	2.73	13.14
	3	29	29	0	18.20	19.58	0.00	0.99	11.19	37.13	61.75
	4	3	3	0	14.05	20.50	0.00	0.00	4.59	37.57	37.57
SDFgamma	1	2	2	0	115.76	0.32	115.54	115.54	115.76	115.99	115.99
	2	5	5	0	1.41	3.16	0.00	0.00	0.00	0.00	7.07
	3	29	29	0	38.96	52.97	0.00	0.00	0.17	104.42	122.05
	4	3	3	0	0.00	0.00	0.00	0.00	0.00	0.00	0.00
SDFgam-ma_percent	1	2	2	0	71.83	52.01	35.05	35.05	71.83	108.60	108.60
	2	5	5	0	0.43	0.95	0.00	0.00	0.00	0.00	2.13
	3	29	29	0	17.74	26.12	0.00	0.00	0.05	34.57	73.88
	4	3	3	0	0.00	0.00	0.00	0.00	0.00	0.00	0.00
SDFtheta	1	2	2	0	48.10	68.02	0.00	0.00	48.10	96.20	96.20
	2	5	5	0	59.71	43.91	0.00	25.37	87.36	92.72	93.08
	3	29	29	0	55.41	45.22	0.00	0.00	80.61	91.36	119.72
	4	3	3	0	66.74	59.89	0.00	0.00	84.40	115.82	115.82
SDFthe-ta_percent	1	2	2	0	45.21	63.94	0.00	0.00	45.21	90.43	90.43
	2	5	5	0	19.31	16.76	0.00	7.62	21.22	24.19	43.52
	3	29	29	0	21.55	19.11	0.00	0.00	24.19	36.28	60.78
	4	3	3	0	25.64	22.36	0.00	0.00	35.84	41.09	41.09

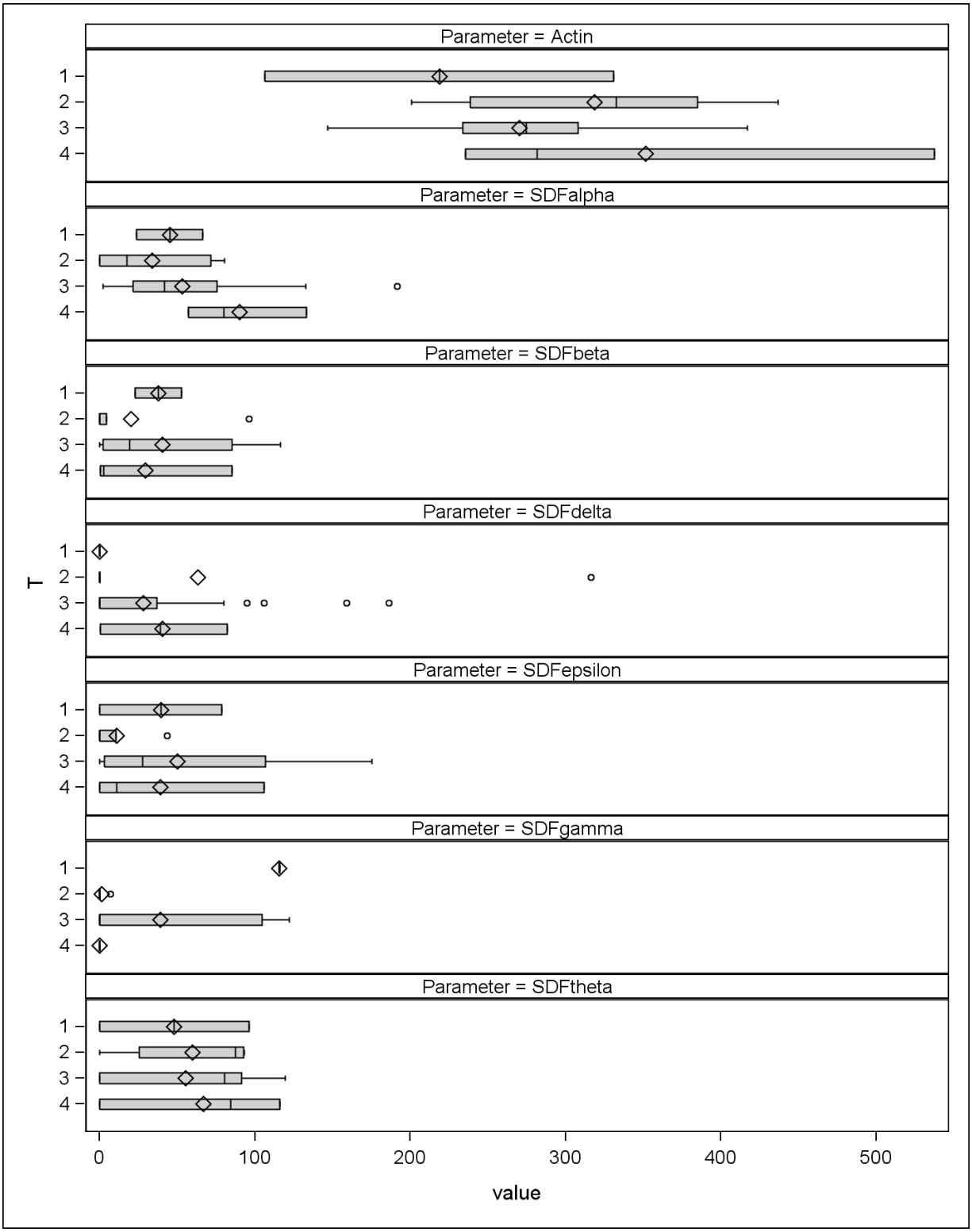
Parameter = Actin
Parameter = SDFalpha
Parameter = SDFbeta
Parameter = SDFdelta
Parameter = SDFepsilon
Parameter = SDFgamma
Parameter = SDFtheta
T
1
2
3
4
0
100
200
300
400
500
value

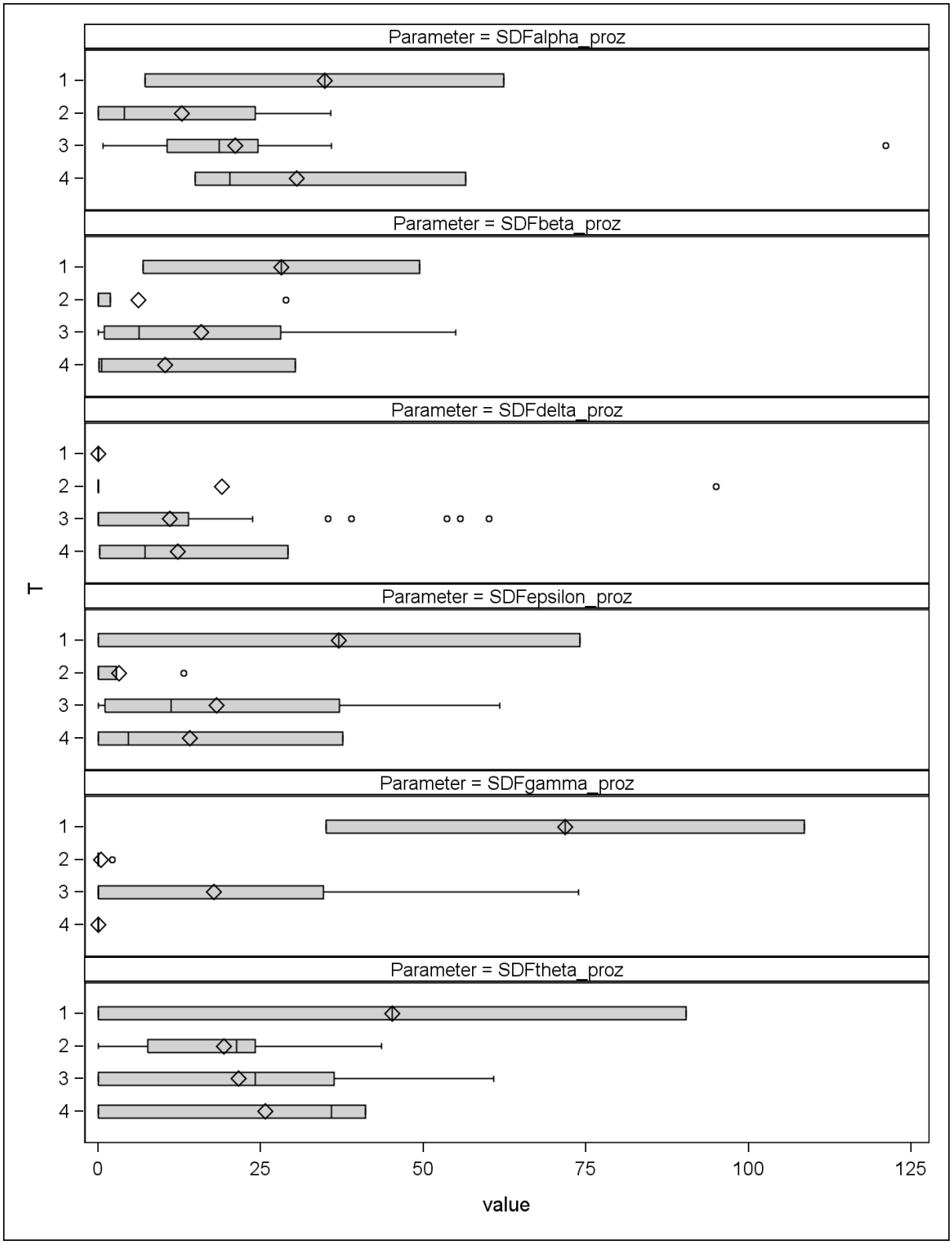

Box plot (1) Correlation of SDFI isoforms with parameter T

7.2.1 p-values for Wilcoxon tests and Kruskal-Wallis tests for association of SDF1 isoforms with clinical parameter-T

Parameter	*p-Wert Kruskall-Wallis-Test*
Actin	0.6591
Alter	0.1410
SDFalpha	0.2426
SDFalpha_percent	0.4916
SDFbeta	0.6006
SDFbeta_percent	0.2761
SDFdelta	0.2151
SDFdelta_percent	0.2900
SDFepsilon	0.3827
SDFepsilon_percent	0.3480
SDFgamma	0.0423
SDFgamma_percent	0.0423
SDFtheta	0.9746
SDFtheta_percent	0.9540

7.3 Correlation of SDFI isoforms with clinical parameter N

Analysis Variable : value											
Parameter	*N*	*N Obs*	*N*	*N Miss*	*Mean*	*Std Dev*	*Mini-mum*	*Lower Quartile*	*Median*	*Upper Quartile*	*Maxi-mum*
Actin	N0	19	19	0	261.69	76.64	106.38	205.09	264.68	308.89	416.96
	N1/N2	19	19	0	284.86	64.50	158.28	235.49	284.08	332.82	436.90
Alter	N0	19	19	0	67.16	11.61	44.00	59.00	68.00	76.00	83.00
	N1/N2	19	19	0	65.63	8.28	47.00	58.00	67.00	72.00	78.00
SDFalpha	N0	19	19	0	49.79	35.05	0.00	21.70	41.95	71.81	132.54
	N1/N2	19	19	0	55.28	47.03	0.00	17.68	49.97	75.74	191.60
SDFalph_ percent	N0	19	19	0	20.60	14.98	0.00	7.41	18.94	29.95	62.33
	N1/N2	19	19	0	22.67	27.33	0.00	4.87	18.22	24.15	121.05
SDFbeta	N0	19	19	0	42.72	39.69	0.00	0.00	24.48	87.36	95.82
	N1/N2	19	19	0	33.10	42.30	0.00	0.34	6.77	85.31	116.51
SDFbet_ percent	N0	19	19	0	18.37	18.49	0.00	0.00	9.81	34.88	54.99
	N1/N2	19	19	0	12.04	16.15	0.00	0.15	3.23	27.06	53.90
SDFdelta	N0	19	19	0	20.81	40.55	0.00	0.00	0.00	36.78	159.23
	N1/N2	19	19	0	43.09	84.14	0.00	0.00	0.00	82.23	316.16
SDFdel-ta_percent	N0	19	19	0	8.25	15.29	0.00	0.00	0.00	13.90	53.63
	N1/N2	19	19	0	15.06	27.53	0.00	0.00	0.00	29.17	95.00
SDFepsilon	N0	19	19	0	42.09	47.65	0.00	3.05	10.51	105.89	122.94
	N1/N2	19	19	0	47.53	56.93	0.00	0.00	11.61	105.89	175.41
SDFepsi-lon_percent	N0	19	19	0	18.13	21.44	0.00	0.99	6.56	38.83	74.04
	N1/N2	19	19	0	16.60	20.65	0.00	0.00	4.59	33.14	61.75
SDFgamma	N0	19	19	0	49.60	56.45	0.00	0.00	0.32	114.65	122.05
	N1/N2	19	19	0	22.42	44.57	0.00	0.00	0.00	7.07	116.94
SDFgam-ma_percent	N0	19	19	0	24.31	32.47	0.00	0.00	0.11	46.20	108.60
	N1/N2	19	19	0	10.44	22.33	0.00	0.00	0.00	2.13	73.88
SDFtheta	N0	19	19	0	64.35	46.37	0.00	0.00	89.19	96.20	119.72
	N1/N2	19	19	0	51.53	43.32	0.00	0.00	79.47	87.40	115.82
SDFthe-ta_persent	N0	19	19	0	27.83	24.47	0.00	0.00	28.87	43.22	90.43
	N1/N2	19	19	0	18.95	17.50	0.00	0.00	21.22	33.88	55.22

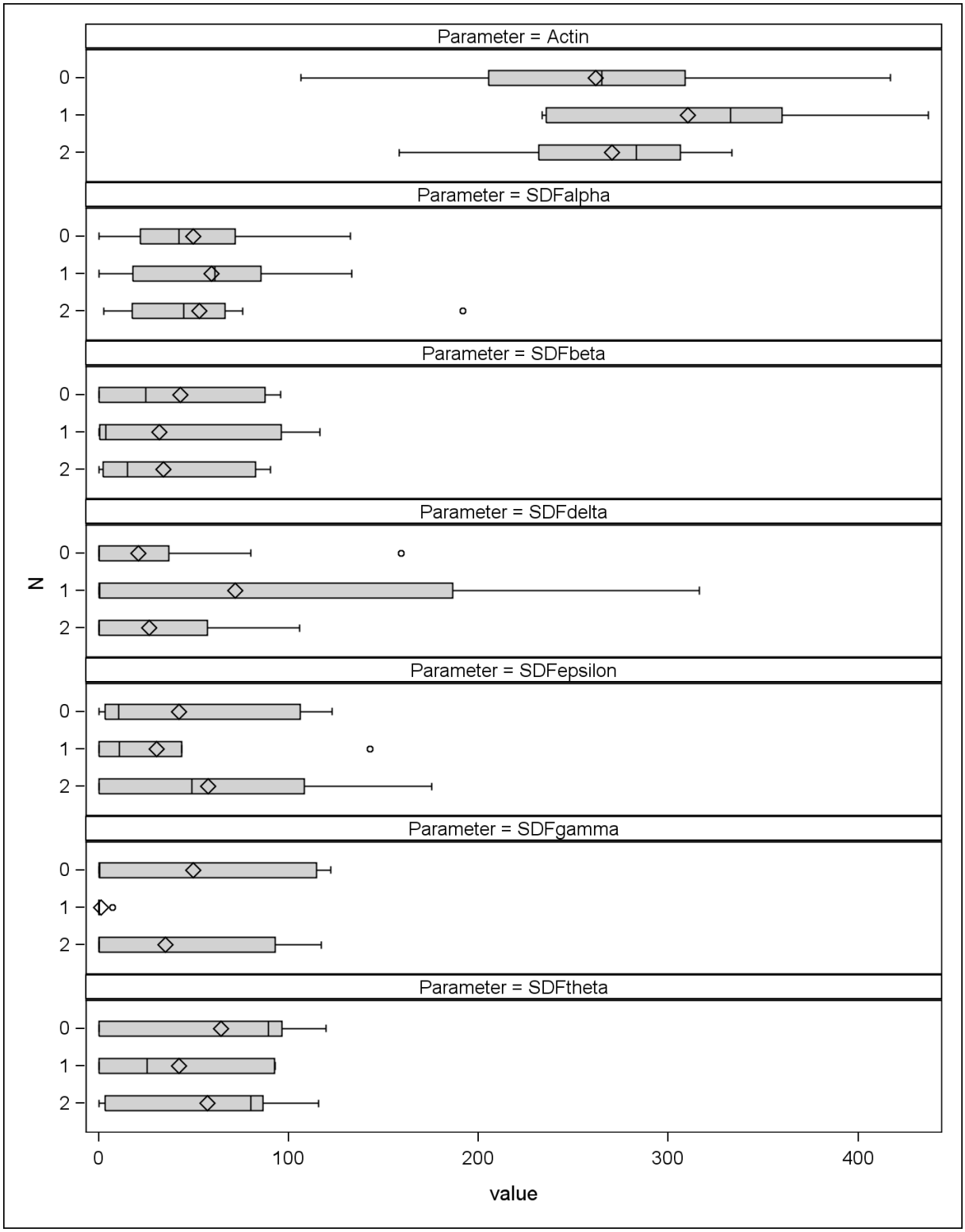
Parameter = Actin
Parameter = SDFalpha
Parameter = SDFbeta
Parameter = SDFdelta
Parameter = SDFepsilon
Parameter = SDFgamma
Parameter = SDFtheta
N
0
1
2
0
100
200
300
400
value

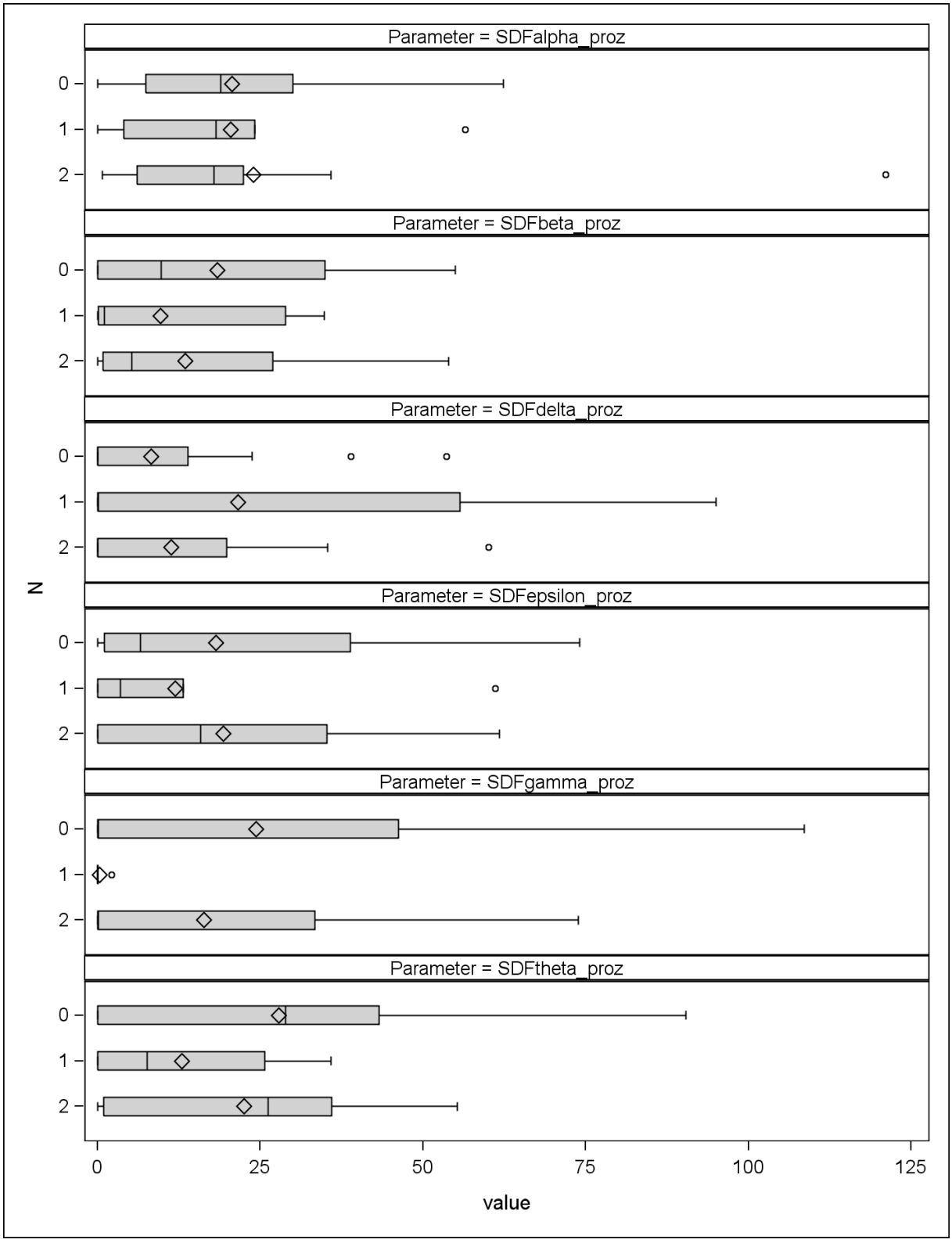

Box plot (2) Correlation of SDFI isoforms with parameter N

7.3.1 p-values for Wilcoxon tests and Kruskal-Wallis tests for association of SDF1 isoforms with clinical parameter -N

Parameter	*p-Wert Wilcoxon-Test*
Actin	0.2933
Alter	0.4301
SDFalpha	0.9186
SDFalpha_percent	0.5691
SDFbeta	0.6585
SDFbeta_ percent	0.4094
SDFdelta	0.6196
SDFdelta_ percent	0.6432
SDFepsilon	1.0000
SDFepsilon_ percent	0.6800
SDFgamma	0.2900
SDFgamma_ percent	0.2759
SDFtheta	0.1172
SDFtheta_ percent	0.2491

7.4 Correlation of SDFI isoforms with clinical parameter M

Analysis Variable : value											
Parameter	*M*	*N Obs*	*N*	*N Miss*	*Mean*	*Std Dev*	*Mini-mum*	*Lower Quartile*	*Median*	*Upper Quartile*	*Maximum*
Actin	0	28	28	0	267.46	72.11	106.38	223.80	269.72	310.45	416.96
	1	11	11	0	312.10	98.75	209.34	235.49	284.08	333.28	537.37
Alter	0	28	28	0	66.43	10.94	44.00	58.50	68.00	74.50	83.00
	1	11	11	0	64.00	10.17	41.00	56.00	67.00	72.00	75.00
SDFalpha	0	28	28	0	55.97	41.67	0.00	30.22	48.90	76.15	191.60
	1	11	11	0	46.30	39.16	2.36	14.15	39.55	75.69	133.05
SDFalpha _percent	0	28	28	0	23.30	23.15	0.00	11.81	19.37	26.69	121.05
	1	11	11	0	16.79	16.62	0.71	4.64	14.90	20.24	56.50
SDFbeta	0	28	28	0	44.10	41.18	0.00	2.83	24.32	86.34	116.51
	1	11	11	0	18.94	34.48	0.00	0.00	2.63	18.71	90.19
SDFbeta_ percent	0	28	28	0	18.19	18.31	0.00	0.94	8.83	33.98	54.99
	1	11	11	0	6.27	11.26	0.00	0.00	0.49	6.14	30.27
SDFdelta	0	28	28	0	40.40	74.05	0.00	0.00	0.00	41.16	316.16
	1	11	11	0	11.06	26.33	0.00	0.00	0.00	0.50	82.23
SDFdelta_ percent	0	28	28	0	14.77	24.72	0.00	0.00	0.00	19.18	95.00
	1	11	11	0	3.33	8.84	0.00	0.00	0.00	0.21	29.17
SDFepsilon	0	28	28	0	42.61	49.11	0.00	1.49	11.06	93.25	142.78
	1	11	11	0	46.33	60.19	0.00	0.00	10.81	105.89	175.41
SDFepsilon_ percent	0	28	28	0	17.38	21.14	0.00	0.41	5.01	37.24	74.04
	1	11	11	0	15.75	20.44	0.00	0.00	4.59	33.14	61.75
SDFgamma	0	28	28	0	42.22	54.87	0.00	0.00	0.09	114.25	122.05
	1	11	11	0	16.93	38.81	0.00	0.00	0.00	0.67	115.40
SDFgamma_ percent	0	28	28	0	20.85	30.79	0.00	0.00	0.03	40.43	108.60
	1	11	11	0	6.95	17.17	0.00	0.00	0.00	0.23	55.13
SDFtheta	0	28	28	0	59.09	44.76	0.00	0.00	86.44	92.80	119.72
	1	11	11	0	49.75	47.46	0.00	0.00	79.47	88.15	115.82
SDFtheta_ percent	0	28	28	0	24.92	22.90	0.00	0.00	24.94	38.44	90.43
	1	11	11	0	17.37	17.23	0.00	0.00	21.22	35.84	41.09

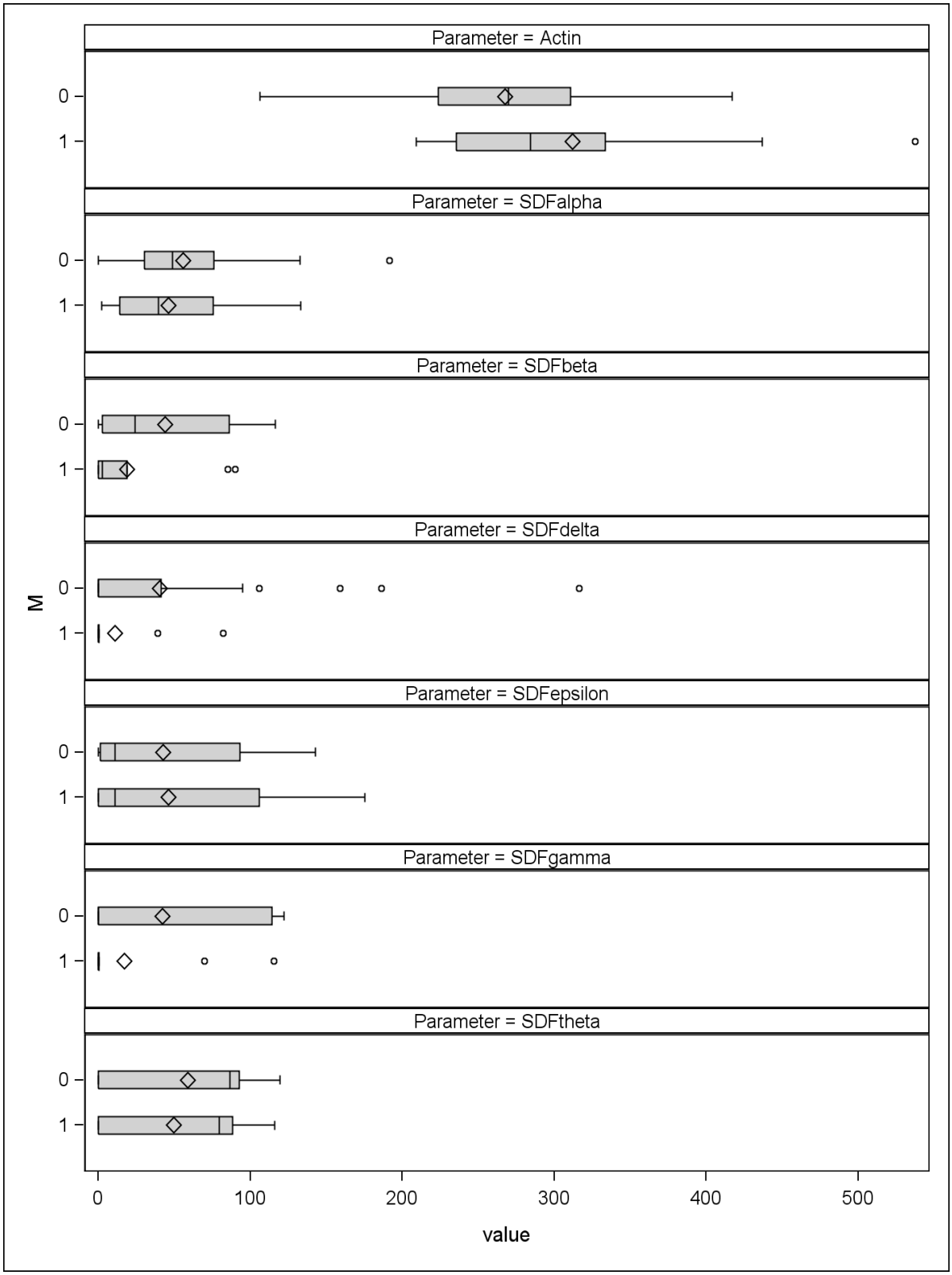
Parameter = Actin
Parameter = SDFalpha
Parameter = SDFbeta
Parameter = SDFdelta
Parameter = SDFepsilon
Parameter = SDFgamma
Parameter = SDFtheta
M
0
1
0
100
200
300
400
500
value

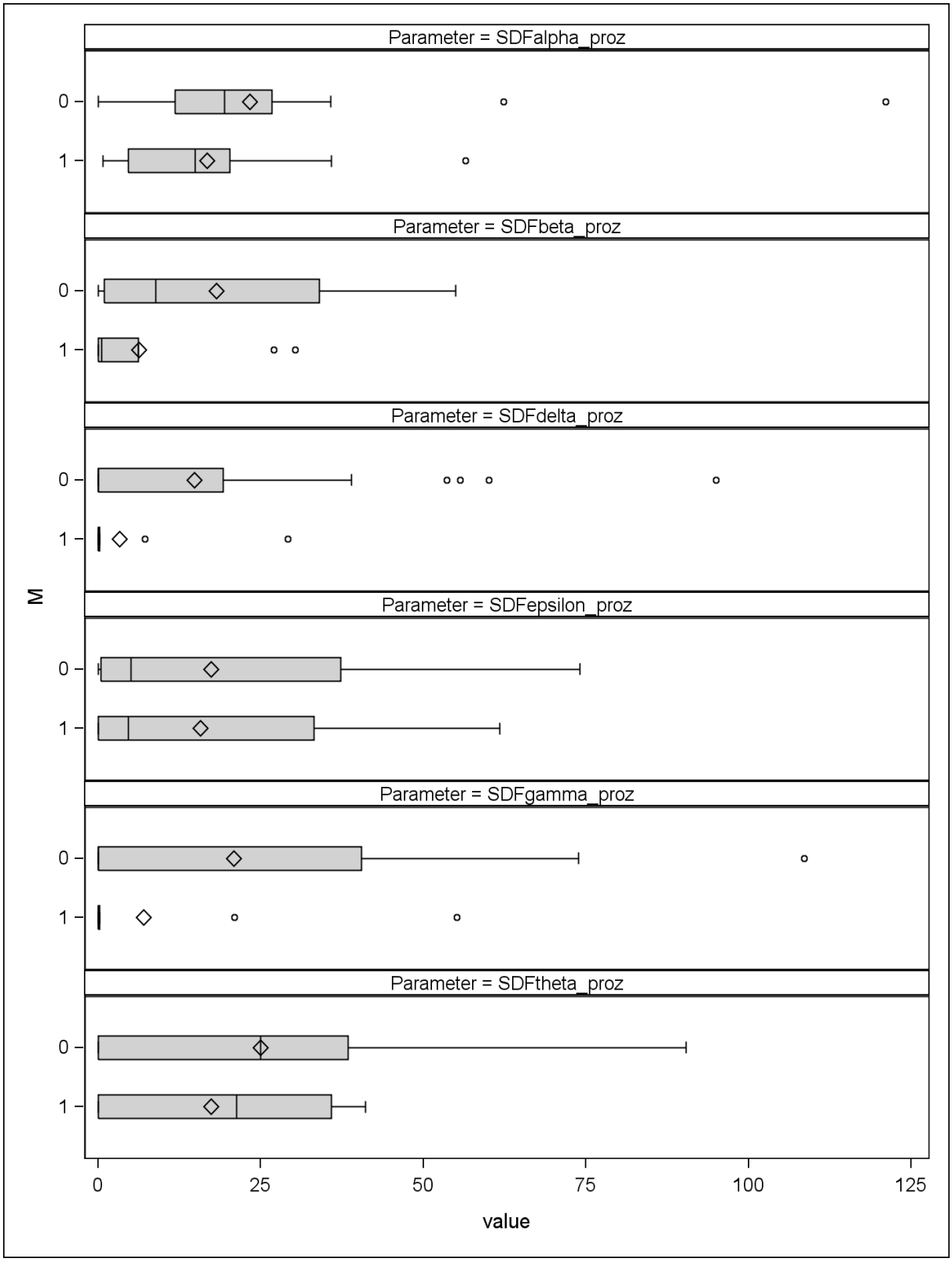

Box plot (3) Correlation of SDFI isoforms with parameter M

7.4.1 p-values for Wilcoxon tests and Kruskal-Wallis tests for association of SDF1 isoforms with clinical parameter -M

Parameter	*p-Wert Wilcoxon-Test*
Actin	0.2958
Alter	0.4534
SDFalpha	0.4633
SDFalpha_ percent	0.2679
SDFbeta	0.0656
SDFbeta_ percent	0.0457
SDFdelta	0.2409
SDFdelta_ percent	0.1894
SDFepsilon	0.8746
SDFepsilon_ percent	0.7885
SDFgamma	0.2412
SDFgamma_ percent	0.2551
SDFtheta	0.3751
SDFtheta_ percent	0.4193

7.5 Correlation of SDFI isoforms with clinical parameter R

Analysis Variable : value											
Parameter	*R*	*N Obs*	*N*	*N Miss*	*Mean*	*Std Dev*	*Mini-mum*	*Lower Quartile*	*Median*	*Upper Quartile*	*Maxi-mum*
Actin	0	29	29	0	273.30	77.49	106.38	233.55	274.76	312.02	436.90
	2	10	10	0	299.62	94.51	209.34	235.49	282.96	331.44	537.37
Alter	0	29	29	0	66.59	10.77	44.00	59.00	68.00	74.00	83.00
	2	10	10	0	63.30	10.44	41.00	56.00	65.50	72.00	75.00
SDFalpha	0	29	29	0	54.65	41.53	0.00	23.94	48.68	75.74	191.60
	2	10	10	0	49.16	40.05	2.36	14.15	47.81	75.69	133.05
SDFalpha_ percent	0	29	29	0	22.64	23.01	0.00	10.58	18.94	26.53	121.05
	2	10	10	0	18.07	16.94	0.71	4.87	15.86	20.24	56.50
SDFbeta	0	29	29	0	42.58	41.26	0.00	2.05	24.16	85.31	116.51
	2	10	10	0	20.83	35.74	0.00	0.00	3.50	18.71	90.19
SDFbeta_ percent	0	29	29	0	17.56	18.29	0.00	0.88	7.85	33.13	54.99
	2	10	10	0	6.90	11.66	0.00	0.00	1.06	6.14	30.27
SDFdelta	0	29	29	0	39.01	73.10	0.00	0.00	0.00	41.16	316.16
	2	10	10	0	12.16	27.48	0.00	0.00	0.00	0.50	82.23
SDFdelta_ percent	0	29	29	0	14.26	24.43	0.00	0.00	0.00	14.63	95.00
	2	10	10	0	3.66	9.25	0.00	0.00	0.00	0.21	29.17
SDFepsilon	0	29	29	0	41.14	48.87	0.00	0.00	10.51	80.61	142.78
	2	10	10	0	50.97	61.35	0.00	0.00	20.55	105.89	175.41
SDFepsilon_ percent	0	29	29	0	16.78	21.01	0.00	0.00	3.47	37.13	74.04
	2	10	10	0	17.32	20.83	0.00	0.00	7.96	33.14	61.75
SDFgamma	0	29	29	0	40.77	54.45	0.00	0.00	0.00	113.86	122.05
	2	10	10	0	18.62	40.48	0.00	0.00	0.00	0.67	115.40
SDFgamma_ percent	0	29	29	0	20.13	30.49	0.00	0.00	0.00	35.05	108.60
	2	10	10	0	7.64	17.94	0.00	0.00	0.00	0.23	55.13
SDFtheta	0	29	29	0	60.25	44.40	0.00	0.00	87.36	92.72	119.72
	2	10	10	0	45.46	47.72	0.00	0.00	42.80	84.40	115.82
SDFtheta_ percent	0	29	29	0	24.80	22.50	0.00	0.00	24.19	38.00	90.43
	2	10	10	0	16.98	18.12	0.00	0.00	13.02	35.84	41.09

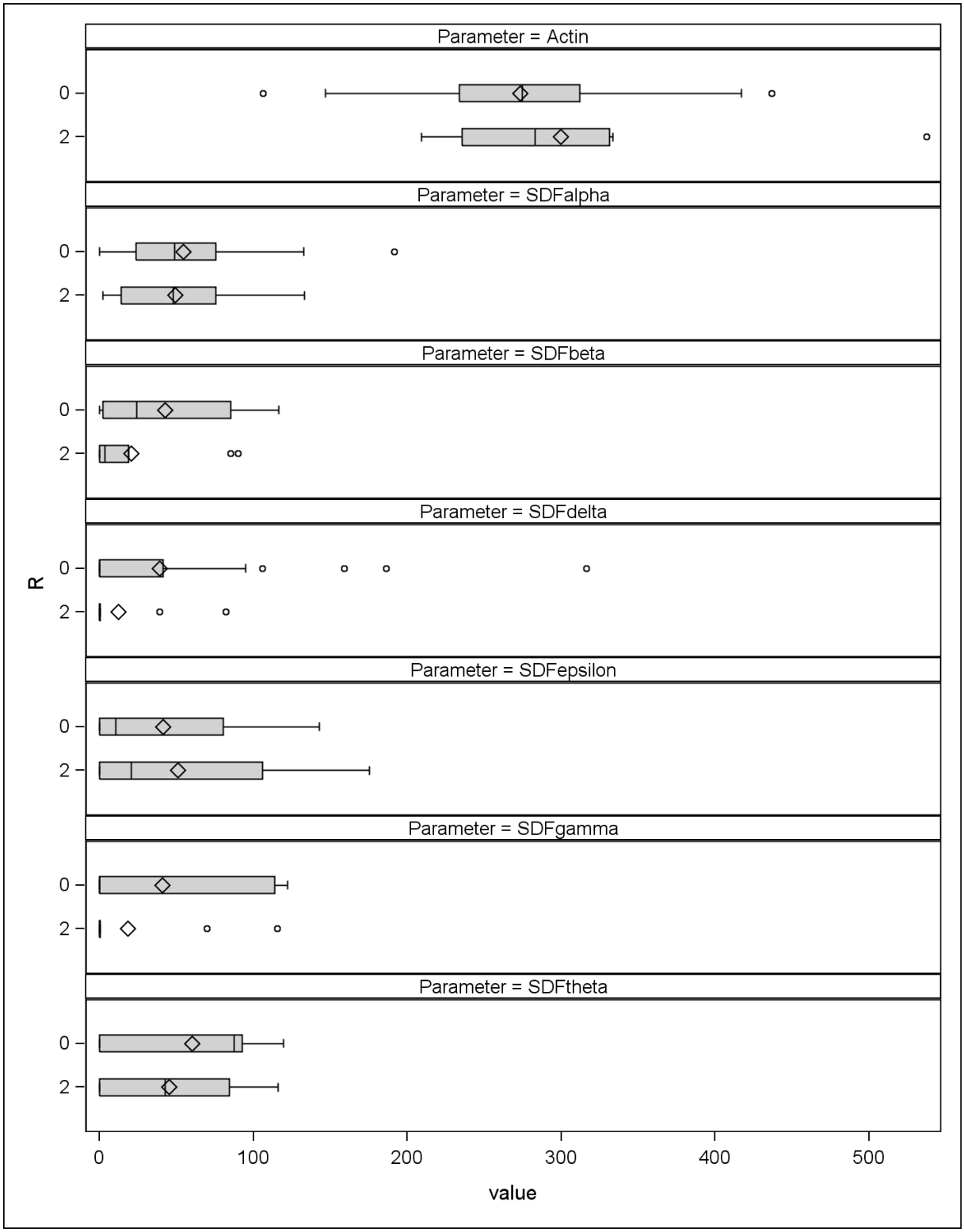
Parameter = Actin
Parameter = SDFalpha
Parameter = SDFbeta
Parameter = SDFdelta
Parameter = SDFepsilon
Parameter = SDFgamma
Parameter = SDFtheta
R
0
2
0
100
200
300
400
500
value

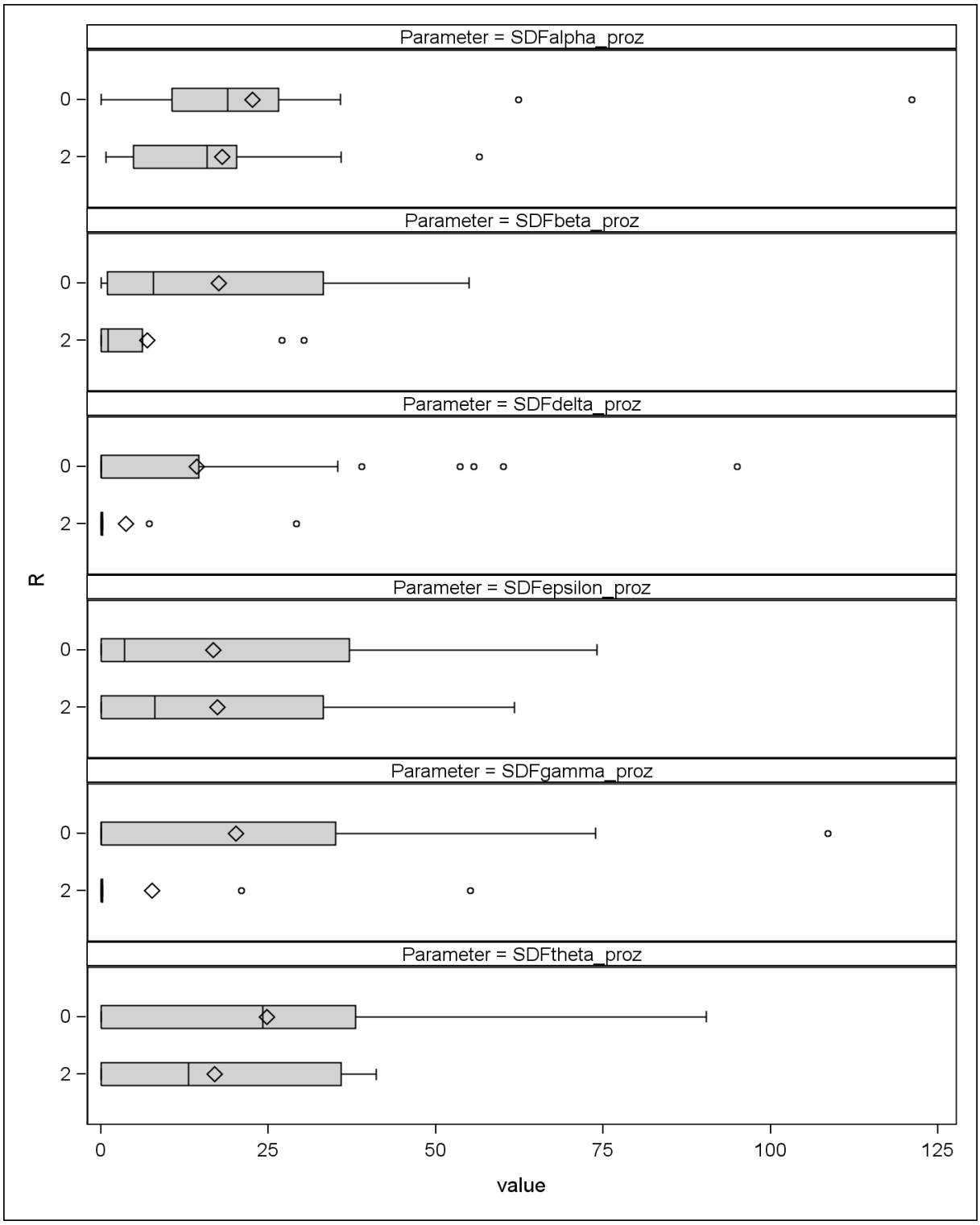

Box plot (4) Correlation of SDFI isoforms with parameter R

7.5.1 p-values for Wilcoxon tests and Kruskal-Wallis tests for association of SDF1 isoforms with clinical parameter -R

Parameter	*p-Wert Wilcoxon-Test*
Actin	0.6181
Alter	0.3674
SDFalpha	0.7115
SDFalpha_ percent	0.5097
SDFbeta	0.1535
SDFbeta_ percent	0.1120
SDFdelta	0.3576
SDFdelta_ percent	0.2873
SDFepsilon	0.7947
SDFepsilon_ percent	0.8836
SDFgamma	0.3720
SDFgamma_ percent	0.3911
SDFtheta	0.2030
SDFtheta_ percent	0.4431

7.6 Correlation of SDFI isoforms with tumor location

Analysis Variable : value											
Parameter	*Location*	*N Obs*	*N*	*N Miss*	*Mean*	*Std Dev*	*Mini-mum*	*Lower Quartile*	*Median*	*Upper Quartile*	*Maxi-mum*
Actin	caecum	3	3	0	236.99	53.96	200.74	200.74	211.23	299.01	299.01
	Colon ascending	5	5	0	312.63	65.43	248.14	281.43	285.20	331.44	416.96
	Colon transverse	1	1	0	173.41	.	173.41	173.41	173.41	173.41	173.41
	Colon descending	2	2	0	359.37	109.64	281.84	281.84	359.37	436.90	436.90
	Sigmoid	13	13	0	297.33	50.58	214.05	264.15	304.89	333.28	384.83
	Rectum	15	15	0	259.35	101.01	106.38	205.09	256.96	308.89	537.37
Alter	caecum	3	3	0	64.33	15.04	47.00	47.00	72.00	74.00	74.00
	Colon ascending	5	5	0	66.00	15.60	44.00	58.00	67.00	79.00	82.00
	Colon transverse	1	1	0	83.00	.	83.00	83.00	83.00	83.00	83.00
	Colon descending	2	2	0	73.00	2.83	71.00	71.00	73.00	75.00	75.00
	Sigmoid	13	13	0	65.38	9.91	47.00	58.00	68.00	73.00	79.00
	Rectum	15	15	0	64.13	9.43	41.00	59.00	65.00	72.00	78.00
SDFalpha	caecum	3	3	0	62.16	20.17	38.98	38.98	71.81	75.69	75.69
	Colon ascending	5	5	0	47.48	56.18	2.36	5.09	20.86	76.56	132.54
	Colon transverse	1	1	0	41.95	.	41.95	41.95	41.95	41.95	41.95
	Colon descending	2	2	0	37.36	27.83	17.68	17.68	37.36	57.04	57.04
	Sigmoid	13	13	0	53.83	39.23	0.00	20.63	56.06	75.74	133.05
	Rectum	15	15	0	55.74	45.62	0.00	23.94	48.68	80.07	191.60
SDFalpha_ percent	caecum	3	3	0	28.21	13.14	13.04	13.04	35.77	35.83	35.83
	Colon ascending	5	5	0	13.76	14.52	0.71	2.05	7.41	26.85	31.79
	Colon transverse	1	1	0	24.19	.	24.19	24.19	24.19	24.19	24.19
	Colon descending	2	2	0	12.14	11.45	4.05	4.05	12.14	20.24	20.24
	Sigmoid	13	13	0	18.67	14.90	0.00	7.26	16.82	23.71	56.50
	Rectum	15	15	0	26.16	29.92	0.00	10.58	18.89	26.53	121.05
SDFbeta	caecum	3	3	0	26.60	46.08	0.00	0.00	0.00	79.81	79.81
	Colon ascending	5	5	0	36.86	41.84	0.00	0.00	24.48	65.34	94.48
	Colon transverse	1	1	0	95.36	.	95.36	95.36	95.36	95.36	95.36
	Colon descending	2	2	0	42.65	60.32	0.00	0.00	42.65	85.31	85.31
	Sigmoid	13	13	0	31.56	42.70	0.00	0.00	3.60	67.33	116.51
	Rectum	15	15	0	39.21	39.32	0.00	4.48	19.33	85.31	96.09
SDFbeta_ percent	caecum	3	3	0	8.90	15.41	0.00	0.00	0.00	26.69	26.69
	Colon ascending	5	5	0	12.44	14.97	0.00	0.00	5.87	23.22	33.13
	Colon transverse	1	1	0	54.99	.	54.99	54.99	54.99	54.99	54.99
	Colon descending	2	2	0	15.13	21.40	0.00	0.00	15.13	30.27	30.27
	Sigmoid	13	13	0	9.89	13.14	0.00	0.00	1.00	22.68	34.82

Analysis Variable : value											
Parameter	*Location*	*N Obs*	*N*	*N Miss*	*Mean*	*Std Dev*	*Mini-mum*	*Lower Quartile*	*Median*	*Upper Quartile*	*Maxi-mum*
	Rectum	15	15	0	18.37	19.43	0.00	1.88	6.93	35.15	53.90
SDFdelta	caecum	3	3	0	35.26	61.08	0.00	0.00	0.00	105.79	105.79
	Colon ascending	5	5	0	8.32	18.36	0.00	0.00	0.00	0.42	41.16
	Colon transverse	1	1	0	41.16	.	41.16	41.16	41.16	41.16	41.16
	Colon descending	2	2	0	41.11	58.14	0.00	0.00	41.11	82.23	82.23
	Sigmoid	13	13	0	31.95	64.01	0.00	0.00	0.00	32.28	186.24
	Rectum	15	15	0	37.79	83.17	0.00	0.00	0.00	38.92	316.16
SDFdelta_ percent	caecum	3	3	0	11.79	20.43	0.00	0.00	0.00	35.38	35.38
	Colon ascending	5	5	0	2.95	6.53	0.00	0.00	0.00	0.10	14.63
	Colon transverse	1	1	0	23.74	.	23.74	23.74	23.74	23.74	23.74
	Colon descending	2	2	0	14.59	20.63	0.00	0.00	14.59	29.17	29.17
	Sigmoid	13	13	0	10.14	20.18	0.00	0.00	0.00	10.48	55.67
	Rectum	15	15	0	14.35	28.42	0.00	0.00	0.00	13.90	95.00
SDFepsilon	caecum	3	3	0	37.24	64.50	0.00	0.00	0.00	111.71	111.71
	Colon ascending	5	5	0	43.97	41.93	9.21	9.61	27.77	67.39	105.89
	Colon transverse	1	1	0	28.72	.	28.72	28.72	28.72	28.72	28.72
	Colon descending	2	2	0	52.94	74.87	0.00	0.00	52.94	105.89	105.89
	Sigmoid	13	13	0	60.30	65.50	0.00	2.97	11.61	115.82	175.41
	Rectum	15	15	0	30.18	39.79	0.00	0.00	9.41	59.40	108.07
SDFepsilon_ percent	caecum	3	3	0	12.45	21.57	0.00	0.00	0.00	37.36	37.36
	Colon ascending	5	5	0	14.86	14.41	2.21	3.42	11.19	20.33	37.13
	Colon transverse	1	1	0	16.56	.	16.56	16.56	16.56	16.56	16.56
	Colon descending	2	2	0	18.79	26.57	0.00	0.00	18.79	37.57	37.57
	Sigmoid	13	13	0	20.94	23.71	0.00	0.83	4.59	39.01	61.75
	Rectum	15	15	0	14.79	21.85	0.00	0.00	4.50	28.96	74.04
SDFgamma	caecum	3	3	0	0.00	0.00	0.00	0.00	0.00	0.00	0.00
	Colon ascending	5	5	0	30.68	49.82	0.00	0.00	0.17	38.60	114.65
	Colon transverse	1	1	0	113.86	.	113.86	113.86	113.86	113.86	113.86
	Colon descending	2	2	0	0.00	0.00	0.00	0.00	0.00	0.00	0.00
	Sigmoid	13	13	0	14.86	37.55	0.00	0.00	0.00	0.32	122.05
	Rectum	15	15	0	60.53	57.98	0.00	0.00	94.97	115.65	122.05
SDFgamma_ percent	caecum	3	3	0	0.00	0.00	0.00	0.00	0.00	0.00	0.00
	Colon ascending	5	5	0	8.22	12.26	0.00	0.00	0.05	13.53	27.50
	Colon transverse	1	1	0	65.66	.	65.66	65.66	65.66	65.66	65.66
	Colon descending	2	2	0	0.00	0.00	0.00	0.00	0.00	0.00	0.00
	Sigmoid	13	13	0	5.20	13.61	0.00	0.00	0.00	0.11	46.20

Analysis Variable : value											
Parameter	*Location*	*N Obs*	*N*	*N Miss*	*Mean*	*Std Dev*	*Mini-mum*	*Lower Quartile*	*Median*	*Upper Quartile*	*Maxi-mum*
	Rectum	15	15	0	32.39	35.55	0.00	0.00	34.57	59.51	108.60
SDFtheta	caecum	3	3	0	57.25	49.61	0.00	0.00	84.40	87.36	87.36
	Colon ascending	5	5	0	82.80	44.84	6.14	87.36	91.36	109.40	119.72
	Colon transverse	1	1	0	105.40	.	105.40	105.40	105.40	105.40	105.40
	Colon descending	2	2	0	104.27	16.34	92.72	92.72	104.27	115.82	115.82
	Sigmoid	13	13	0	52.59	44.34	0.00	0.00	80.61	92.42	95.82
	Rectum	15	15	0	41.22	43.40	0.00	0.00	25.37	87.40	104.42
SDFtheta_ percent	caecum	3	3	0	23.92	22.08	0.00	0.00	28.22	43.52	43.52
	Colon ascending	5	5	0	28.30	17.72	1.85	21.91	30.63	38.87	48.25
	Colon transverse	1	1	0	60.78	.	60.78	60.78	60.78	60.78	60.78
	Colon descending	2	2	0	31.16	14.05	21.22	21.22	31.16	41.09	41.09
	Sigmoid	13	13	0	18.21	16.23	0.00	0.00	24.19	28.91	43.22
	Rectum	15	15	0	21.06	26.63	0.00	0.00	7.62	37.96	90.43

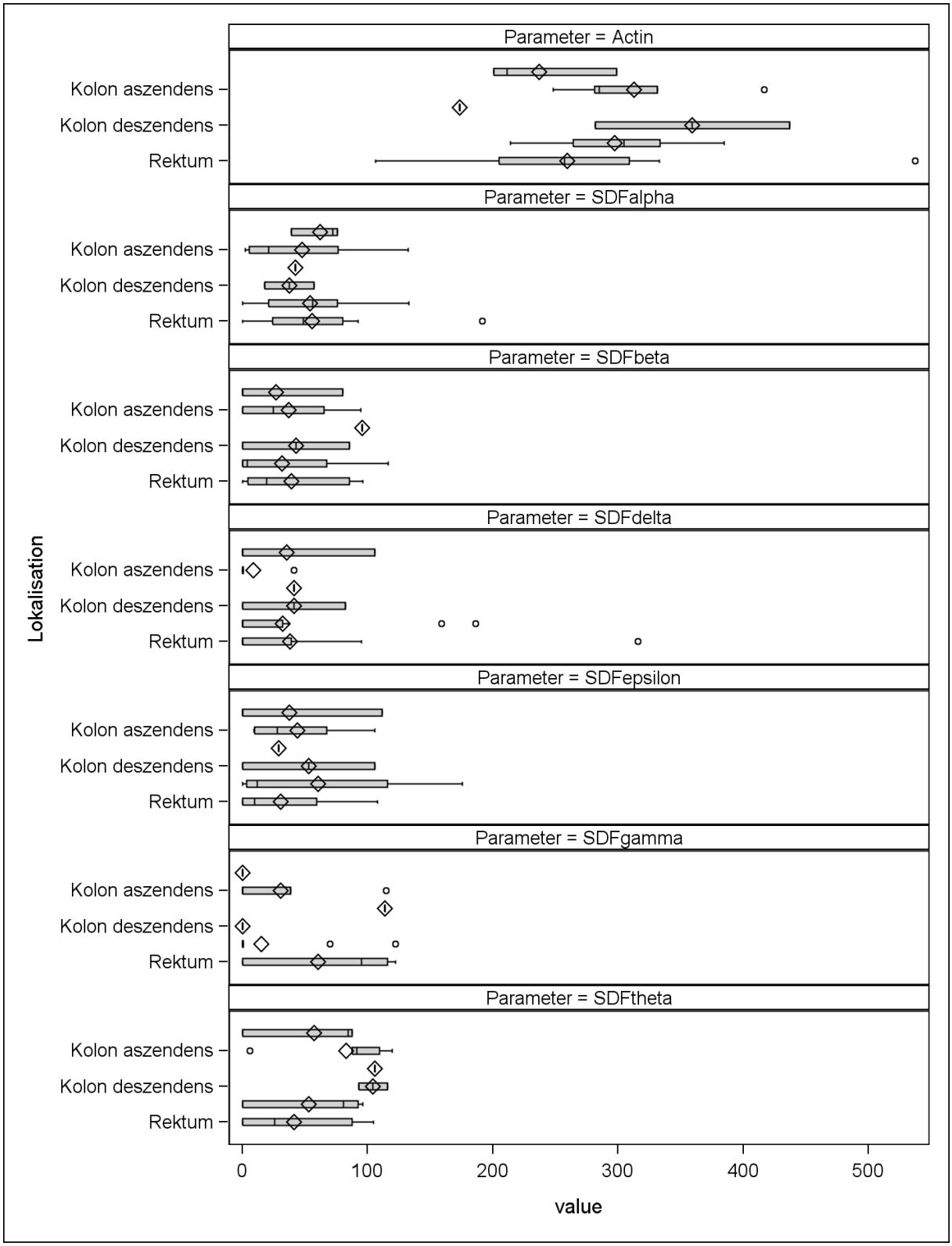
Parameter = Actin
Parameter = SDFalpha
Parameter = SDFbeta
Parameter = SDFdelta
Parameter = SDFepsilon
Parameter = SDFgamma
Parameter = SDFtheta
Kolon aszendens
Kolon deszendens
Rektum
Lokalisation
0
100
200
300
400
500
value

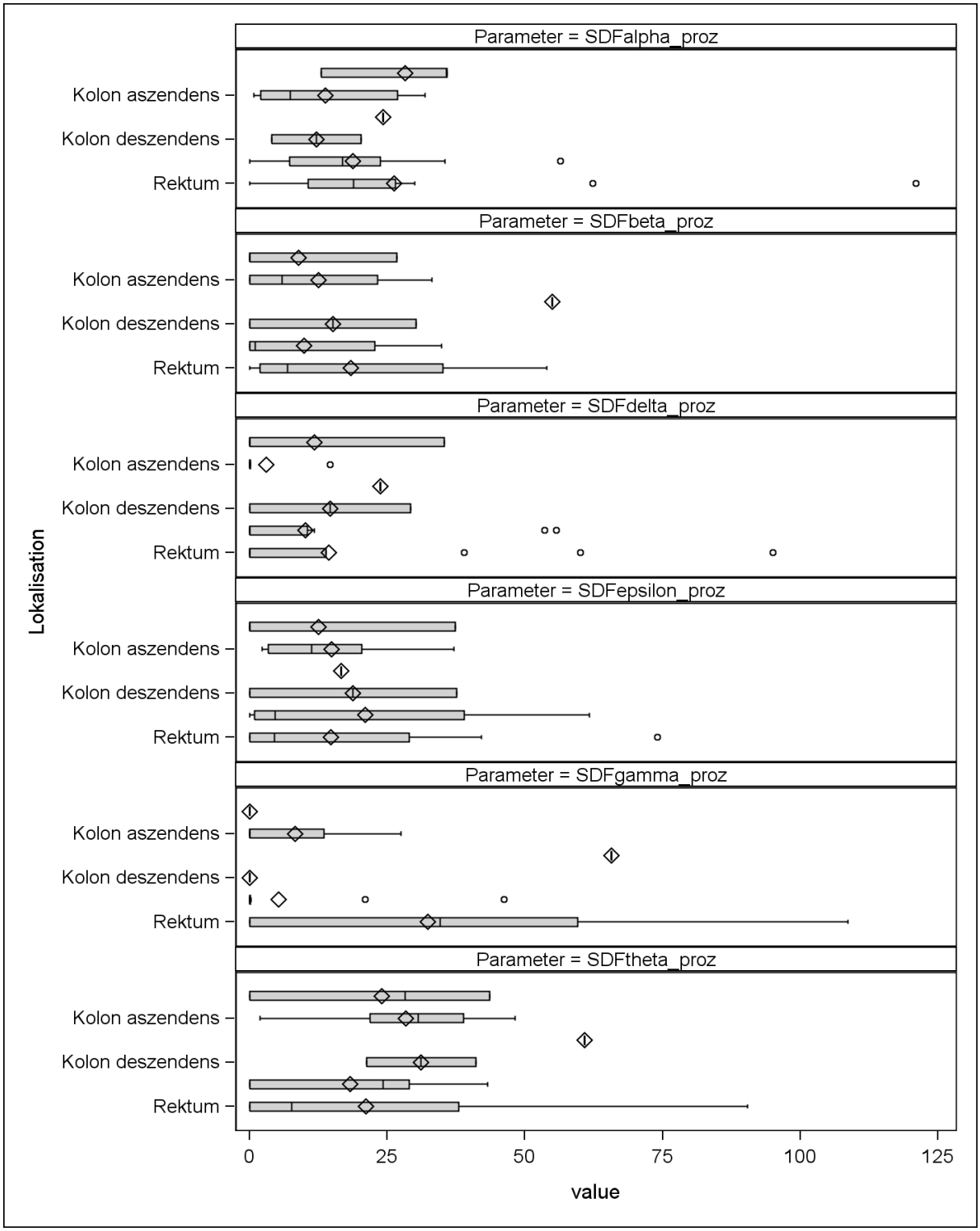

Box plot (5) Correlation of SDFI isoforms with tumor location

7.6.1 p-values for Wilcoxon tests and Kruskal-Wallis tests for association of SDF1 isoforms with tumor location

Parameter	*p-Wert Wilcoxon-Test*
Actin	0.1286
Alter	0.9575
SDFalpha	0.8651
SDFalpha_ percent	0.5311
SDFbeta	0.5039
SDFbeta_ percent	0.2016
SDFdelta	0.9815
SDFdelta_ percent	0.9850
SDFepsilon	0.4253
SDFepsilon_ percent	0.6915
SDFgamma	0.1407
SDFgamma_ percent	0.0992
SDFtheta	0.2319
SDFtheta_ percent	0.5595

7.7 Scatter plot

7.7.1 Correlation among SDF-1 isoforms

Actin and the SDF1 isoforms did exhibit correlation with age. Further, there was significant association among the SDF1 isoforms. Also **SDF γ** tends to decrease when actin increases. After standardisation, some correlations are substantially different from zero, in particular SDF1 β and SDF1θ.

Pearson Correlation Coefficients Prob > |r| under H0: Rho=0 Number of Observations								
	Alter	*Actin*	*alpha*	*beta*	*gamma*	*delta*	*epsilon*	*theta*
Alter Alter	1.00000 39	-0.13972 0.3962 39	-0.04777 0.7728 39	-0.02730 0.8690 39	0.19317 0.2387 39	0.07543 0.6481 39	-0.21384 0.1912 39	0.10631 0.5195 39
Actin Actin	-0.13972 0.3962 39	1.00000 40	-0.01916 0.9066 40	-0.08372 0.6075 40	-0.35767 0.0235 40	0.10351 0.5250 40	-0.05144 0.7526 40	-0.09977 0.5402 40
alpha alpha	-0.04777 0.7728 39	-0.01916 0.9066 40	1.00000 40	0.23404 0.1461 40	0.16911 0.2969 40	0.21220 0.1887 40	-0.04299 0.7922 40	0.11430 0.4825 40
beta beta	-0.02730 0.8690 39	-0.08372 0.6075 40	0.23404 0.1461 40	1.00000 40	0.16463 0.3100 40	0.60533 <.0001 40	0.28580 0.0738 40	0.03862 0.8130 40
gamma gamma	0.19317 0.2387 39	-0.35767 0.0235 40	0.16911 0.2969 40	0.16463 0.3100 40	1.00000 40	-0.15802 0.3301 40	-0.12948 0.4258 40	0.25850 0.1073 40
delta delta	0.07543 0.6481 39	0.10351 0.5250 40	0.21220 0.1887 40	0.60533 <.0001 40	-0.15802 0.3301 40	1.00000 40	0.05196 0.7502 40	-0.25492 0.1124 40
epsilon epsilon	-0.21384 0.1912 39	-0.05144 0.7526 40	-0.04299 0.7922 40	0.28580 0.0738 40	-0.12948 0.4258 40	0.05196 0.7502 40	1.00000 40	-0.16050 0.3225 40
theta theta	0.10631 0.5195 39	-0.09977 0.5402 40	0.11430 0.4825 40	0.03862 0.8130 40	0.25850 0.1073 40	-0.25492 0.1124 40	-0.16050 0.3225 40	1.00000 40

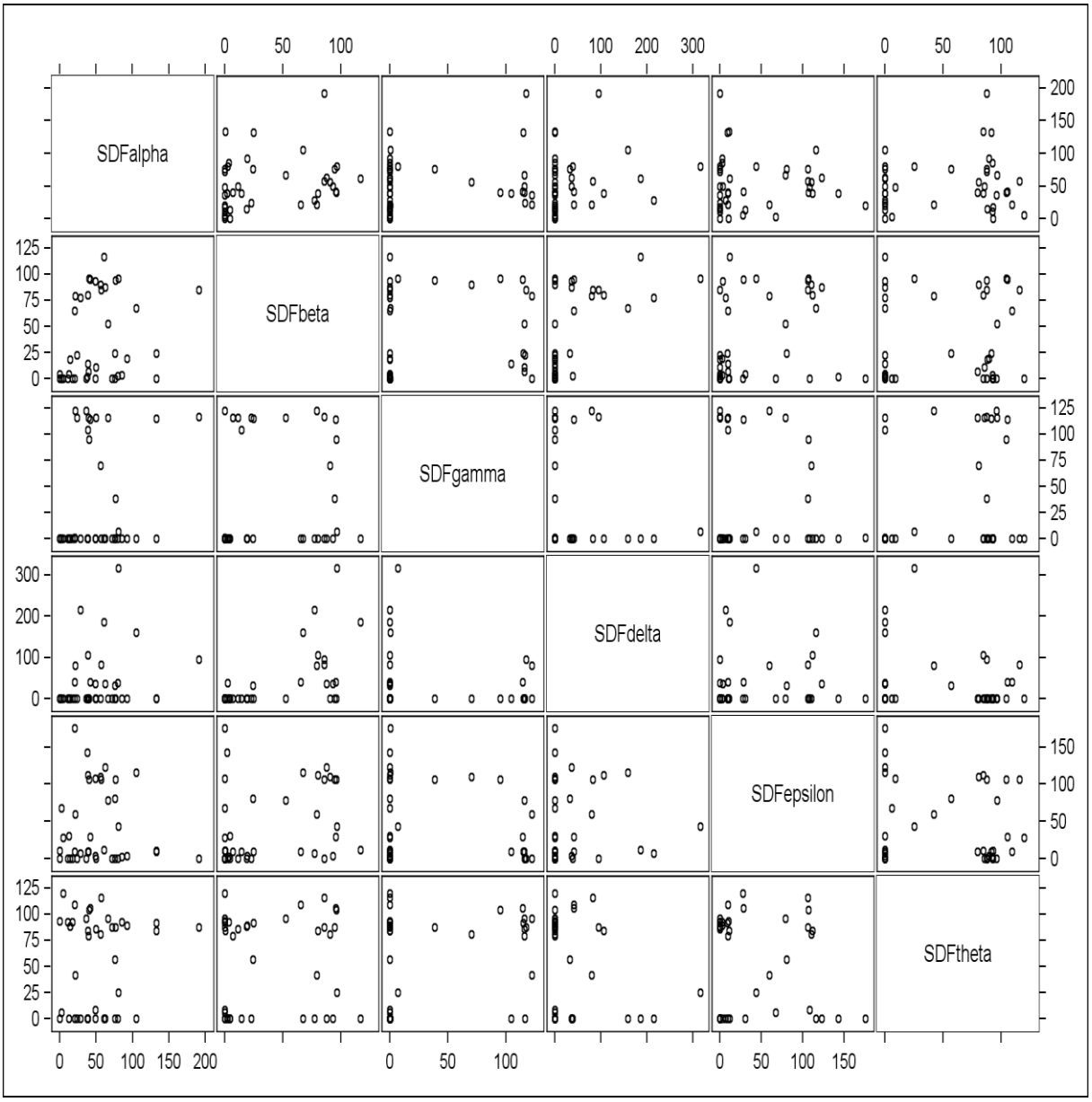

Scatter plot (1) Correlation among SDF-1 isoforms

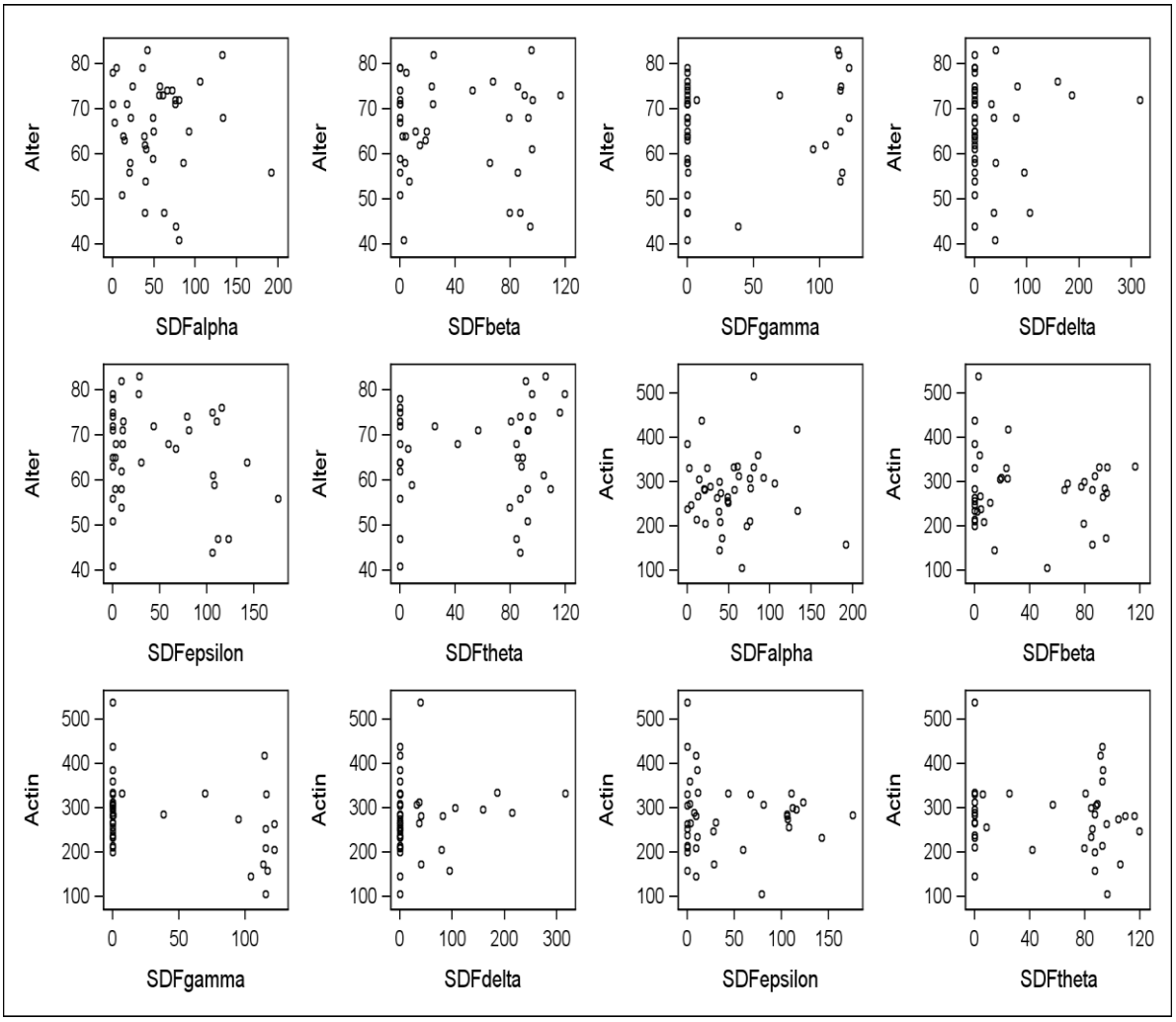

Scatter plot (2) Correlation between SDF-1 isoforms with actin and age

7.7.2 Correlation among SDF-1 isoforms- percent

Actin and the SDF1 isoforms_percent did exhibit correlation with age. **SDF α, SDF β, SDF γ** and **SDF1θ** tend to decrease when actin increases.

SDFIbeta isoform was correlated with isoforms of SDFIalpha (P= 0.048). SDFIgamma isoform was correlated with isoforms of SDFI alpha (P= 0.0023) and SDFIbeta (P= 0.001). SDFIdelta isoform was correlated with isoforms of SDFIbeta (P= 0.000). SDFIepsilon isoform was correlated with isoforms of SDFIbeta (P= 0.047). SDFItheta isoform was correlated with isoforms of SDFIalpha (0.008),SDFIbeta (P= 0.023) and gamma (0.000).

Pearson Correlation Coefficients Prob > |r| under H0: Rho=0 Number of Observations								
	Alter	*Actin*	*alpha_percent*	*beta_percent*	*gamma_percent*	*delta_percent*	*epsilon_percent*	*theta_percent*
Alter Alter	1.00000 39	-0.13972 0.3962 39	-0.02286 0.8902 39	0.02145 0.8969 39	0.13937 0.3974 39	0.07224 0.6621 39	-0.13369 0.4172 39	0.12114 0.4626 39
Actin Actin	-0.13972 0.3962 39	1.00000 40	-0.40136 0.0103 40	-0.32314 0.0420 40	-0.54909 0.0002 40	-0.00248 0.9879 40	-0.22619 0.1605 40	-0.42788 0.0059 40
*alpha_* percent alpha_ percent	-0.02286 0.8902 39	-0.40136 0.0103 40	1.00000 40	0.43695 0.0048 40	0.46757 0.0023 40	0.25954 0.1058 40	0.05407 0.7404 40	0.41089 0.0084 40
*beta_* percent beta_ percent	0.02145 0.8969 39	-0.32314 0.0420 40	0.43695 0.0048 40	1.00000 40	0.48248 0.0016 40	0.56648 0.0001 40	0.31493 0.0478 40	0.35834 0.0232 40
*gamma_* perc gamma_ perc	0.13937 0.3974 39	-0.54909 0.0002 40	0.46757 0.0023 40	0.48248 0.0016 40	1.00000 40	-0.00486 0.9763 40	0.14699 0.3654 40	0.53831 0.0003 40
*delta_* percent delta_ percent	0.07224 0.6621 39	-0.00248 0.9879 40	0.25954 0.1058 40	0.56648 0.0001 40	-0.00486 0.9763 40	1.00000 40	-0.01127 0.9450 40	-0.11986 0.4613 40
*epsilon_* perc epsilon_ perc	-0.13369 0.4172 39	-0.22619 0.1605 40	0.05407 0.7404 40	0.31493 0.0478 40	0.14699 0.3654 40	-0.01127 0.9450 40	1.00000 40	0.08839 0.5876 40
*theta_* percent theta_percent	0.12114 0.4626 39	-0.42788 0.0059 40	0.41089 0.0084 40	0.35834 0.0232 40	0.53831 0.0003 40	-0.11986 0.4613 40	0.08839 0.5876 40	1.00000 40

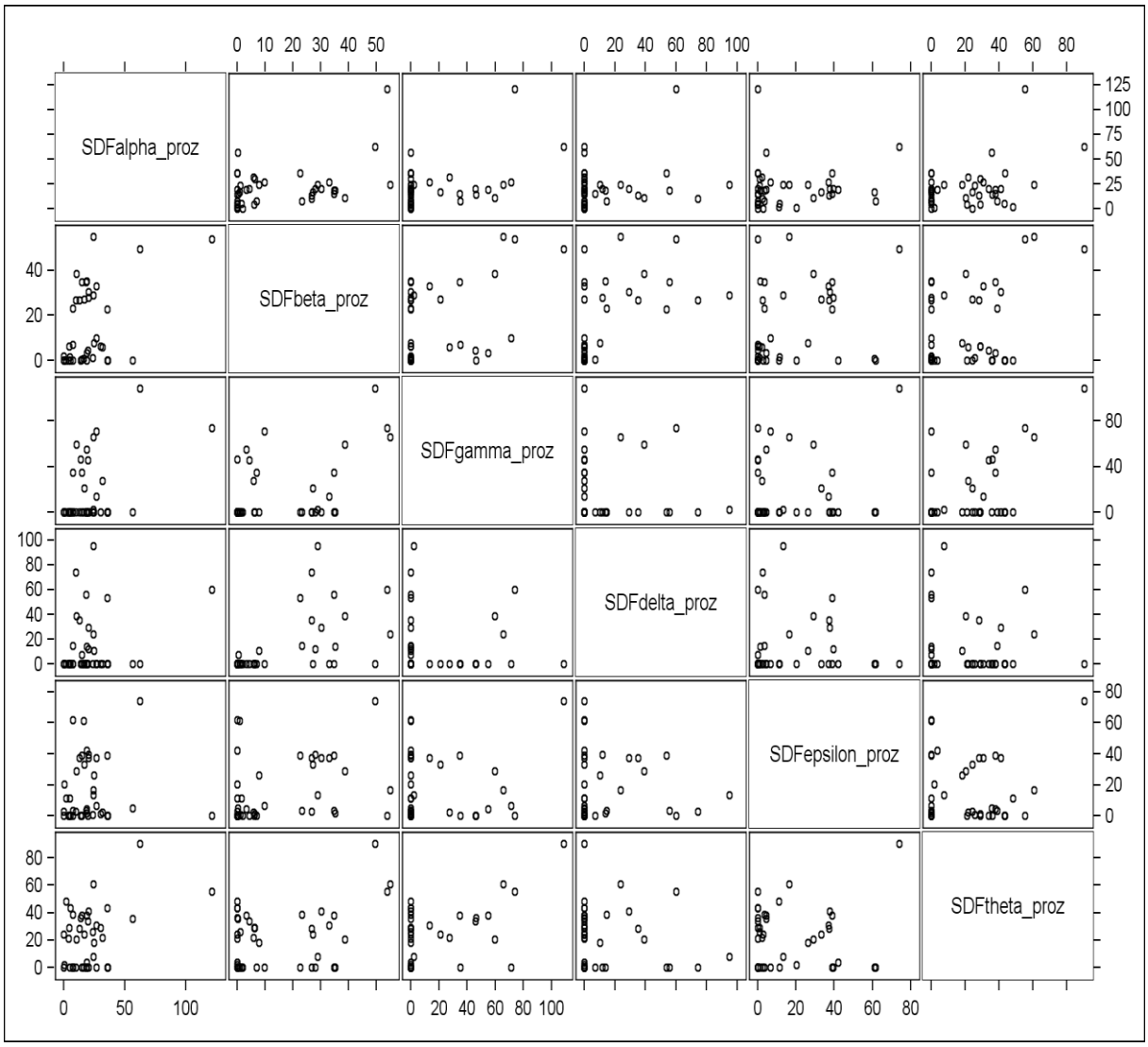

Scatter plot (3) Correlation among SDF-1 isoforms_percent

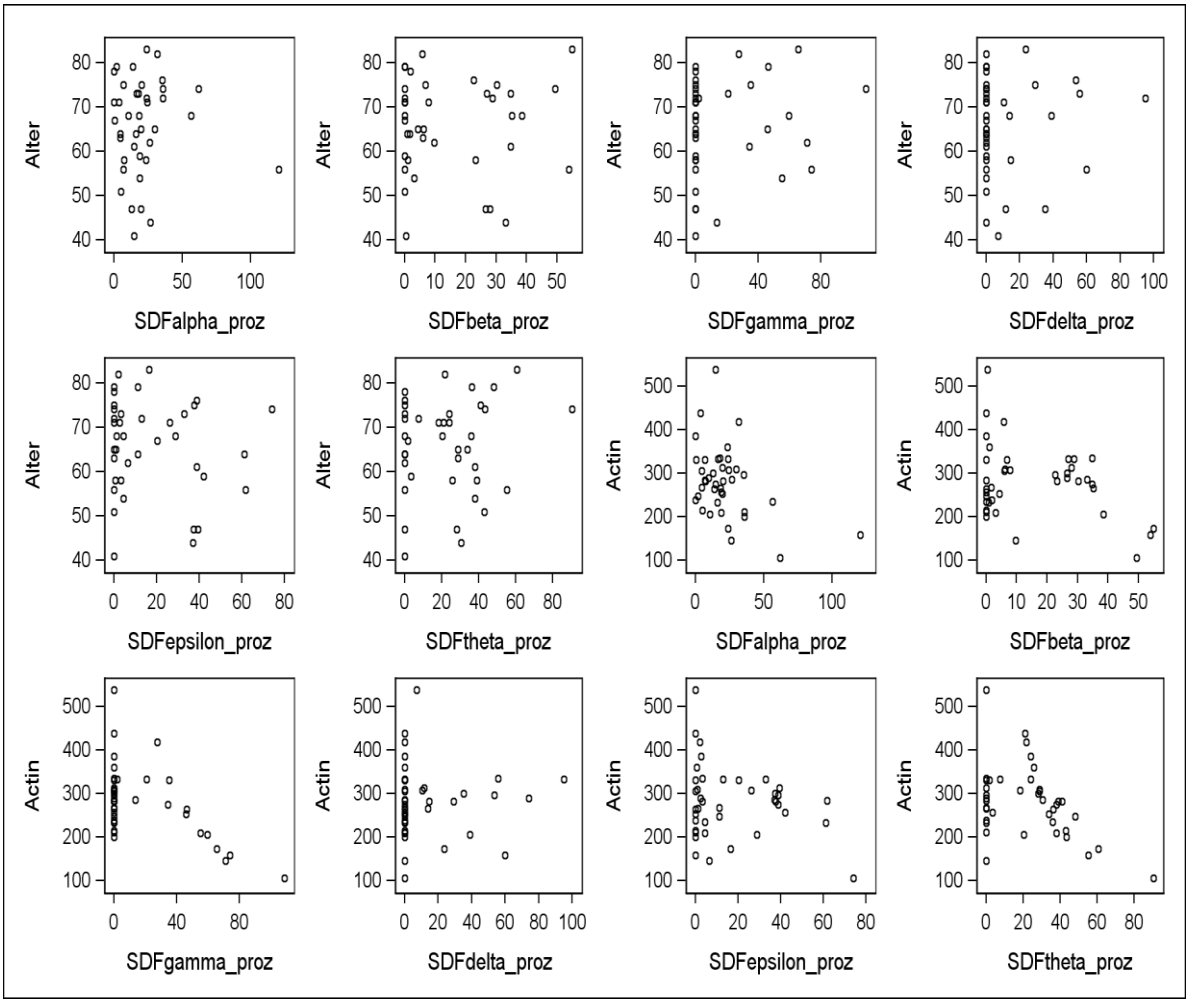

Scatter plot (4) Correlation between SDF-1 isoforms_percent with actin and age

8. CURRICULUM VITAE

Personal Details	
Name: Date/Place of birth: Nationality: Marital status:	Risala Allami March 17. 1975, Baghdad,Iraq Iraqi Married
Education	
Schooling: Studies:	1980-1989: Basic primary school 1990-1993: High school graduation 1994-1998: B.sc Degree in Biology-Baghdad University-Iraq 1999-2001: M.sc Degree in Genetic Engineering and Biotechnology Faculty of Science - Baghdad university- Iraq
Work Experience	
	Since Jan -2010 Postgraduate studies (PhD) Project. Performance of RT-PCR, RFLP analyses, immunohistochemical staining, Western blot analysis, nucleic acid and protein isolation, flow cytometry, cloning, transfection with si-RNA and plasmids, cell culture techniques ,animal testing.

Field of responsibility:	Sep2001- Dec 2006 A member of staff in Department of Biology / Faculty of Arts and Science –Libya. Aug1999- Aug 2001 Postgraduate studies (M.SC) project. Aug1998- Juli1999 Lab-technician in Department of Biology / Faculty of science Baghdad university
Interships	
	1.11.09-20.12.2009 at the Johannes Gutenberg university, interdisciplinary translational oncological laboratory of PD.Dr.Schimanski and Prof.Dr.Gockel 1.02.2008-28.02.2008 at the Johannes Gutenberg university, institute of molecular genetics and biosafety research, laboratory of Prof.Dr.E.Schmidt
Personal skills	
Languages Computer	Arabic (mother tongue) English German MS Word, MS Power Point, Adobe Photoshop, PubMed